AN ABSTRACT OF THE THESIS OF

Duangchit Panomvana for the degree of Doctor of Philosophy

in Pharmacy presented on August 31, 1979

Title: PROLONGED DURATION OF ACTION OF DYPHYLLINE THROUGH PRODRUGS.

Redacted for privacy

Abstract approved: _____
Dr. James W. Ayres

A series of four diesters and four monoesters of dyphylline were synthesized to slowly liberate dyphylline upon in vivo enzymatic attack and thus prolong the duration of action of dyphylline. These synthesized prodrugs were characterized by infrared (IR), proton nuclear magnetic resonance (PMR) and mass spectrometry. Analysis of dyphylline and each of its mono- and di- esters was also conducted using high pressure liquid chromatography (HPLC). Due to the unsatisfactory separation provided by a single mobile phase, appropriate solvent programming conditions for the separation of dyphylline and all of the mono- and di- esters synthesized here had to be developed. It was confirmed by PMR at approximately -40°C that all four monoesters formed at the α-hydroxy position. The hydroxy peak of monopropionyl dyphylline at -40°C was shifted approximately one ppm downfield relative to the room temperature spectrum and showed a clear doublet. Similar results were obtained for the three other monoesters.

An attempt was also made to synthesize secondary monopivaloyl dyphylline by using triphenylmethyl chloride to protect the primary hydroxyl function of dyphylline. However, after the protecting group was removed with glacial acetic acid, the compound which was purified was identified to be the primary monopivaloyl dyphylline.

There was always an "unknown" peak on each HPLC chromatogram of the primary monoester when the compound was stored in aqueous solution, but not when stored in a nonpolar organic solution. The "unknown" was identified to be the secondary monoester by collecting both the "unknown" and the primary monopropionyl dyphylline from the HPLC outlet followed by evaluation via mass spectrometry. The primary and secondary monoesters were found to be in equilibrium in aqueous solution.

The stability of dipropionyl dyphylline was investigated at several pH values and temperatures in buffered aqueous solutions. Either the concentration of intact drug or some function of the concentration was linear with respect to time. Specific rate constants were determined from the slopes of these straight lines and utilized to generate Arrhenius plots. Both the experimental activation energies and the frequency factors varied markedly with pH. Some of this variation might be explained by large variations in entropy. It was found that the free energies of activation were quite constant and were higher with the slower reaction rates, as would be expected. The stability

of monopropionyl dyphylline was also studied at two different pH values at 60°C. The experimental and predicted monopropionyl dyphylline concentration-time curves generated from the degradation of dipropionyl dyphylline at this temperature and two pH values were compared.

Pharmacokinetic models for both the diester and monoester were developed. Simulations for both single and multiple doses were performed on the computer utilizing the Runge-Kutta numerical method. The sensitivity of dyphylline mass level to each rate constant in the models was determined. The results showed that the conversion rates from the diester to the monoester and/or from the monoester to dyphylline were the rate controlling steps. Predicted dyphylline mass levels versus time curves generated from the simulated administration of dyphylline, monopropionyl dyphylline and dipropionyl dyphylline *via* the intravenous route were compared and showed that the prodrugs provided less fluctuation in dyphylline mass level versus time curves than that provided by dyphylline itself. The absorption rate of the prodrug did not have much effect on dyphylline mass level when this rate was assumed to be equal to the absorption rate of theophylline or a few times slower, the rate of absorption started to produce an effect when it dropped to one-tenth of the absorption rate of theophylline. These simulation experiments indicate that the use of prodrugs as an approach to prolonging the duration of action of dyphylline has very high potential.

Prolonged Duration of Action of Dyphylline through Prodrugs

by

Duangchit Panomvana

A THESIS

submitted to

Oregon State University

in partial fulfillment of
the requirements for the
degree of

Doctor of Philosophy

Completed August 1979

Commencement June 1980

APPROVED:

Redacted for privacy

Professor of Pharmacy
in charge of major

Redacted for privacy

Dean of Pharmacy School

Redacted for privacy

Dean of Graduate School

Date thesis is presented August 31, 1979

Typed by Opal Grossnicklaus for Duangchit Panomvana

ACKNOWLEDGEMENTS

I am very thankful for the pleasure of having Dr. J. W. Ayres as my major professor. His friendliness, patience, encouragement, constant guidance and helpful advice throughout my graduate study are deeply appreciated.

I wish to express my sincere appreciation to Dr. J. H. Block for his guidance and helpful suggestions throughout this research work.

My special appreciation is also extended to Dr. T. Lindstrom for his teaching and comments concerning the mathematics and computer program for the pharmacokinetic models.

Special thanks is given to D. R. Henry for being such a helpful consultant in everything and especially in the computer field. Thanks to D. R. Henry and C. Lins for making the pharmaceutical chemistry laboratory an enjoyable place to work.

I am also particularly indebted to my friends Somrat and Nuannaid Yindepit for helping me taking care of my daughter while I was working on this research.

I am deeply grateful to my parents for their never ending love, encouragement and financial support.

Finally, the patience, encouragement and assistance of my husband, Patipan, is greatly acknowledged. The joy brought to me by my daughter, Piyachit, makes this work meaningful.

TABLE OF CONTENTS

LIST OF FIGURES

LIST OF SCHEMES

LIST OF TABLES

CHAPTER I

DYPHYLLINE PRODRUGS: SYNTHESIS AND HPLC SOLVENT PROGRAMMING ANALYSIS

INTRODUCTION

Dyphylline (dihydroxypropyltheophylline) was synthesized in 1946 (1) (Figure 1). The presence of the hydrophilic dihydroxypropyl group overcomes the disadvantages of low solubility which exist for theophylline. Dyphylline is reported to have the therapeutic activity of theophylline with much lower toxicity (1, 2, 3). An early pharmacokinetic study reported the half-life of dyphylline to be 2.11 ± 0.36 hours (4). With such a short half-life, dosing every half-life to maintain desired serum concentrations is impractical. A very large dose administered less frequently will result in large plasma concentration fluctuations between doses. An alternative to frequent dosing is to administer a sustained-release product. Simon et al. (5) studied the bioavailability and serum concentrations of dyphylline after administering sustained-release tablets (40 mg/kg) and reported 67.8 (range 36.8 to 86.0) percent bioavailability of dyphylline from their tablets compared to those from conventional tablets. The mean half-life of dyphylline from the sustained-release formulation was reported to be 3.42 ± 0.94 hours which is, of course, inconsistent with the earlier report and may reflect prolonged absorption rather than a longer half-life. The serum concentrations were reported to be maintained above 7.88 μg/ml once steady state was achieved when the sustained-release tablets were given once every 8 hours (5).

However, the suggested minimum effective serum concentration for dyphylline is 12 μg/ml (3). Further studies are needed to determine whether or not dyphylline serum concentrations can be maintained within the therapeutic range without causing toxic effects.

The purpose of this study was to prepare prodrugs to prolong the duration of action of dyphylline. A series of derivatives of dyphylline were synthesized which are expected to liberate dyphylline upon *in vivo* enzymatic attack. The ester derivatives were chosen because of the widespread distribution of enzyme esterases throughout the body, including the blood stream. The duration of action is anticipated to increase with the size of the ester substituents which has been reported to correlate inversely with the rate of hydrolysis of esters (6-13). Therefore, one approach to controlling the rate of cleavage of dyphylline ester prodrugs is through chain length optimization.

A series of four diesters and four monoesters were chosen for synthesis as shown in Table I. These ester derivatives of dyphylline were prepared and characterized by Infrared (IR), proton nuclear magnetic resonance (PMR) and mass spectrometry. Analysis of dyphylline and each of its mono- and diesters also was conducted using solvent programming high-pressure liquid chromatography (HPLC).

EXPERIMENTAL

Instrumentation

Melting points were determined using a capillary melting point apparatus.[1]

A thin layer chromatography (TLC)[2] solvent system consisting of distilled n-butanol-chloroform (1:1) was employed.

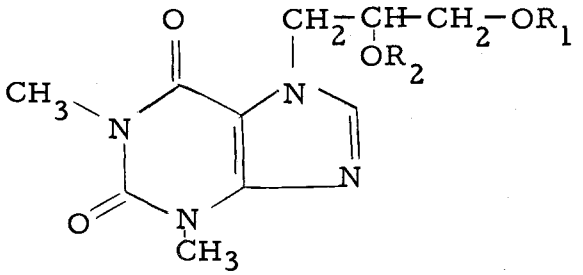

Figure 1. General structure of dyphylline and its derivatives

Table I. Summary of the structure of dyphylline and its ester derivatives

	Compound	R_1	R_2
I	Dyphylline	—H	—H
II	Monopropionyldyphylline	$-C(=O)-CH_2-CH_3$	—H
III	Dipropionyldyphylline	$-C(=O)-CH_2-CH_3$	$-C(=O)-CH_2-CH_3$
IV	Monoisobutyryldyphylline	$-C(=O)-CH-(CH_3)_2$	—H
V	Diisobutyryldyphylline	$-C(=O)-CH-(CH_3)_2$	$-C(=O)-CH-(CH_3)_2$
VI	Monopivaloyldyphylline	$-C(=O)-C(CH_3)_3$	—H
VII	Dipivaloyldyphylline	$-C(=O)-C(CH_3)_3$	$-C(=O)-C(CH_3)_3$
VIII	Mono-p-Cl-benzoyldyphylline		—H
IX	Di-p-Cl-benzoyldyphylline	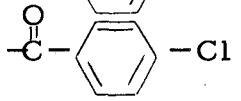	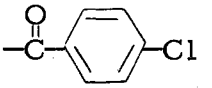

Infrared[3] (IR) spectra of dyphylline and its ester derivatives were determined as a mineral oil dispersions. Polystyrene standard[4] was used for calibration at a frequency of 699 cm^{-1}.

Mass spectra[5] were obtained by direct entry probe. Volatilization of the compounds into the ion source occurred at probe temperatures of 80-150°C. All mass spectra were obtained at 70 ev ionization potential with an electron current of 300 μA. The source temperature was 200°C. For samples II-VII the mass range scanned was 50-500 atomic mass units (amu), the upper limit was increased to 600 amu for samples VIII and IX. All samples were dissolved in $CHCl_3$.

Proton Nuclear Magnetic Resonance PMR Spectra[6] were obtained using chloroform-d as the solvent and tetramethylsilane as the internal reference standard.[7] Proton shifts were recorded in δ, parts per million (ppm), relative to the reference standard. Room temperature PMR's were run on 60 MHZ instrument while cold PMR's (-40°C to -55°C) were run on 100 MHz instrument.

The high pressure liquid chromatograph (HPLC) system consisted of two mobile phase delivery pumps,[8] a programmer,[9] a sample injection apparatus,[10] a 30-cm reversed-phase HPLC column,[11] a UV detector[12] with the wavelength set at 280 nm, and a potentiometric recorder.[13]

Synthesis

Monopropionyldyphylline (II): Dyphylline[14] 0.1 mole (25.4 g) was dissolved in approximately 120 ml of anhydrous pyridine[15] by heating until the solution was clear. This solution was then cooled in an ice bath and 0.1 mole (9.25 g) of propionyl chloride[16] was slowly added into the cold solution of dyphylline. The mixture was allowed to stir at room temperature overnight. The next day, pyridine hydrochloride was removed by suction filtration. The filtrate was evaporated in vacuo using a rotatory evaporator[17] to produce a yellow oily substance. Diethyl ether[18] was then added and the mixture shaken vigorously. The monopropionyl ester derivative of dyphylline appeared as a white precipitate which was collected by suction filtration, washed with 3-5 ml of distilled water, and recrystallized twice from 95% ethanol.[19] TLC of a solution of the product in chloroform showed only one spot. The melting point was determined and the compound was characterized by IR, PMR and mass spectrometry.

Dipropionyl dyphylline (III): Same as for II, except the amount of propionyl chloride was increased to 0.22 mole (20.36 g). After the pyridine hydrochloride was removed by suction filtration, the filtrate was evaporated in vacuo to produce a dry dark brown solid instead of an oily substance. This dark brown solid was then purified by crystallizing twice from 95% ethanol.

Monoisobutyryl dyphylline (IV): The procedure was similar to the synthesis of II except 0.1 mole (10.7 g) of isobutyryl chloride[20] was used in place of propionyl chloride and was dissolved in approximately 40 ml of anhydrous pyridine before mixing. The solutions were mixed at room temperature instead of cooling in the ice bath.

Diisobutyryl dyphylline (V): The procedure was the same as the synthesis of IV except the amount of isobutyryl chloride was increased to approximately 0.22 mole (23.4 g) and the order of mixing was reversed, i.e., dyphylline solution was added into isobutyryl chloride solution.

Monopivaloyl dyphylline (VI): The procedure was the same as the synthesis of IV except 0.1 mole (12.0 g) of pivaloyl chloride[21] was used instead of isobutyryl chloride.

Dipivaloyl dyphylline (VII): The procedure was the same as for V except 0.22 mole (26.5 g) of pivaloyl chloride was used in place of isobutyryl chloride.

Mono-p-chlorobenzoyl dyphylline (VIII): A solution of p-chlorobenzoyl chloride[22] of 0.1 mole (17.5 g) in 30 ml of anhydrous pyridine was added into a clear solution of 0.1 mole (25.4 g) of dyphylline dissolved in about 120 ml of pyridine. The mixture was allowed to stir overnight at room temperature. After 24 hours a white precipitate appeared which was a mixture of pyridine hydrochloride and the product. The mixture was collected by filtration and washed several times with 2-4 ml of distilled water to remove pyridine hydrochloride.

The product became hard and sticky, was allowed to dry at room temperature, and was recrystallized from 95% ethanol. One gram of the product requires 50 ml or more of 95% ethanol for complete dissolution. Upon cooling, a very light precipitate formed. The precipitate was collected, dried, dissolved in chloroform and TLC showed only one spot. The structure was characterized using IR, PMR and mass spectrometry.

Di-p-chlorobenzoyl dyphylline (IX): The procedure was the same as for VIII but the solution of dyphylline 0.1 mole (25.4 g) was added into p-chlorobenzoyl chloride 0.25 mole (43.75 g) previously dissolved in about 40 ml of pyridine.

Solvent programming HPLC analysis of dyphylline esters

A single mobile phase could not be used satisfactorily for separation of dyphylline from its mono- and di- ester derivatives (II-IX) because of their marked differences in polarities. Appropriate solvent programming conditions for separation and quantitation of dyphylline and all of the mono- and di-esters synthesized here were developed. For pump A, the mobile phase was 10% acetonitrile in distilled water (v/v) and for pump B the mobile phase was 60% acetonitrile in distilled water (v/v). The initial condition was 0% B and the final condition was 100% B. The programming time was 3 minutes using a straight line curve. The solvent flow rate was 2 ml per minute.

Secondary Monoesters

Synthesis of the secondary monopivaloyl dyphylline: Triphenylmethy (trityl) chloride[23] was used to protect the primary hydroxyl function of dyphylline since tritylation was reported to be an especially useful method for the selective blocking of primary hydroxyl groups in polyols (18). Trityl chloride 0.1 mole (28 g) was dissolved in approximately 100 ml of pyridine, mixed well with a clear solution of 0.1 mole of dyphylline in pyridine, and heated at 80°-100°C for one hour. Then 15 ml (slightly in excess of 0.1 mole) of pivaloyl chloride in 40 ml of pyridine was slowly added into the previous mixture of dyphylline and trityl chloride, stirred at room temperature overnight, filtered and the precipitate washed several times with distilled water to remove pyridine chloride and the remaining solid dried at room temperature overnight. Glacial acetic acid was then added and heated until all the solid was completely dissolved, stirred at 80°-90°C for 48 hours to assure complete removement of the trityl protecting group, and evaporated in vacuo to remove the glacial acetic acid. When the mixture became gummy ether was slowly added and the mixture was shaken vigorously until a white precipitate formed. This white precipitate was recrystallized in 95% ethanol three times, had the same melting point, and gave the same PMR spectrum as the primary ester, monopivaloyl dyphylline (VI). The retention times on

HPLC were also identical.

It has also been found that there was always a peak in the HPLC tracings prior to the appearance of the primary monoester peak when the primary monoester was dissolved in aqueous solvent. An excess of the primary monopropionyl dyphylline was placed in approximately 2 ml of distilled water to obtain a saturated solution, and allowed to stand at room temperature for at least 4 days to assure equilibrium between the unknown and the primary monopropionyl ester. The undissolved solid was removed by filtration, and the clear filtrate was injected into the HPLC. The unknown compound and the primary monopropionyl ester were each collected from the outlet of the HPLC into two separate test tubes containing 10 ml of spectral grade chloroform. The contents of each test tube were immediately mixed thoroughly using a vortex mixer in order to allow partitioning of the compound from the mobile phase (which contained 80% water) into the chloroform phase. As soon as possible after mixing, both test tubes were placed in an acetone-dry ice bath to freeze the water present. This cooling was also to minimize any interconversion between the unknown and the primary monoester. The cold chloroform phase was collected and dried over approximately 2-3 g of anhydrous sodium sulfate. After vortexing well, the sodium sulfate was discarded. The contents in each test tube were concentrated by evaporation with a nitrogen stream until the volume was about one ml. The unknown

sample and the primary monopropionyl sample were injected into the HPLC to assure the purity of each compound and the mass spectra of both the unknown and the primary monopropionyl dyphylline were then obtained.

RESULTS AND DISCUSSIONS

Scheme I illustrates the general pathway used to prepare the hydroxy esters of dyphylline. In general, the order of mixing was reversed when the desired compounds were diesters compared to those of monoesters. However, some minor changes were needed for preparation of each compound. Synthesis of the propionyl esters required reaction in the cold since these reactions were quite exothermic. For p-chlorobenzoyl esters, the products did not remain dissolved in the reaction solvent (pyridine) as did other esters of dyphylline but, rather, formed a white precipitate mixed with the by-product, pyridine hydrochloride. Therefore, p-chlorobenzoyl esters could not be separated from pyridine hydrochloride by suction filtration but were separated by washing with several ml of water since pyridine hydrochloride was very water soluble but the products were not.

Table II summarizes some of the physical characteristics of dyphylline and its hydroxy esters. The percent yields were much lower for the propionyl esters when compared to others. This may be

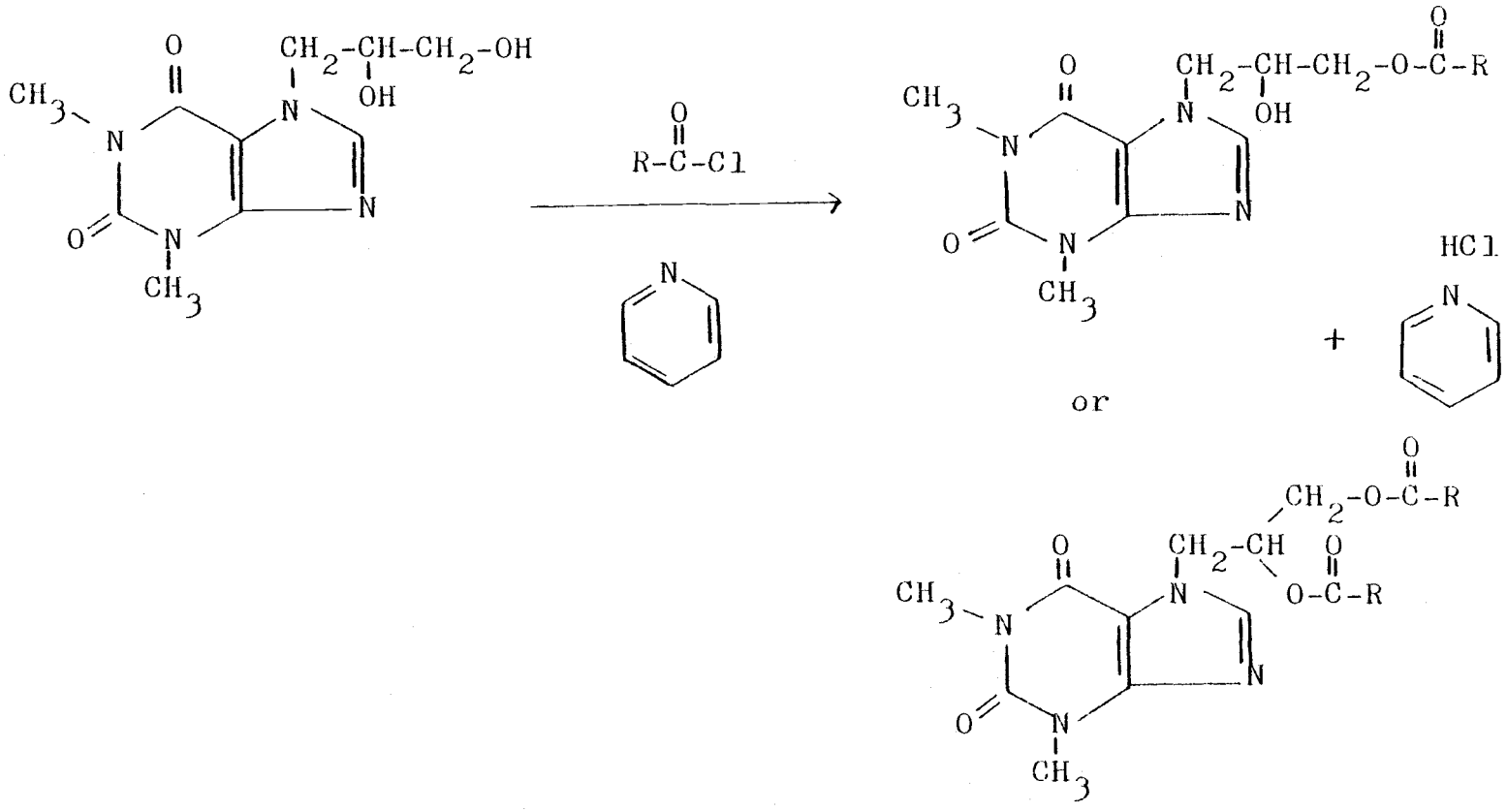

Scheme I. Chemical pathway for the synthesis of dyphylline esters

Table II. Summary of Some Physical Characteristics of Dyphylline and its Hydroxy Esters.

Compound	Molecular formulae	Molecular weight* (Error = 0.010)	Uncorrected melting point (C)	TLC** R_f value	% Yield***
I	$C_{10}H_{14}N_4O_4$	254.102	160-165	0.27	--
II	$C_{13}H_{18}N_4O_5$	310.128	137-138	0.63	28.06
III	$C_{16}H_{22}N_4O_6$	366.154	116-118	0.84	38.96
IV	$C_{14}H_{20}N_4O_5$	324.143	80-85	0.69	89.14
V	$C_{18}H_{26}N_4O_6$	394.185	106-108	0.84	67.89
VI	$C_{15}H_{22}N_4O_5$	338.159	142-144	0.74	60.02
VII	$C_{20}H_{30}N_4O_6$	422.216	122-114	0.87	81.96
VIII	$C_{17}H_{17}N_4O_5Cl$	392.089	189-191	0.67	48.15
IX	$C_{24}H_{20}N_4O_6Cl_2$	530.076	156-157	0.93	89.10

*Molecular weights of compounds II-IX were confirmed by high resolution mass spectra performed in a private laboratory.

**Silica gel PF-254 + 366, E. Merck Ag, Darnstadt (Germany). The mobile phase was n-butanol-chloroform (1:1)

***%yield after recrystallization.

due to the effect of the heat evolved when dyphylline and propionyl chloride solution were mixed since the mixture turned brown which might indicate production of undesirable by-products. Another reason might be their higher solubility in water as the products were washed with several ml of distilled water to remove any dyphylline or other polar impurities which might contaminate the products.

Infrared Spectrometry: The infrared spectra of dyphylline and its mono- and di-ester derivatives using mineral oil as the mulling agent are shown in Figures 2-10. The infrared spectra of ester derivatives exhibit carbonyl absorption around 1700 cm^{-1}. The CO-absorption of the purine ring appears as two bands, the first between 1720 and 1690 cm^{-1} and the second between 1670 and 1640 cm^{-1} (14, 15). Thus, there were peaks in the 1690-1720 region for the spectrum of dyphylline and its ester derivatives. However, the spectra of the esters showed more intensity and more vibrational peaks in this region than the spectra of dyphylline. The diesters showed even higher intensity and more vibrational peaks than the monoesters. The two —OH groups of the aliphatic alcohol side chain of dyphylline appear as stretching absorption at about 3325 and 3450 cm^{-1}. Only one —OH peak appeared for the monoester derivatives. This peak was much broader and shifted from 3325 cm^{-1} to about 3200 cm^{-1}. For the diesters, both —OH peaks disappeared as would be expected. Mono-isobutyryl dyphylline was the only mono-ester which showed a broad

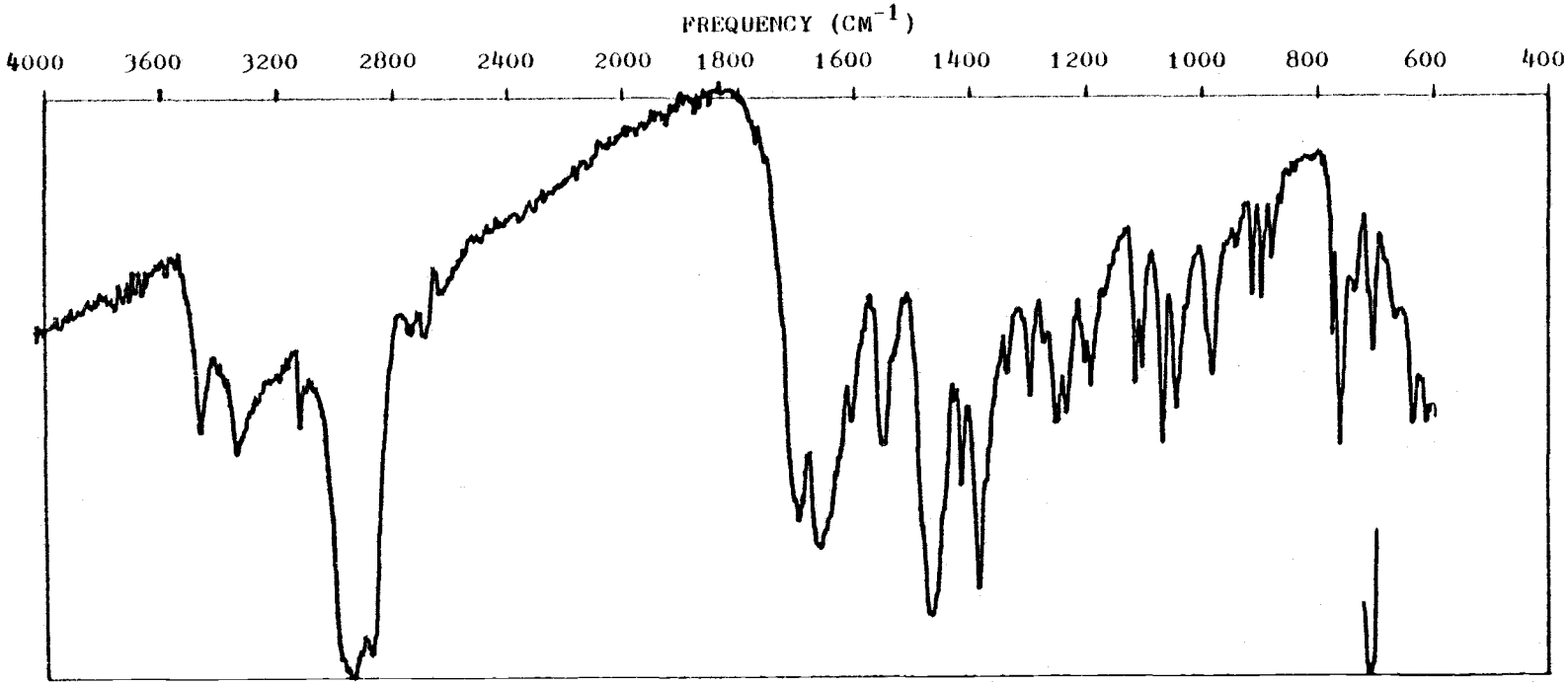

Figure 2. Infrared Spectrum of Dyphylline

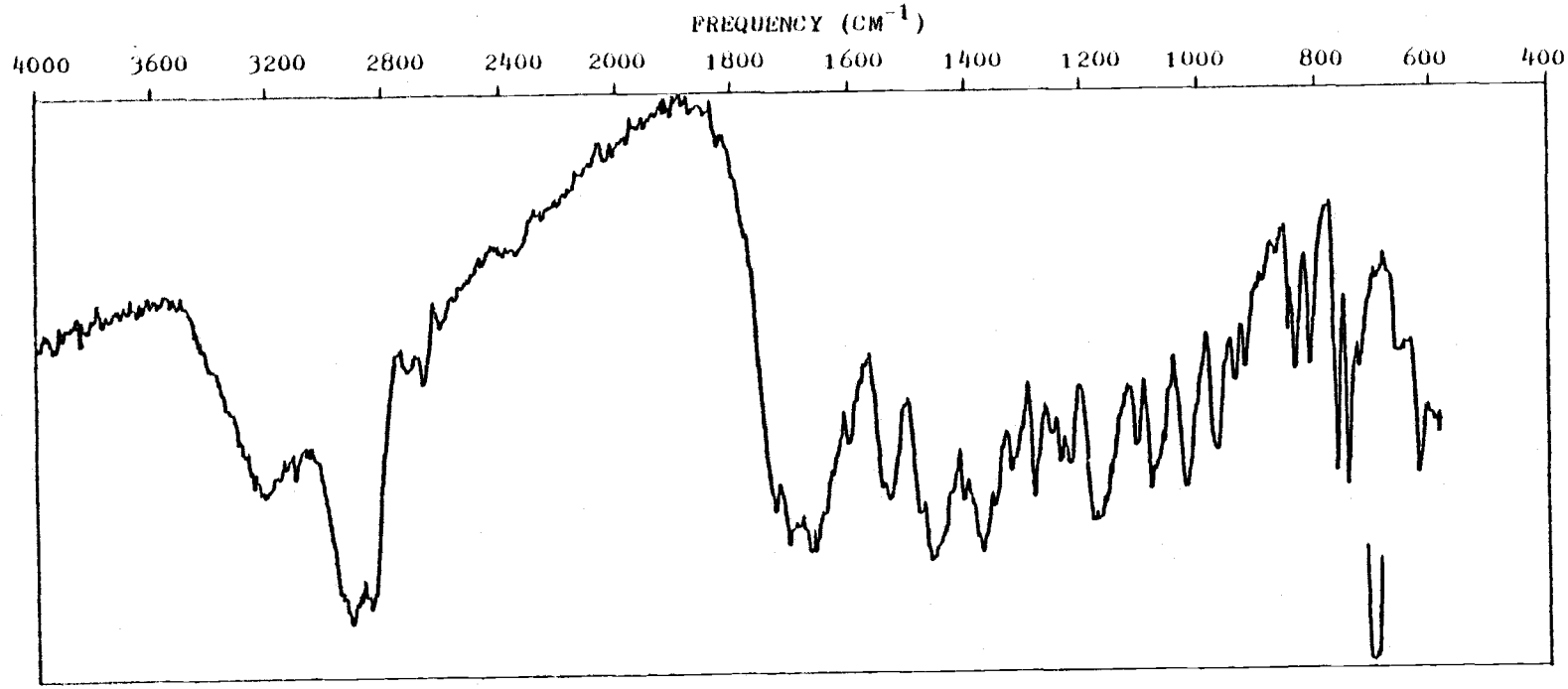

Figure 3. Infrared Spectrum of Primary Monopropionyl Dyphylline

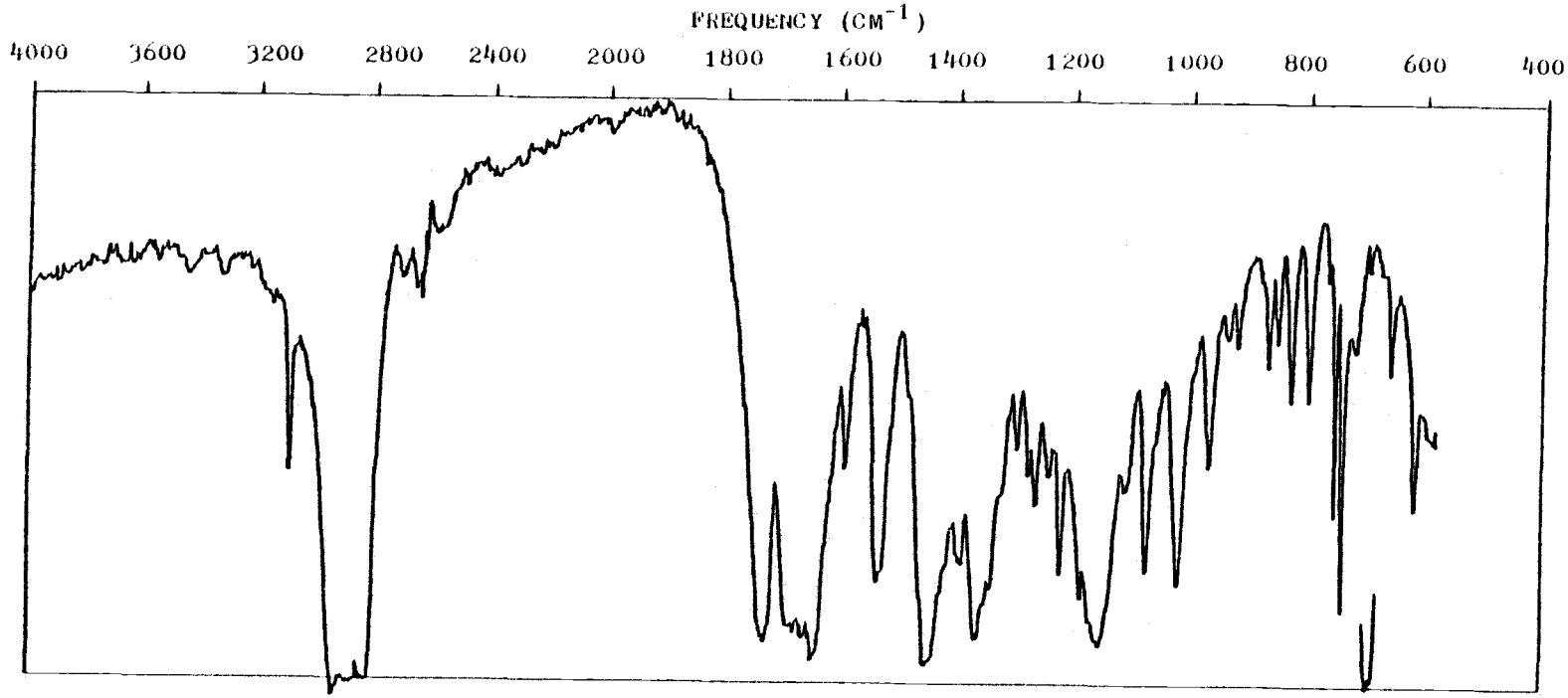

Figure 4. Infrared Spectrum of Dipropionyl Dyphylline

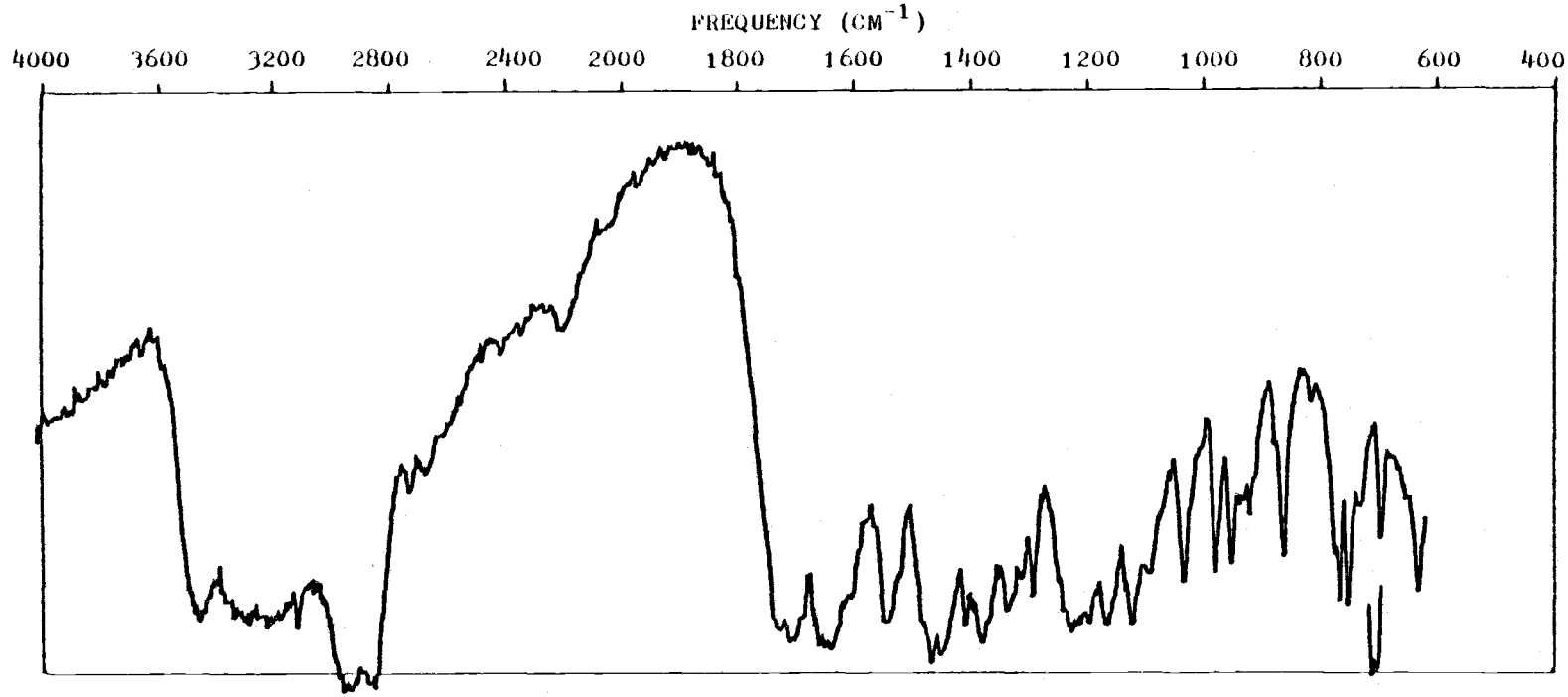

Figure 5. Infrared Spectrum of Primary Mono-isobutyryl Dyphylline

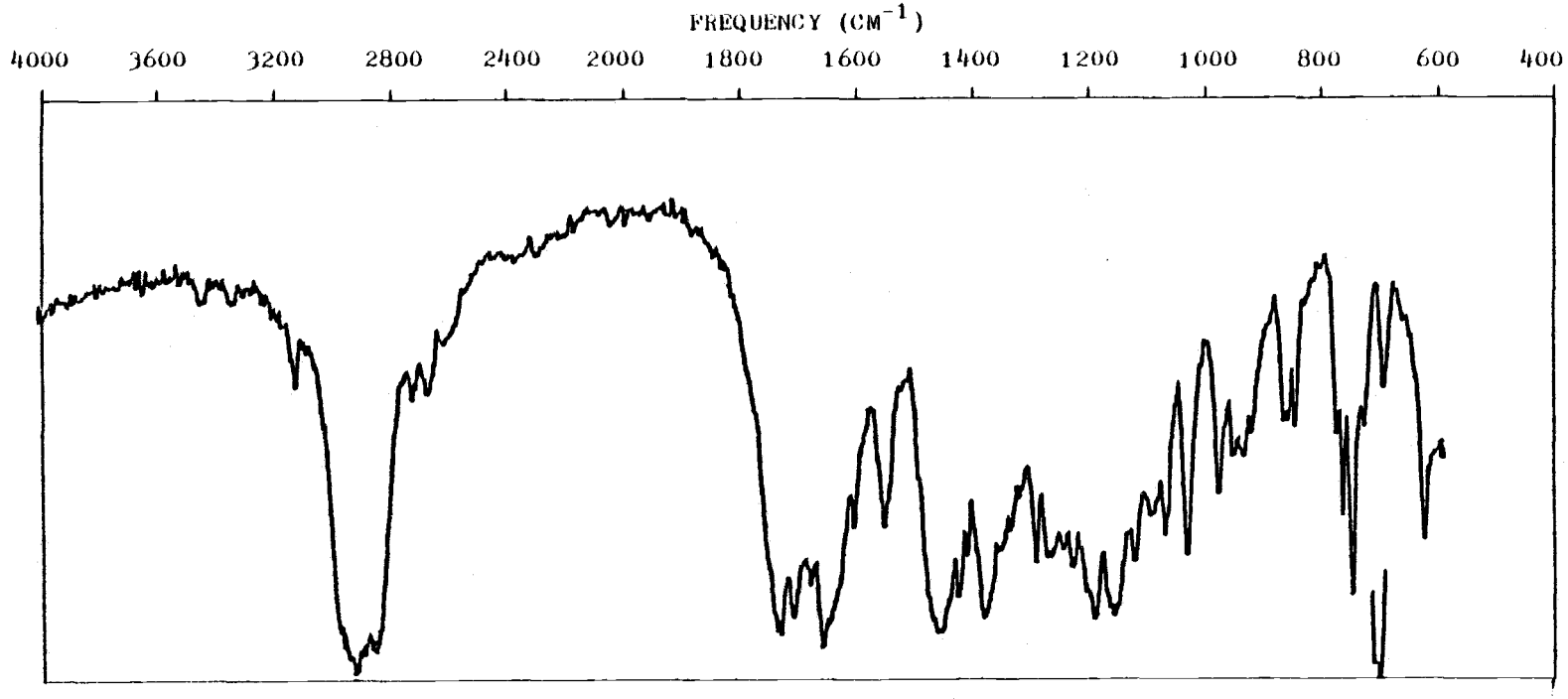

Figure 6. Infrared Spectrum of Di-isobutyryl Dyphylline

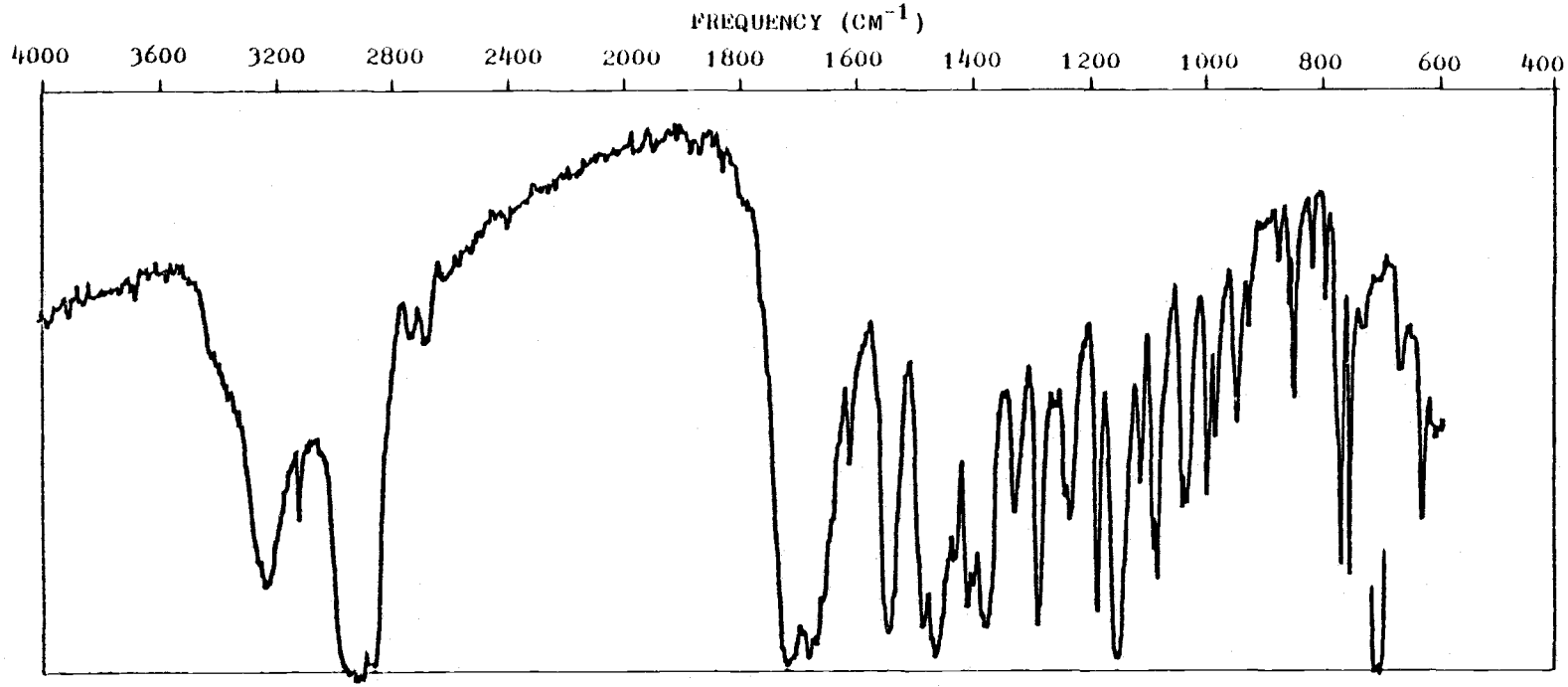

Figure 7. Infrared Spectrum of Primary Monopivaloyl Dyphylline

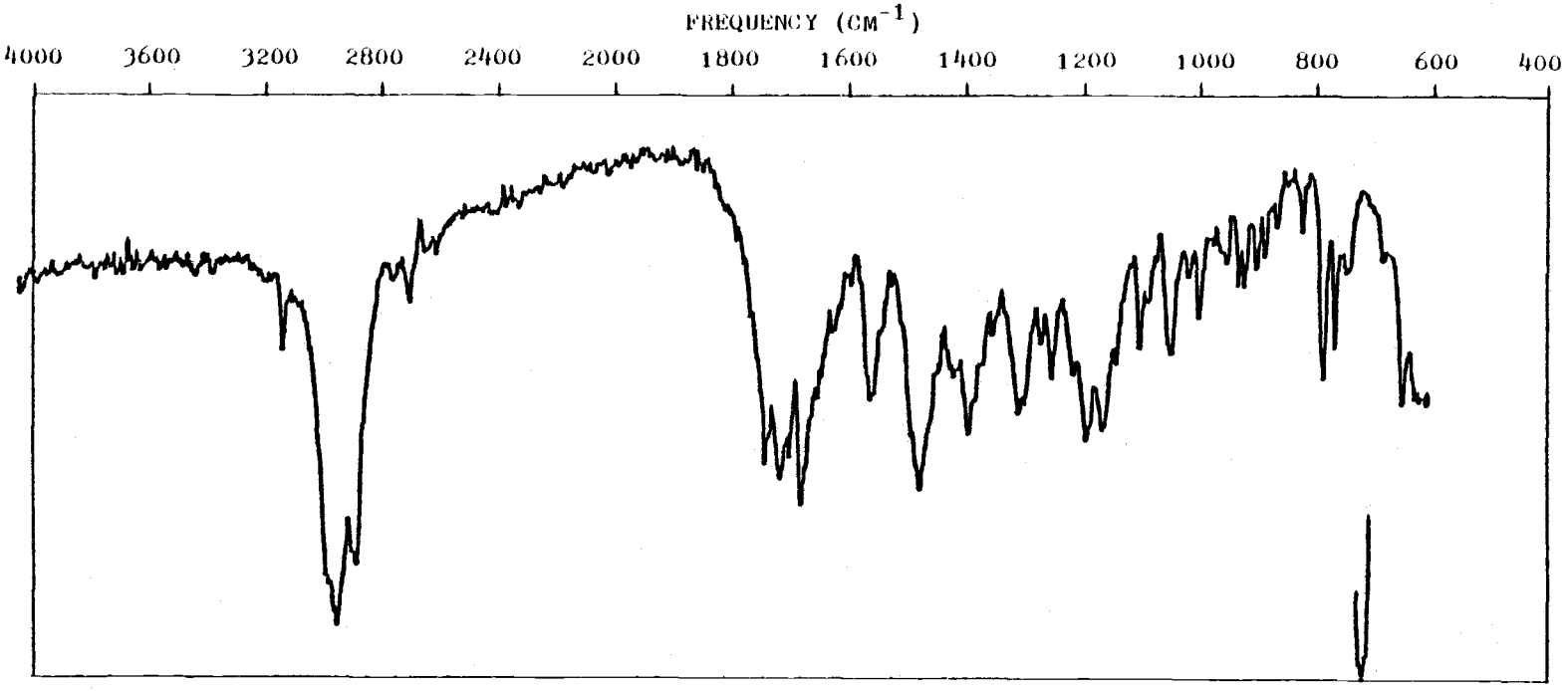

Figure 8. Infrared Spectrum of Dipivaloyl Dyphylline

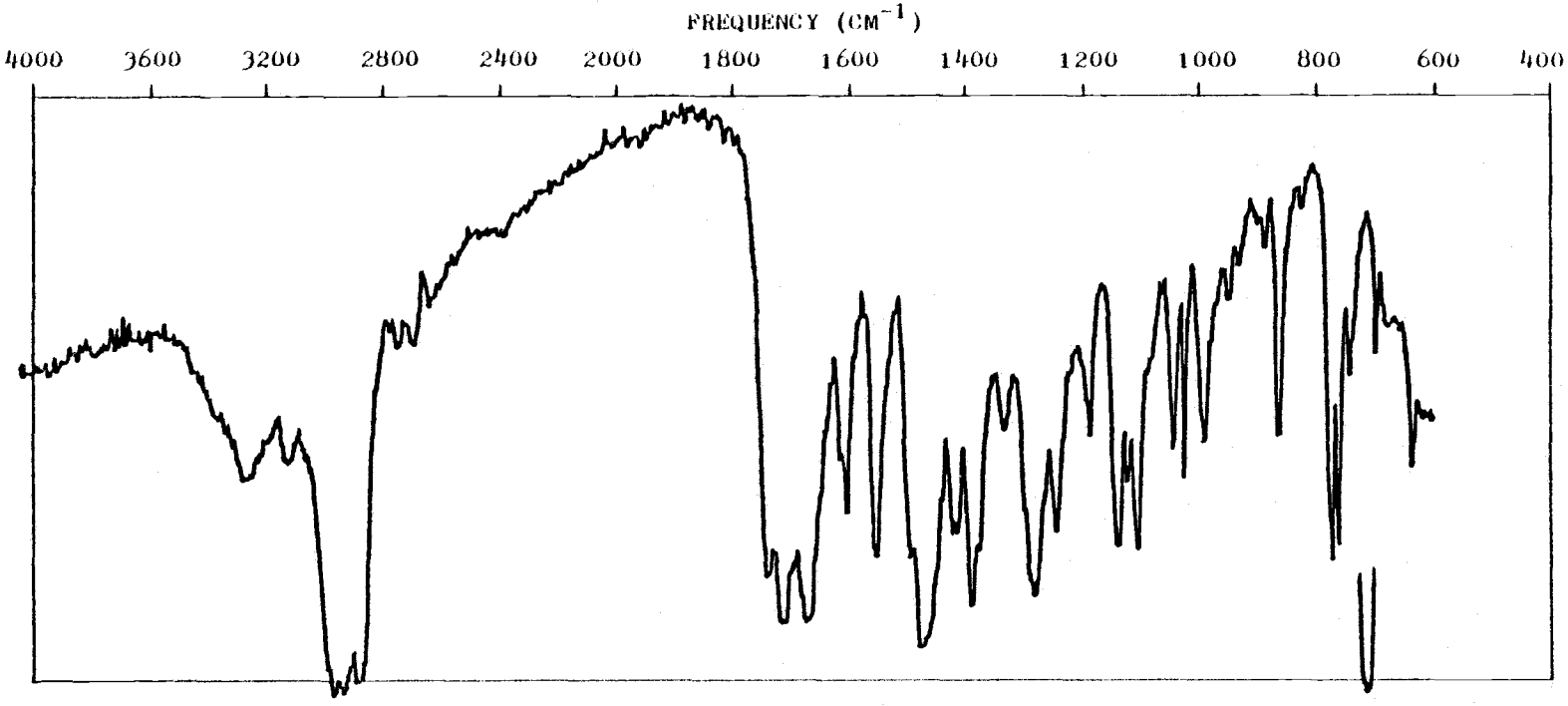

Figure 9. Infrared Spectrum of Primary Mono-p-Cl-benzoyl Dyphylline

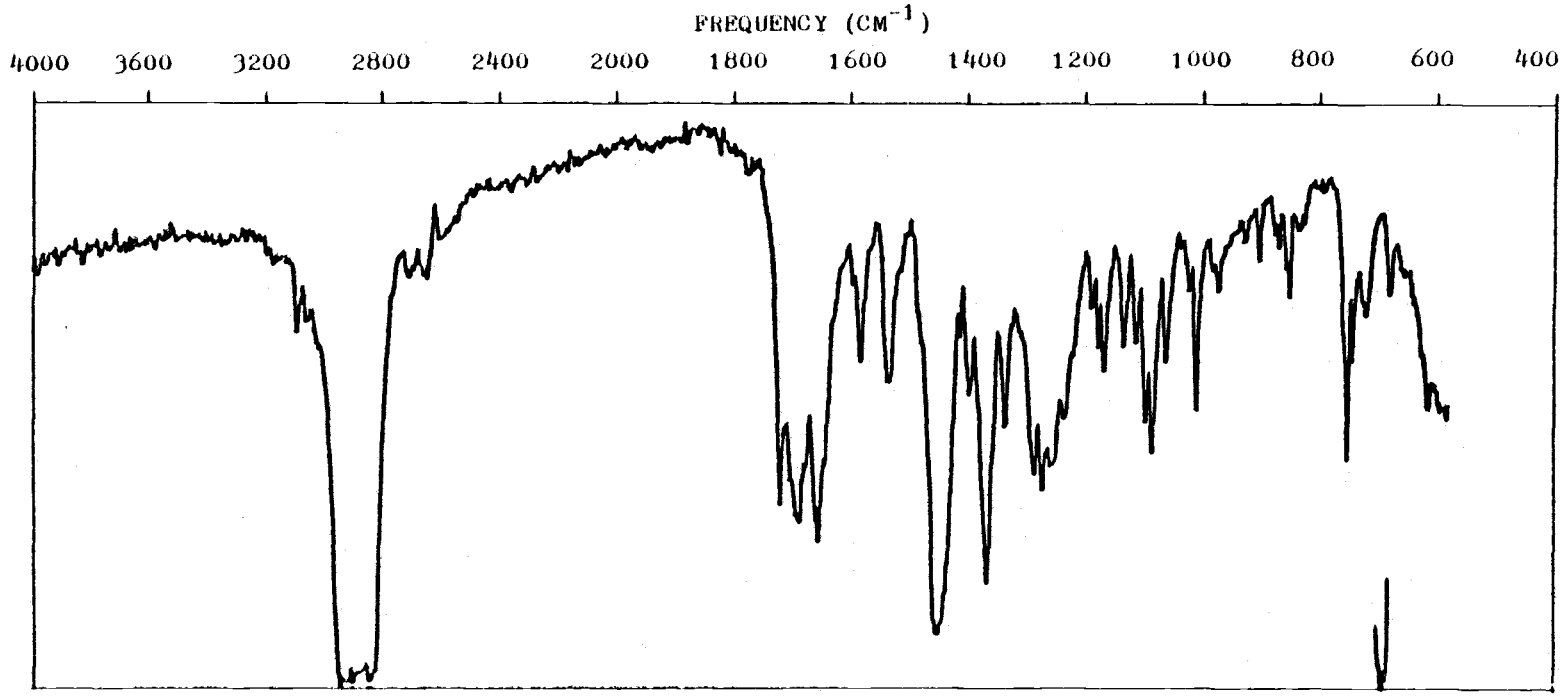

Figure 10. Infrared Spectrum of Di-p-Cl-benzoyl Dyphylline

extra peak in the OH group region. This peak remained even after drying the compound at 50°C under high vacuum for 3 hours. Its cause is currently unknown.

Mass spectrometry: The molecular ion peaks of dyphylline and all of the mono- and di- ester derivatives synthesized here were observed as distinct peaks. The dyphylline molecular ion peak produced from its ester derivatives was small. Only small peaks appeared for the molecular ion of the appropriate monoester in the mass spectrum of the corresponding diester. The $M-H_2O$ ion peaks for all monoesters were small but present. An ion peak at m/e 223 was present and could be produced through β-fission of the aliphatic alcohol group (eliminated - CH_2—OH) of the molecular ion of dyphylline. This ion peak was usually higher for the monoesters than for the diesters and was the parent peak of the dyphylline spectrum. The fragment ions at m/e 194 and 180 might be ionized caffeine ($C_8H_{10}O_2N_4$) and theophylline or theobromine ($C_7H_8O_2N_4$) respectively (figure 11). The diesters provided much lower peaks at m/e 194 compared to the monoesters. The bond may have more readily broken between the gamma carbon and the nitrogen atom when the secondary —OH was also esterified, which resulted in a much higher

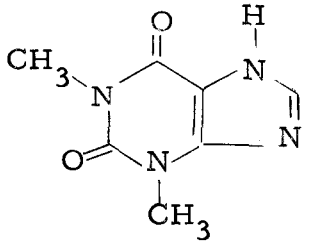

Theophylline
m/e 180

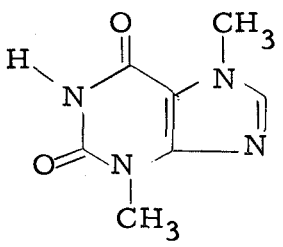

Theobromine
m/e 180

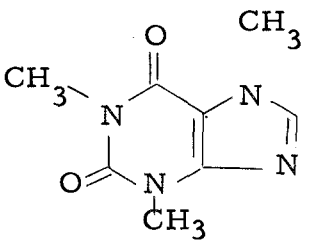

Caffeine
m/e 194

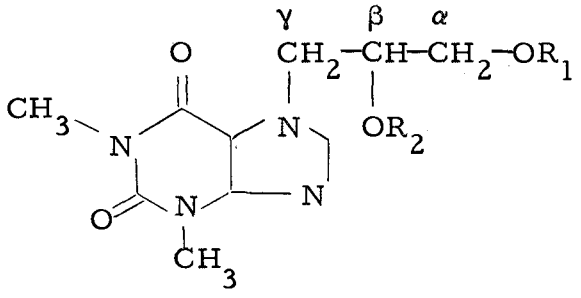

Dyphylline ester
derivatives

Figure 11. Structures of theophylline, theobromine, caffiene and dyphylline ester derivatives.

m/e 180 peak for the diesters while the primary monoesters being esterified only at the primary —OH underwent easier bond cleavage between the beta and gamma carbon which resulted in a higher m/e 194 peak. These m/e 194 and 180 fragment ions could then undergo further fragmentation which resembled the decomposition of caffeine and theophylline or theobromine respectively. Some of the major peaks in the mass spectra of these compounds besides their molecular ion peaks were m/e 53-55, m/e 67-68, m/e 81-82, m/e 94-95, m/e 105, m/e 123, m/e 136-137, m/e 151 and m/e 165-166 (16). The

fragment ions of the esters exhibited the above peaks as well as abundant peaks at m/e 57, m/e 71, m/e 85 and m/e 139 for the propionyl ion, iso-butyryl ion, pivaloyl ion and p-Cl-benzoyl ion respectively and these ion peaks were much higher for the diesters than the monoesters as expected. The fragment ion peaks at m/e 131 and m/e 187 of the mono- and di- propionyl esters, m/e 145 and m/e 215 of the mono- and di- isobutyryl esters, m/e 159 and m/e 243 of the mono- and di- pivaloyl esters, m/e 213 and m/e 351 of the mono- and di-p-Cl-benzoyl esters were the m/e fragment ions of the entire side chains which confirms the higher preference of the dyphylline ester derivatives for mass spectrometer cleavage at the bond between the gamma carbon and the nitrogen compared to the breaking of the ester bond to produce dyphylline. If the ester derivatives were first cleaved between the beta and gamma carbons, further breaking of the side chain fragments occurred so fast at the ester bond that no peak could be seen for the m/e of the complete side chain fragment. The mass spectra of dyphylline and the mono- and di- esters synthesized here are shown in detail in figures 12-20.

PMR Spectra: The PMR data for various hydroxy esters of dyphylline are summarized in Table III and shown in detail in figures 21-28. The hydroxy protons of the mono-ester compounds appeared as expected. The hydroxy peaks on the PMR spectra for all of the monoesters appeared as a broad singlet somewhere close to 3.8 when

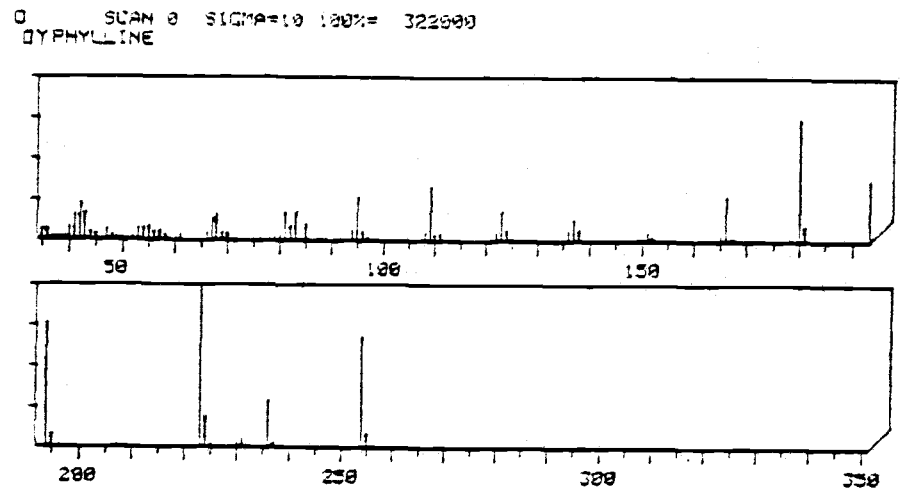

55	7.4	66	4.9	97	1.3	130	0.1
56	6.7	67	13.7	98	0.4	131	0.5
57	2.4	68	15.2			132	0.1
58		69		100	0.3	133	0.3
59		70	4.6	101	0.1	134	1.0
60		71	0.7			135	2.4
61	15.6	72	0.5	104	0.1	136	0.4
62	23.9	73	0.7	105	0.2	137	13.4
63	16.5	74	0.1	106	0.4	138	0.9
64	5.5	75	0.5	107	1.2	139	1.0
65	3.9			108	5.5	140	0.5
66	7.4	77	0.9	109	30.3	141	0.5
67	3.5	78	0.7	110	4.3		
68	2.1	79	1.3	111	5.1	143	0.1
69	1.2	80	13.4	112	0.7	144	0.2
70		81	17.7	113	0.2	145	0.3
71		82	9.5	114	0.2		
72		83	17.6	115	0.1	147	0.4
73		84	1.2			148	0.5
74		85	18.3	117	0.5	149	1.3
75		86	0.2	118	0.5	150	1.4
76		87	1.9	119	0.5	151	5.9
77				120	1.0	152	2.8
78		89	0.1	121	1.3	153	0.5
79				122	0.2	154	0.1
80		91	0.4	123	17.8	155	0.1
81		92	0.3	124	6.5		
82		93	1.5	125	1.1	159	0.6
83	0.2	94	6.7	126	0.3	160	0.2
		95	26.7	127	0.3	161	0.2
85	1.0	96	5.5			162	0.6

163	0.3			227	0.3		
164	0.3	200	0.1	228	0.9	287	0.1
165	3.5	201	0.3	229	1.6		
166	27.9	202	0.7	230	3.3	290	0.7
167	2.2	203	0.3	231	5.8	291	0.4
168	0.7	204	0.1	232	1.0		
169	0.5	205	0.2			310	1.4
170	0.1	206	0.9	234	0.1	311	0.1
		207	2.5	235	0.1		
177	0.3	208	1.3	236	23.9	390	0.2
178	0.6	209	0.3	237	3.7		
				238	0.5	392	0.1
180	74.9	215	0.3				
181	9.2	216	1.5	246	0.1	421	0.1
182	0.3	217	0.3			422	0.1
		218	0.3	252	0.6	423	0.2
190	0.1	219	1.1			424	0.3
191	0.5	220	1.4	254	67.3		
		221	0.6	255	8.7	426	0.3
193	38.1			256	1.3		
194	76.9	223	100.0	257	0.2	428	0.2
195	8.3	224	19.9				
196	1.3	225	2.2	265	0.1	496	0.1
197	0.4	226	0.6				

Figure 12. Mass Spectrum of Dyphylline

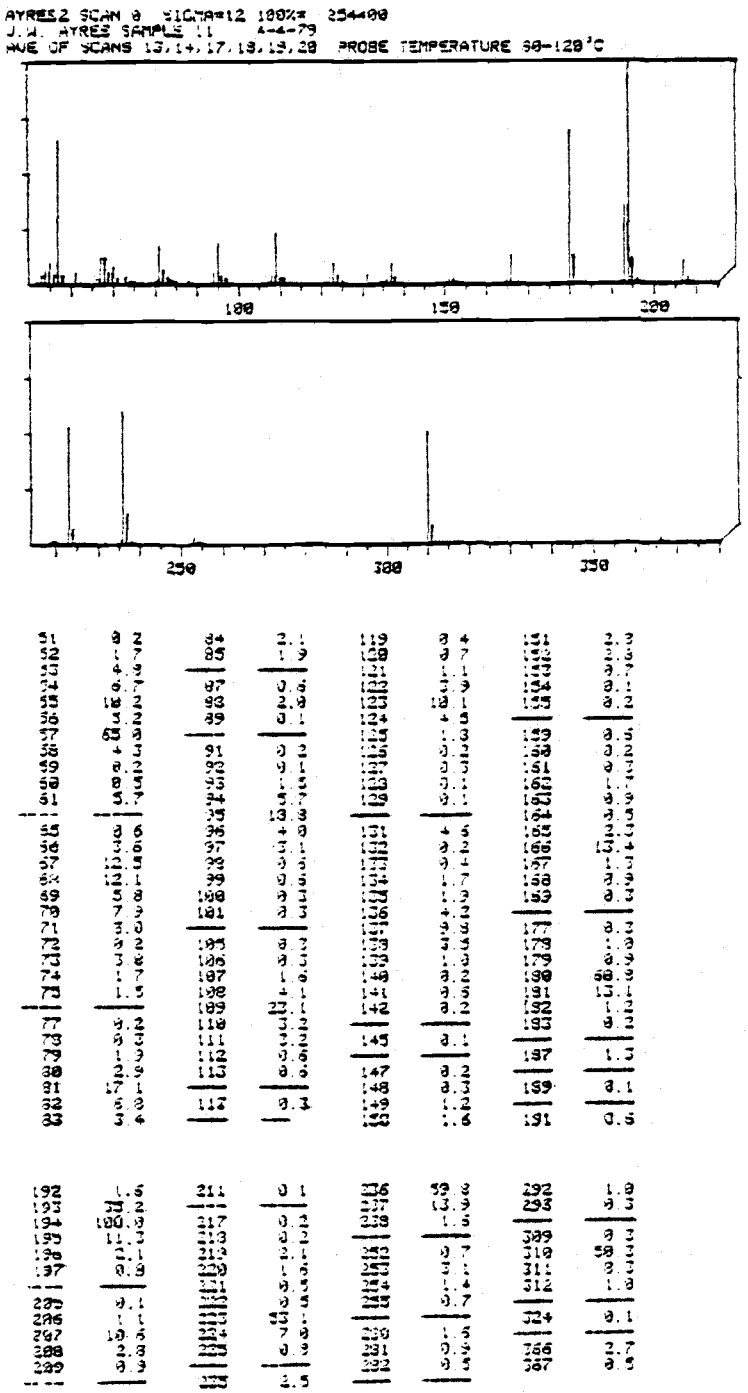

Figure 13. Mass Spectrum of Primary Monopropionyl Dyphylline

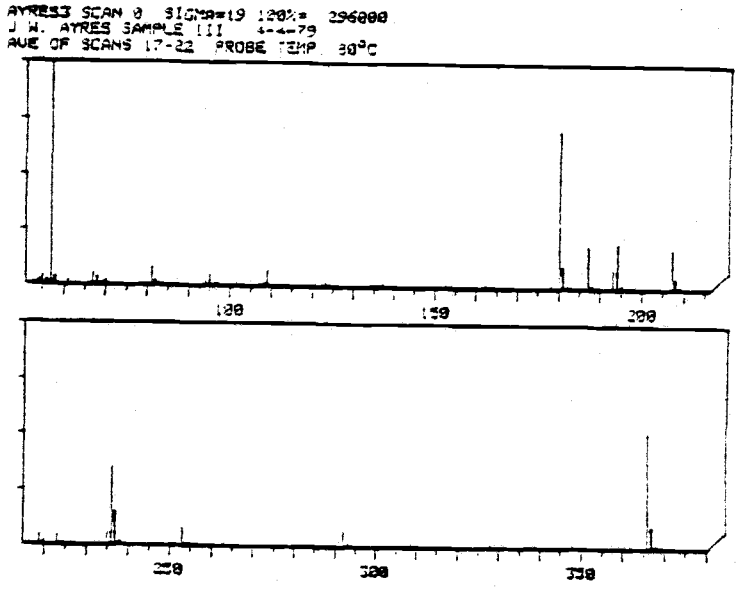

92	0.4	92	0.4	151	0.9	218	0.9
93	1.5	93	0.3	152	0.9	219	4.8
94	2.6	94	2.9			220	2.8
95	4.5	95	0.2	162	1.8	221	0.7
96	2.5	96	1.2	163	0.7	222	0.1
97	100.0	97	0.7	164	0.3	223	4.5
98	4.2			165	0.1	224	1.8
99	0.1	106	0.1	166	1.8		
100	0.2	107	1.9			234	0.5
101	2.5	108	1.3	178	0.6	235	5.8
		109	0.9	179	0.6	236	15.1
116	1.4	110	0.9	180	0.2	237	15.1
117	0.4	111	0.6	181	0.6	238	1.7
118	0.7	112	0.2	182	0.2	239	0.1
119	1.6	113	1.1				
120	2.5			197	18.9	252	0.7
121	0.5	120	0.2	198	1.8	253	7.9
		121	0.1	199	0.1	254	1.1
122	1.2	122	1.6	200	0.1	255	0.7
		123	2.6	201	0.7		
123	0.3	124	1.1	202	1.8	280	0.7
		125	0.2	203	0.8	281	0.1
129	0.3			204	20.1		
130	1.3	134	1.3	205	2.2	292	7.2
131	0.8	135	1.2	206	0.5	293	2.8
132	2.5	136	1.3	207	0.2	294	0.2
133	1.8	137	1.4				
134	0.3	138	0.6	286	0.3	309	1.1
				287	17.8	310	1.8
88	1.1	149	0.2	288	4.5		
		150	0.3	289	0.8		
363	0.2	366	31.4	367	9.6	368	1.3

Figure 14. Mass Spectrum of Dipropionyl Dyphylline

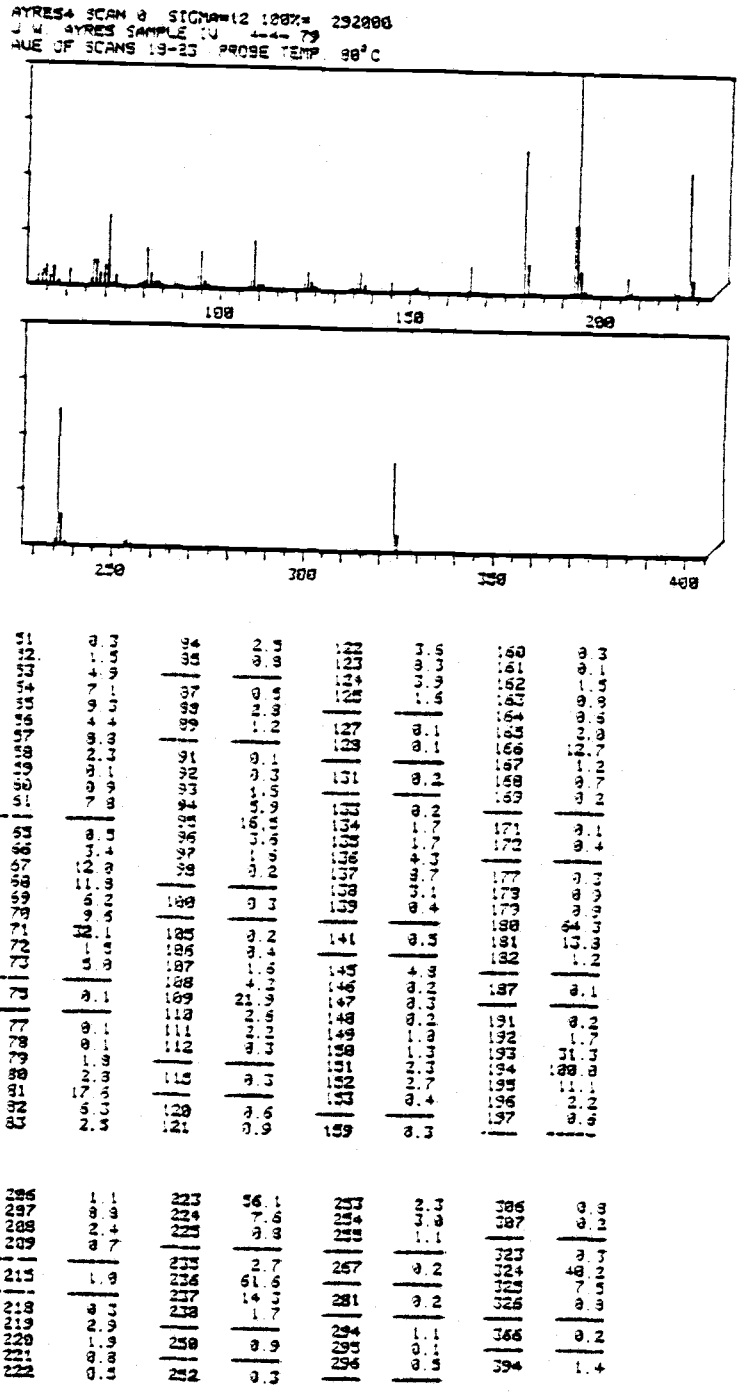

Figure 15. Mass Spectrum of Primary Mono-isobutyryl Dyphylline

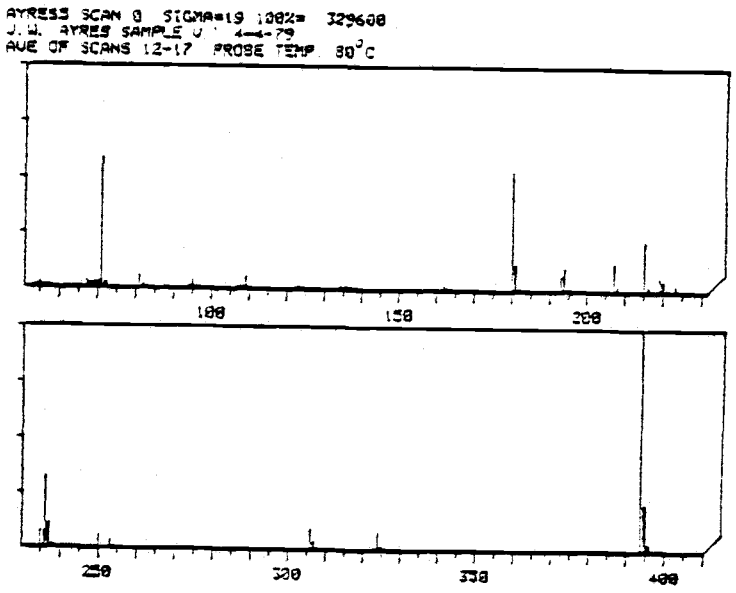

52	0.1	97	0.1	149	0.1	205	0.1
53	1.0			150	0.3	206	0.5
54	1.7	106	0.2	151	0.5	207	13.1
55	2.6	107	2.1	152	0.7	208	2.0
56	1.2	108	1.7			209	0.3
57	1.5	109	5.9	159	0.1		
58	0.4	110	0.8	160	0.1	214	0.1
				161	0.1	215	22.5
61	0.1	118	0.1	162	2.1	216	2.5
				163	0.8	217	0.1
66	0.3	120	0.2	164	0.2	218	0.9
67	1.0	121	0.2	165	0.5	219	5.5
68	2.4	122	1.4	166	0.7	220	4.4
69	2.8	123	1.8			221	1.2
70	3.1	124	0.9	168	0.1	222	0.3
71	58.5	125	0.2			223	3.2
72	2.2			170	0.2	224	0.4
73	0.5	127	0.4			225	0.1
				178	0.1		
79	0.5	133	0.2	179	0.3	234	0.2
80	0.9	134	2.2	180	3.7	235	7.8
81	5.5	135	1.2	181	12.1	236	12.2
82	1.9	136	2.2	182	1.8	237	10.3
83	0.6	137	1.8			238	1.4
84	0.2	138	0.4	192	0.9		
				193	5.9	248	5.7
92	0.1	142	0.1	194	10.7	251	0.9
93	0.6			195	1.0		
94	2.2	145	0.2			263	1.8
95	3.7			283	0.4	264	0.9
96	0.8	148	0.1	284	0.2	265	0.6
253	0.1	294	0.7	322	1.6		
256	0.6	305	0.2	324	7.9	392	0.2
257	0.7	306	0.8	325	1.4	393	0.4
258	0.1	307	3.5			394	100.0
		308	0.6	331	0.1	395	21.3
279	0.1	309	0.7			396	3.2
				379	0.5	397	0.2

Figure 16. Mass Spectrum of Di-isobutyryl Dyphylline

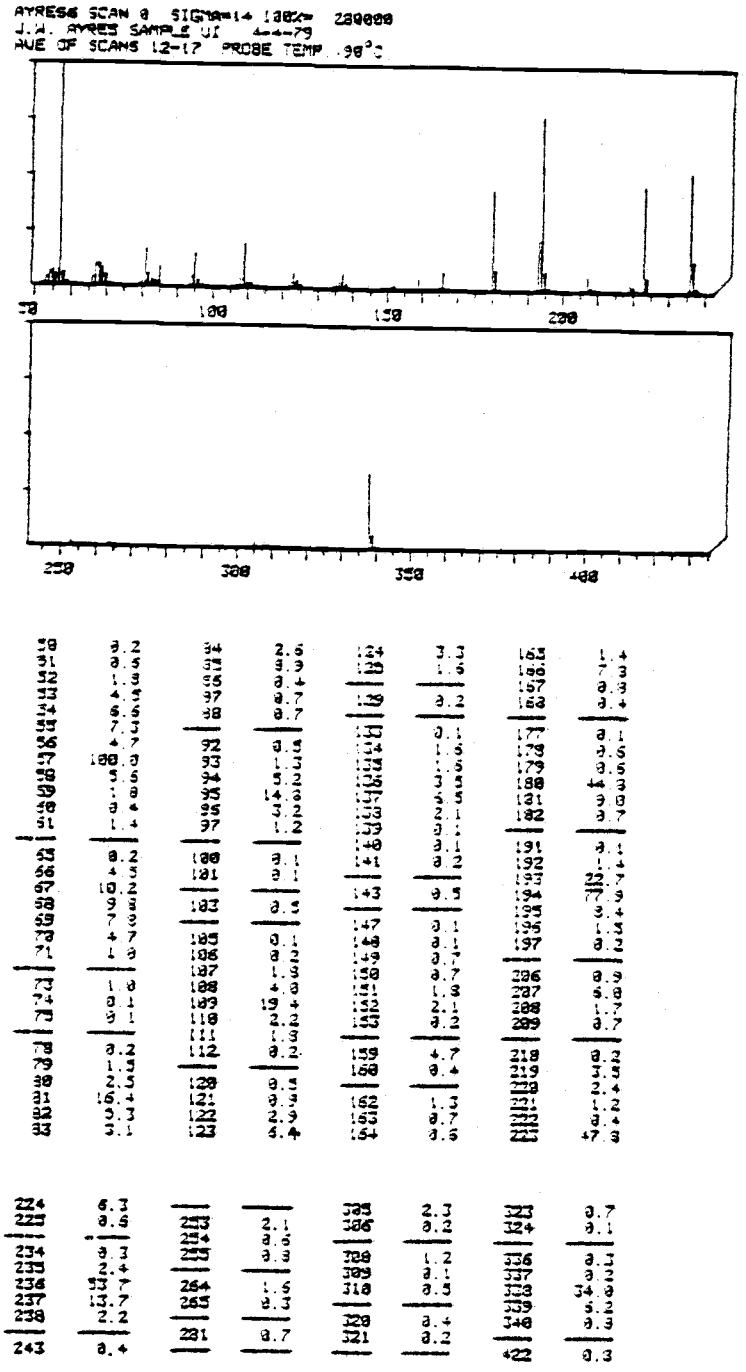

Figure 17. Mass Spectrum of Primary Monopivaloyl Dyphylline

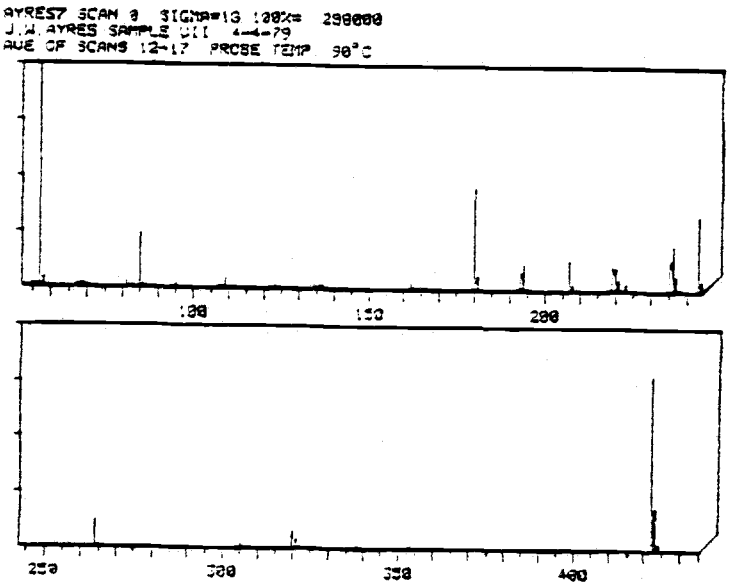

53	3.7	106	0.1	162	3.1	219	10.3
54	1.8	107	1.8	163	1.9	220	18.8
55	2.5	108	1.4	164	0.3	221	4.9
56	1.4	109	4.3	165	0.4	222	0.7
57	100.0	110	0.6	166	1.0	223	3.4
58	4.3	111	0.1	167	0.1	224	0.3
59	0.1						
		120	0.2	173	0.4	227	0.9
66	0.6	121	0.1	179	0.3		
67	2.2	122	1.3	180	45.4	234	0.2
68	1.5	123	1.7	181	6.1	235	14.1
69	2.6	124	0.0	182	0.6	236	20.0
70	1.0					237	6.4
		130	0.1	184	0.2	238	0.8
79	0.2	134	2.6				
80	0.1	135	1.5	191	0.2	241	0.1
81	3.2	136	2.3	192	1.4		
82	1.0	137	1.4	193	0.5	243	11.6
83	1.3	138	0.3	194	11.7	244	4.5
84	0.2			195	1.1	245	0.6
85	24.0	141	0.2				
86	1.2			203	0.5	252	0.1
		147	0.1			253	2.2
92	0.2	148	0.1	285	0.1	254	0.1
93	0.5	149	0.2	286	0.4	255	0.5
94	1.5	150	0.5	287	13.7		
95	2.1	151	0.6	288	2.3	264	12.2
96	0.6	152	0.7	289	0.2	265	1.5
103	0.4	159	0.5	217	0.1	298	0.3
				218	1.4	281	0.4
		321	4.0	333	0.4	420	0.1
385	2.8	322	1.1			421	0.2
386	0.2	323	1.5	356	0.1	422	23.5
387	0.1	324	0.1			423	10.6
388	0.3			407	1.5	424	2.9
		337	1.8	408	0.2	425	0.2
329	7.6	333	0.3				

Figure 18. Mass Spectrum of Dipivaloyl Dyphylline

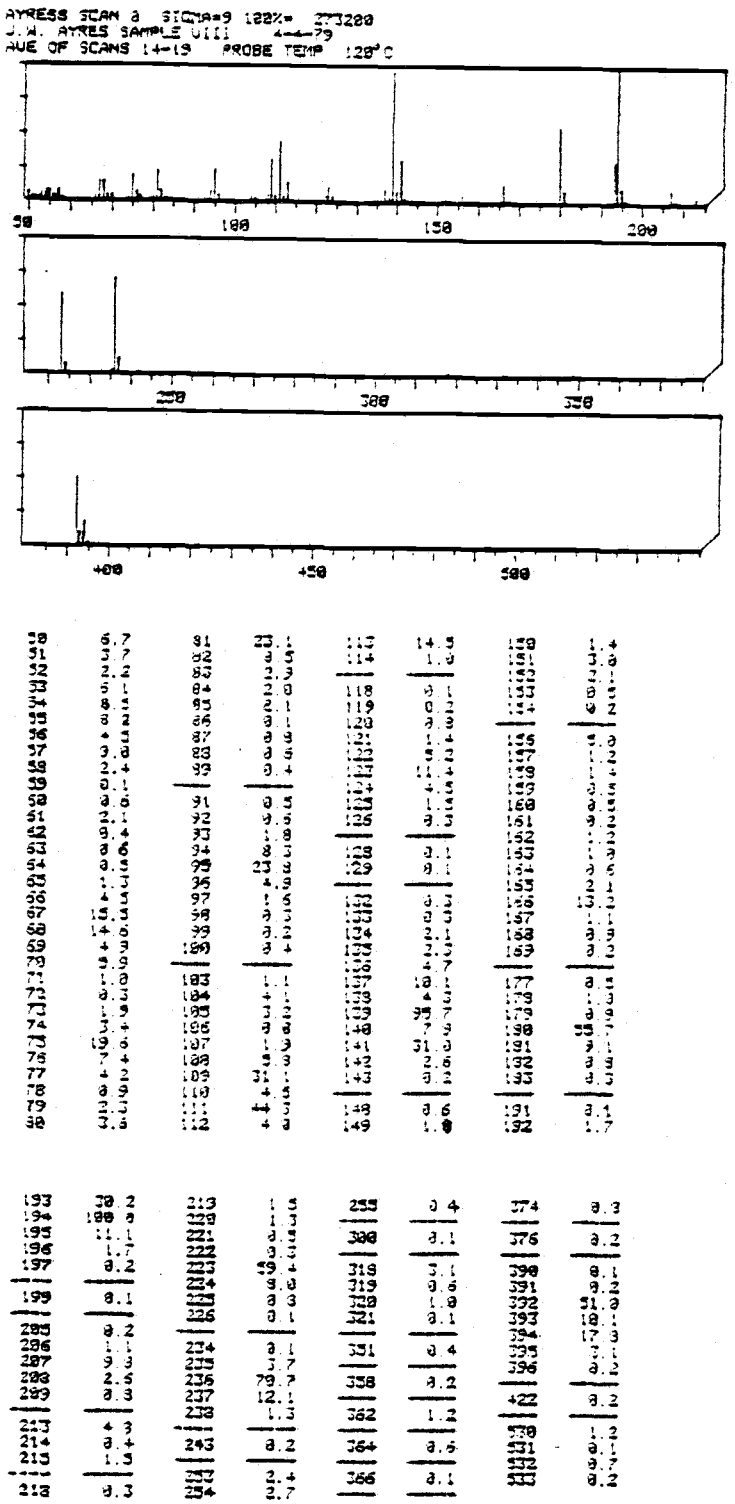

Figure 19. Mass Spectrum of Primary Mono-p-Cl-benzoyl Dyphylline

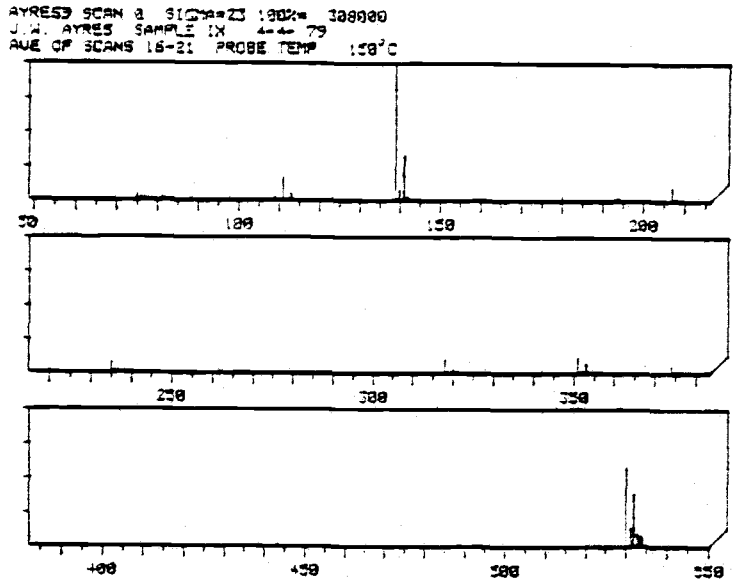

Figure 20. Mass Spectrum of Di-p-Cl-benzoyl Dyphylline

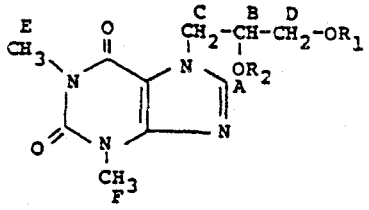

Table III. Summary of relative chemical shift values (δ, ppm) for dyphylline esters using chloroform-d as the solvent and TMS as the internal standard reference

Compound	H_A	H_B	H_C,H_D	H_E,H_F	R_2	R_1
Dyphylline **	δ 7.83 (s,1)	δ 2.45 (m,1)	δ 3.54-4.53 (m,4)	δ 3.12 (s,3) δ 3.30 (s,3)	δ 4.53-4.97 (m,2)	
Monoproionyl dyphylline	δ 7.6 (s,1)	δ 4.1 - δ 4.8 (m,5)		δ 3.35 (s,3) δ 3.55 (s,3)	δ 3.85 (s,1)	δ 2.45* (q,2,J=3.5) δ 1.25 (t,3,J=3.5)
Dipropionyl dyphylline	δ 7.5 (s,1)	δ 5.4 (p,1, J=2.0)	δ 3.95 - δ 4.90 (m,4)	δ 3.35 (s,3) δ 3.55 (s,3)	δ 2.3 (m,4) δ 1.15 (m,6)	
Monoisobutyryl dyphylline	δ 7.6 (s,1)	δ 3.9 - δ 4.7 (m,5)		δ 3.35 (s,3) δ 3.55 (s,3)	δ 3.75 (s,1)	δ 2.5 (m,1) δ 1.2 (d,6 J=3.5)
Diisobutyryl dyphylline	δ 7.5 (s,1)	δ 5.4 (p,1, J=2.0)	δ 3.95 - δ 4.85 (m,4)	δ 3.35 (s,3) δ 3.55 (s,3)	δ 2.5 (m,2) δ 1.0 - δ 1.3 (m,12)	
Monopivaloyl	δ 7.6 (s,1)	δ 4.1 - δ 4.8 (m,5)		δ 3.35 (s,3) δ 3.55 (s,3)	δ 3.9 (s,1)	δ 1.25 (s,9)
Dipivaloyl dyphylline	δ 7.5 (s,1)	δ 5.4 (p,1, J=2.0)	δ 3.9 - δ 4.7 (m,4)	δ 3.35 (s,3) δ 3.55 (s,3)	δ 1.15 (s,9) δ 1.25 (s,9)	
Mono-p-chlorobenzoyl dyphylline	δ 7.6 (s,1)	δ 4.45 (m,5)		δ 3.35 (s,3) δ 3.55 (s,3)	δ 3.75 (s,1)	δ 7.2 δ 8.05 (m,4)
Di-p-chlorobenzoyl dyphylline	δ 7.5 (s,1)	δ 5.75 (p,1, J=2.0)	δ 4.55 - δ 4.85 (m,4)	δ 3.35 (s,3) δ 3.55 (s,3)	δ 7.9 (m,4) δ 7.35 (m,4)	

*J was recorded as cycles per second (cps).

**Due to solubility, the spectrum of dyphylline was generated using DMSO-d_6 as the solvent while its esters were dissolved in chloroform-d.

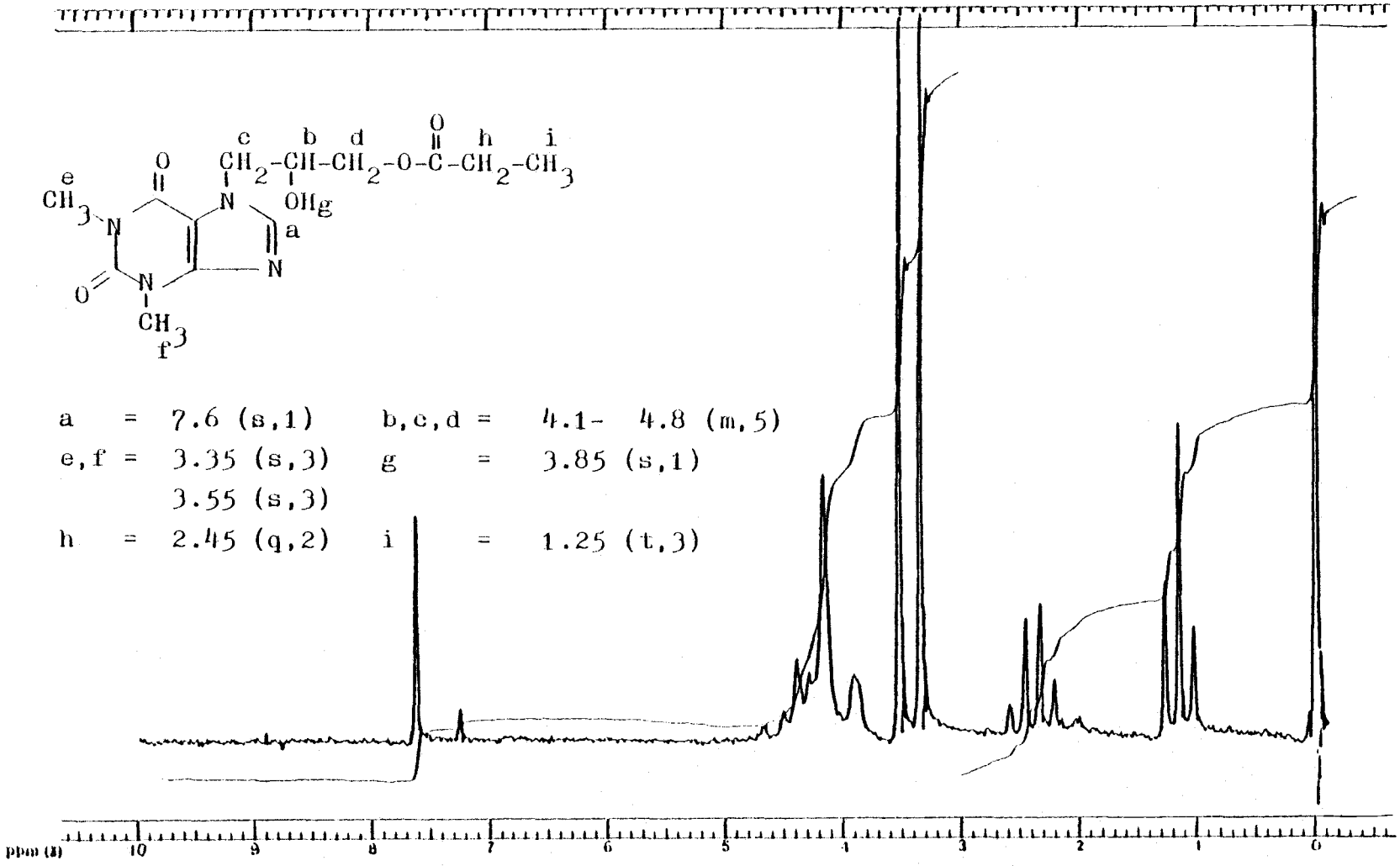

Figure 21. PMR Spectrum of Primary Monopropionyl Dyphylline

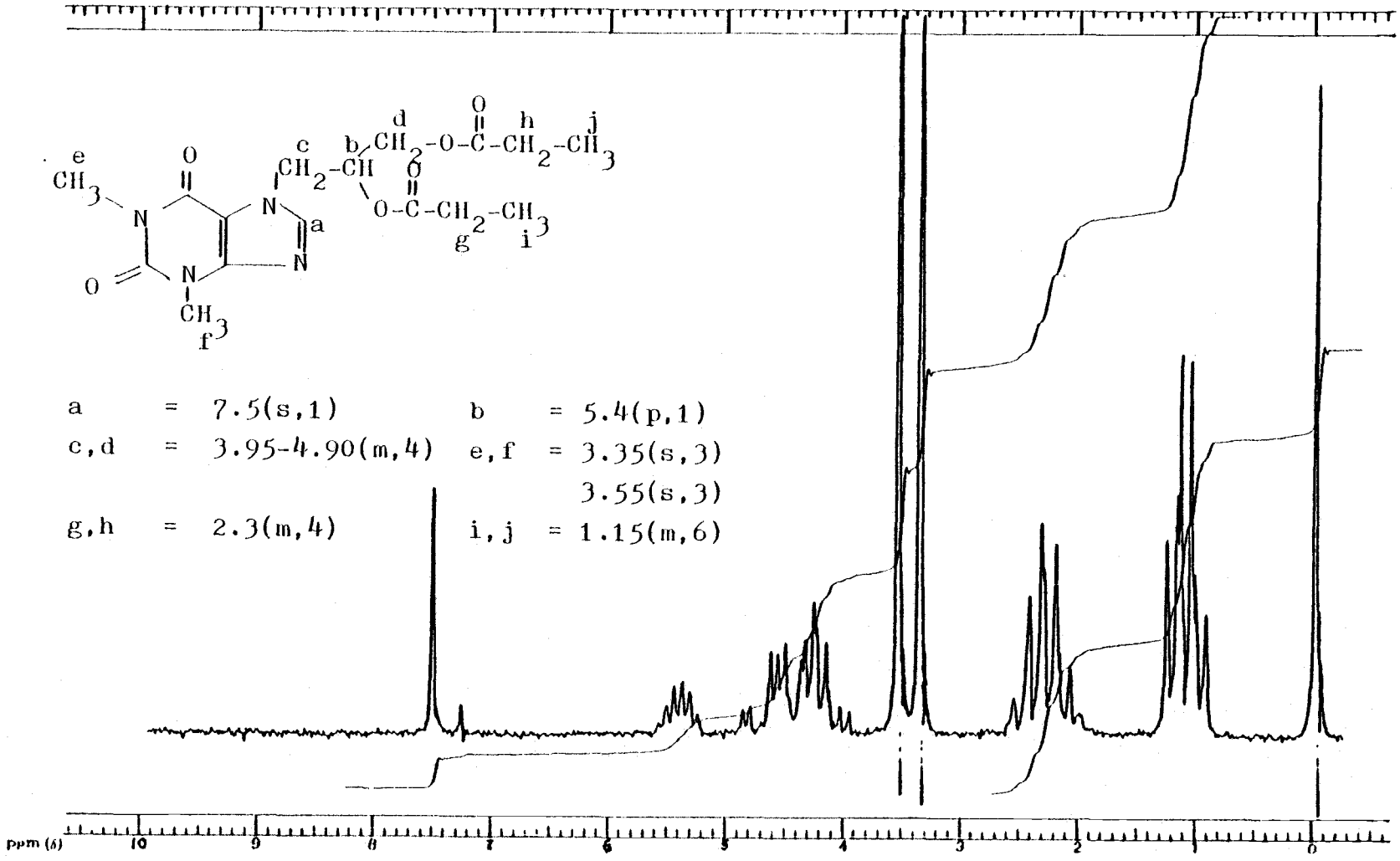

Figure 22. PMR Spectrum of Dipropionyl Dyphylline

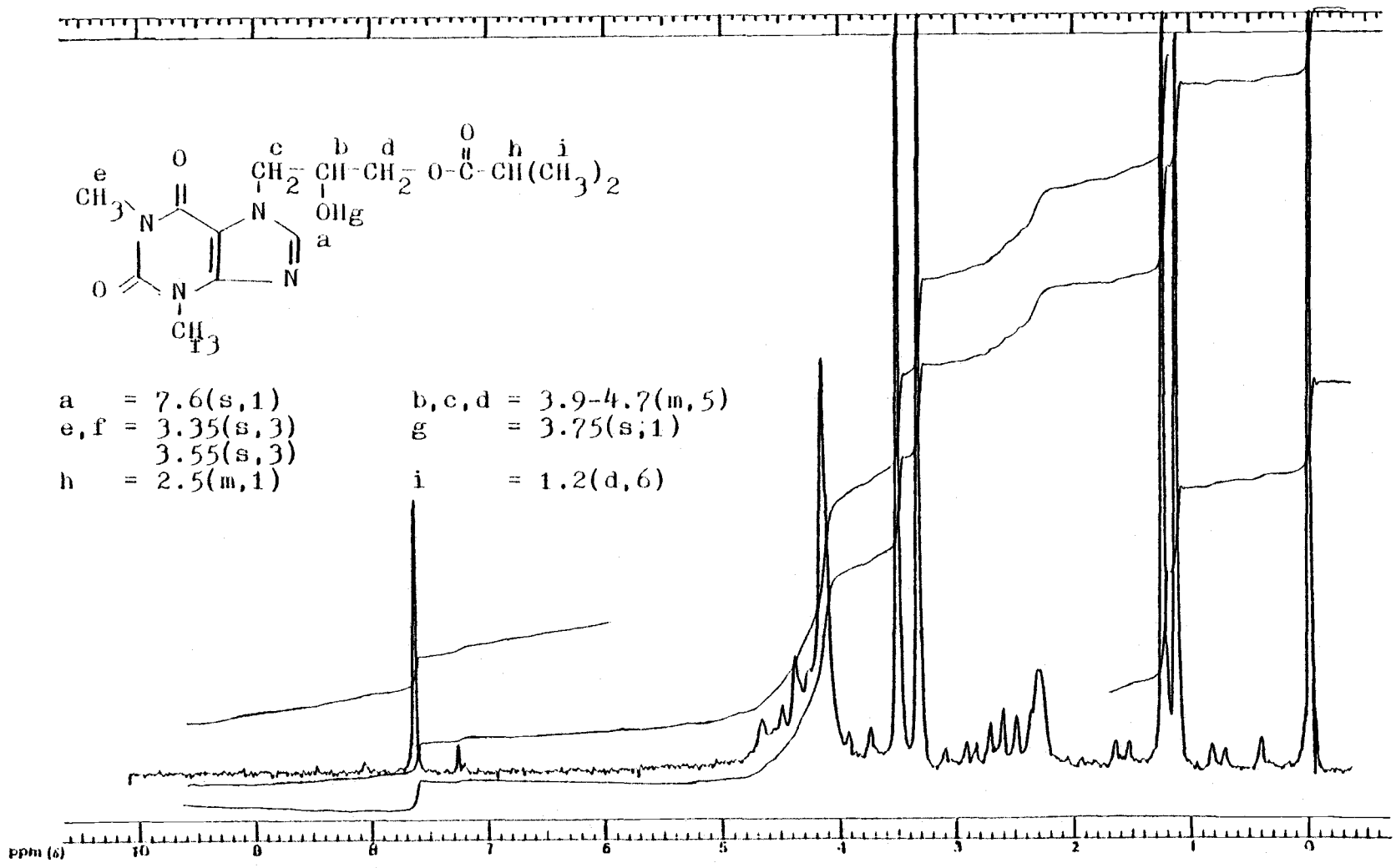

Figure 23. PMR Spectrum of Primary Mono-isobutyryl Dyphylline

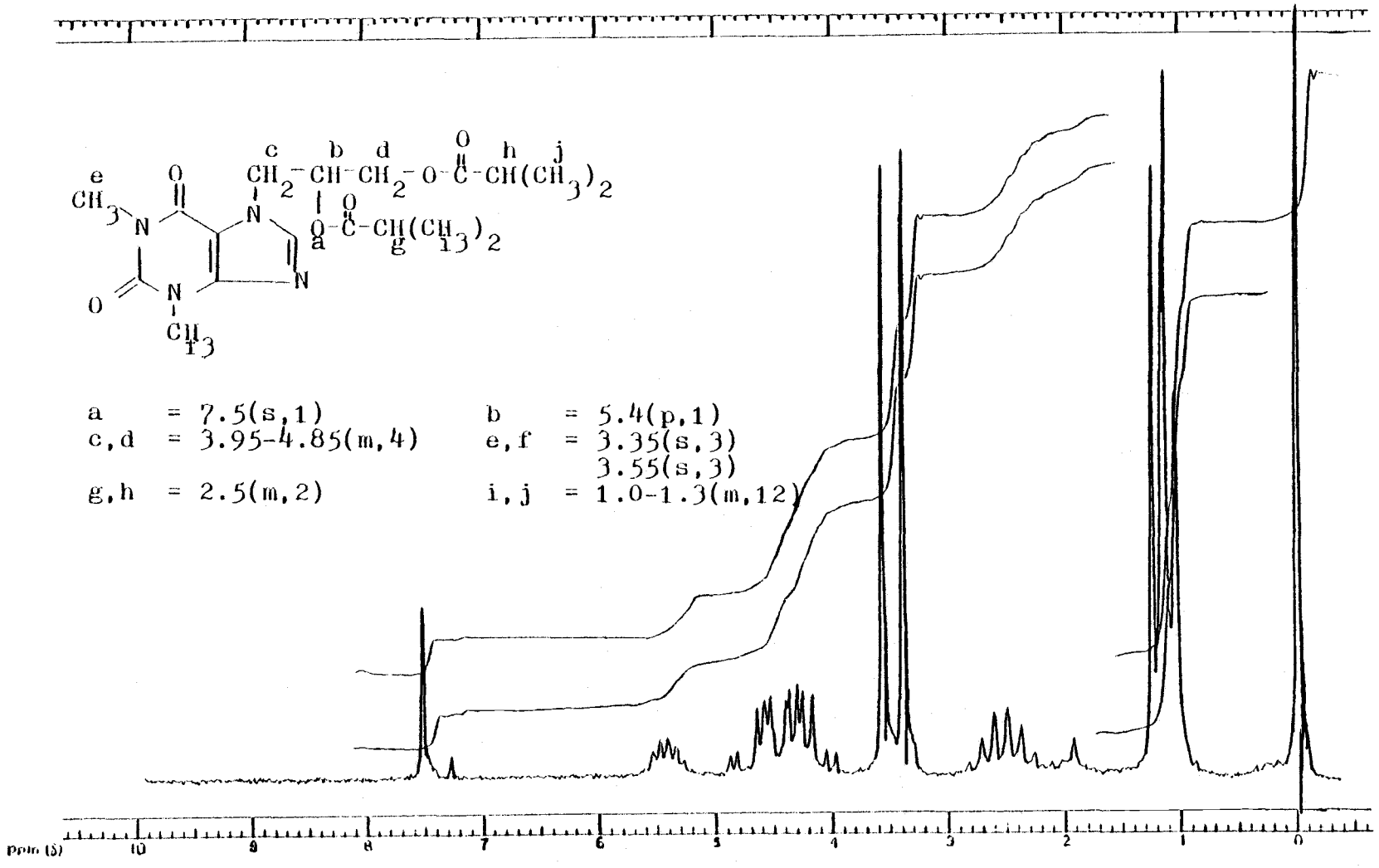

Figure 24. PMR Spectrum of Di-isobutyryl Dyphylline

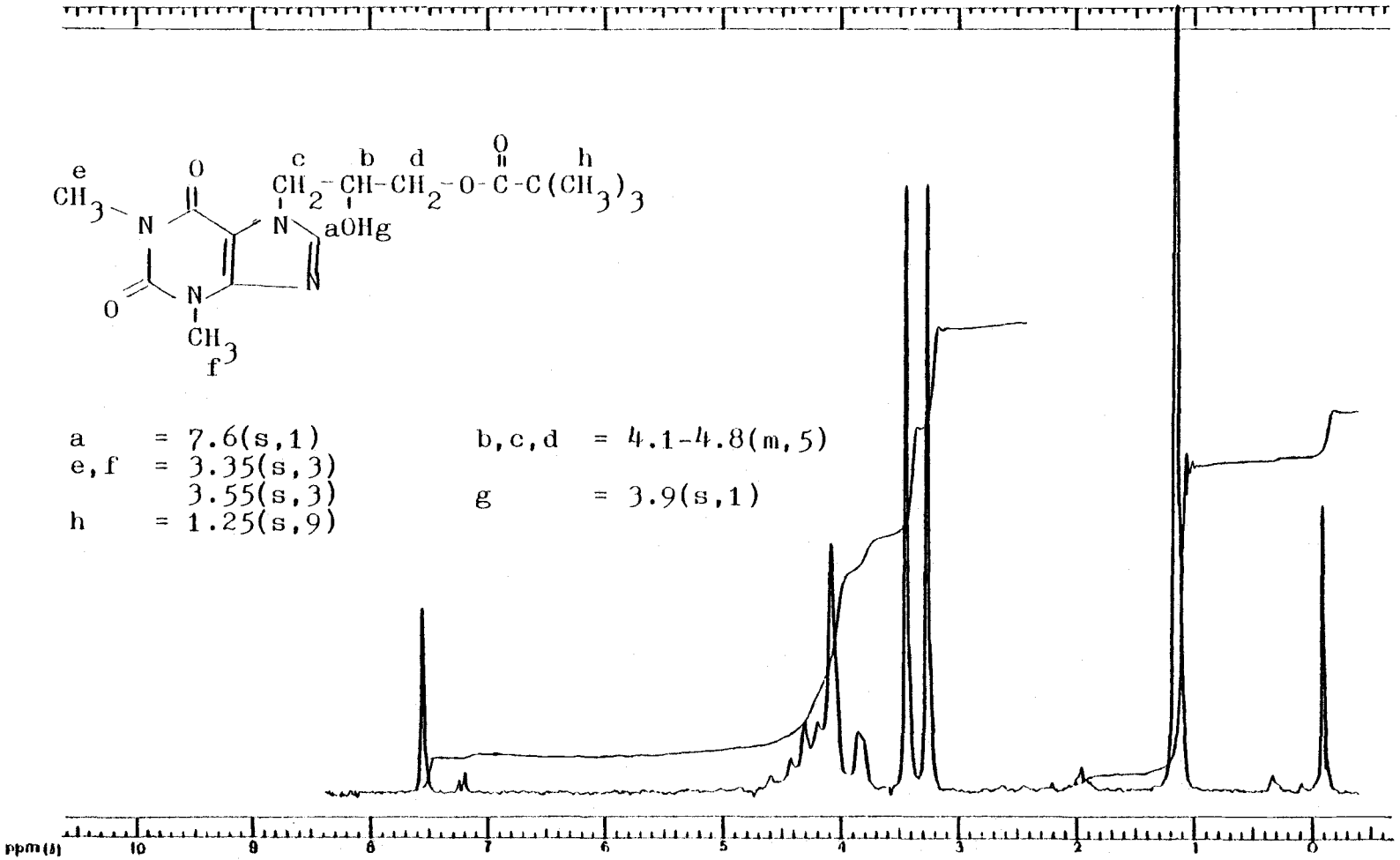

Figure 25. PMR Spectrum of Primary Monopivaloyl Dyphylline

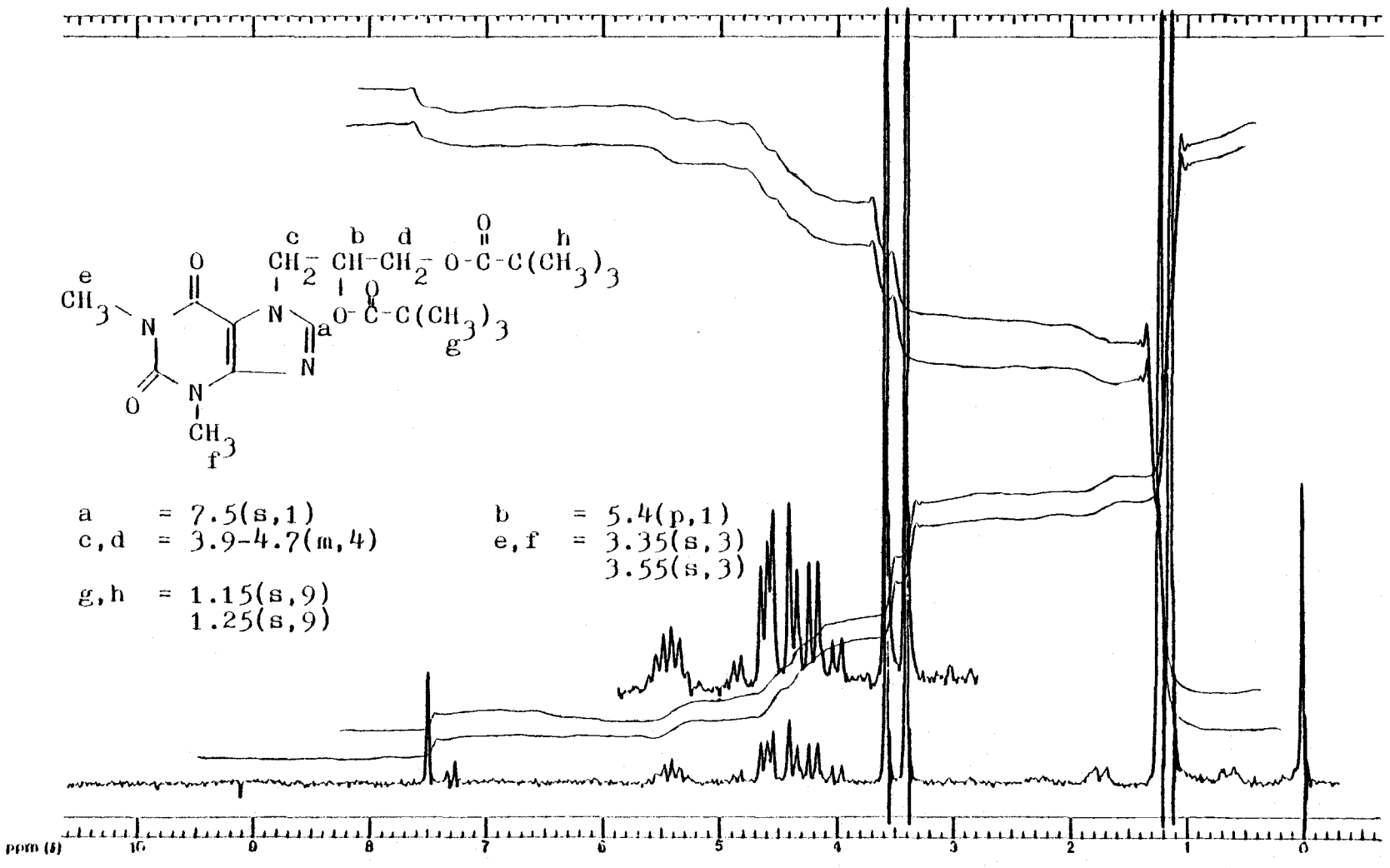

Figure 26. PMR Spectrum of Dipivaloyl Dyphylline

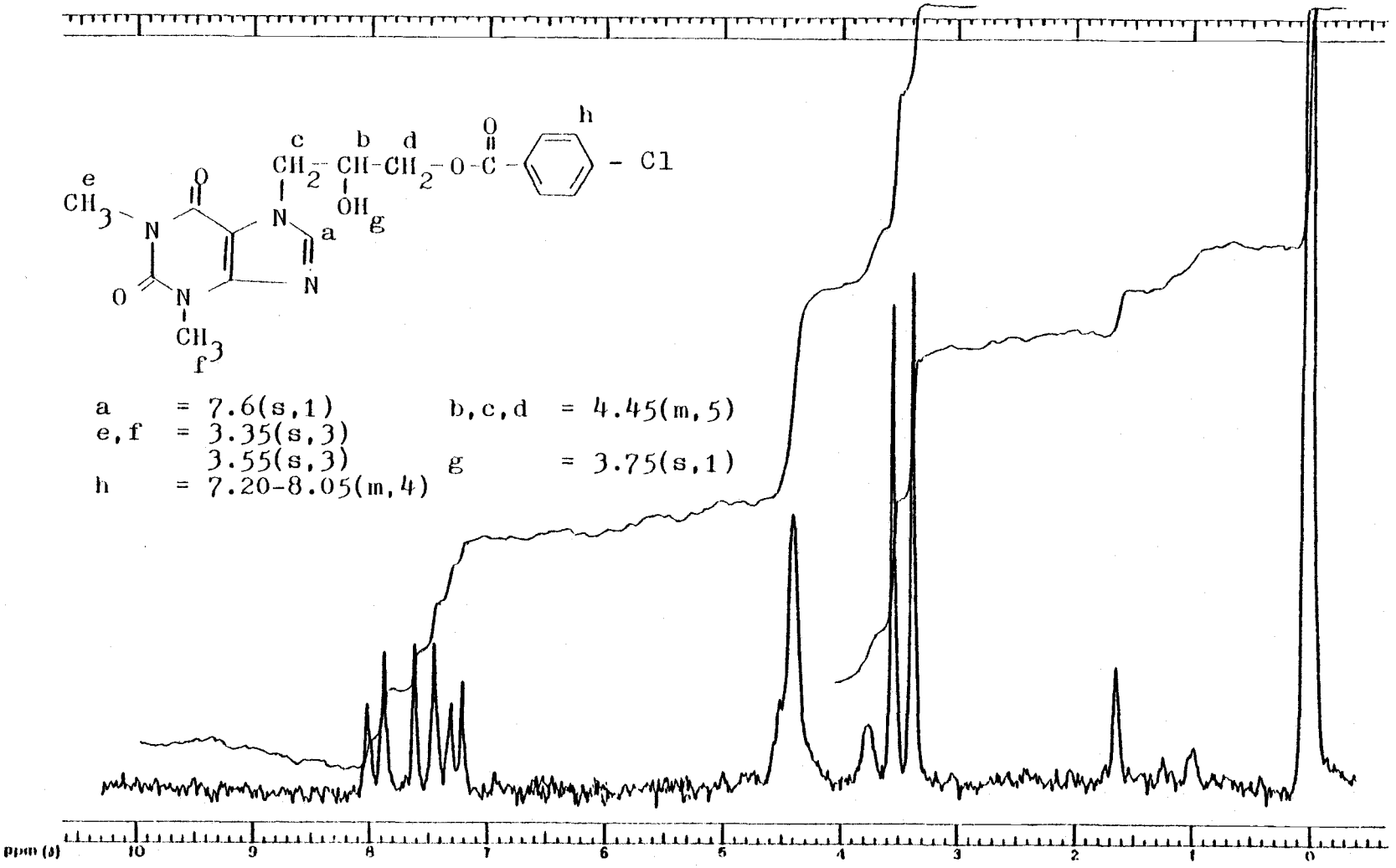

Figure 27. PMR Spectrum of Primary Mono-p-Cl-Benzoyl Dyphylline

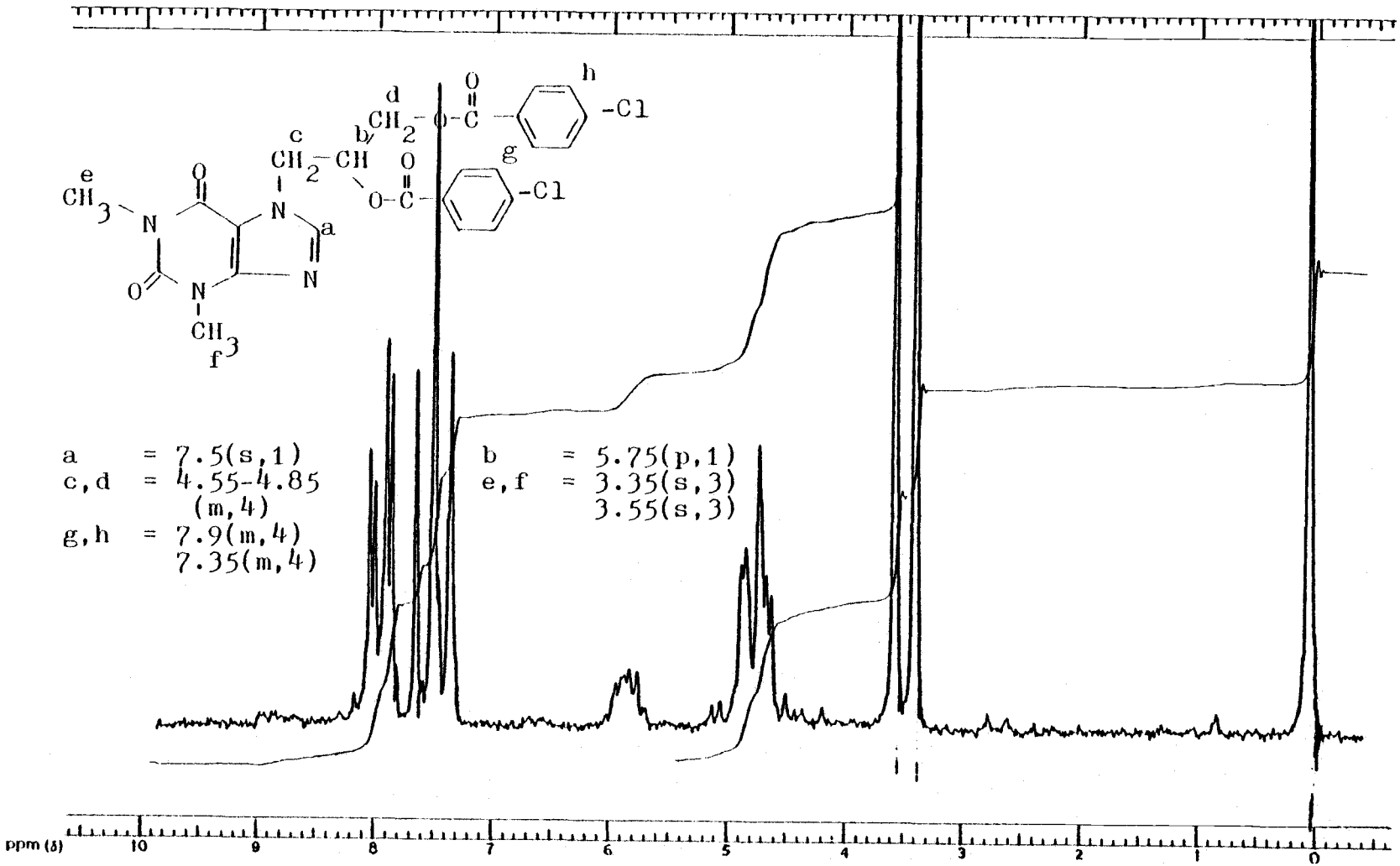

Figure 28. PMR Spectrum of Di-p-Cl-benzoyl Dyphylline

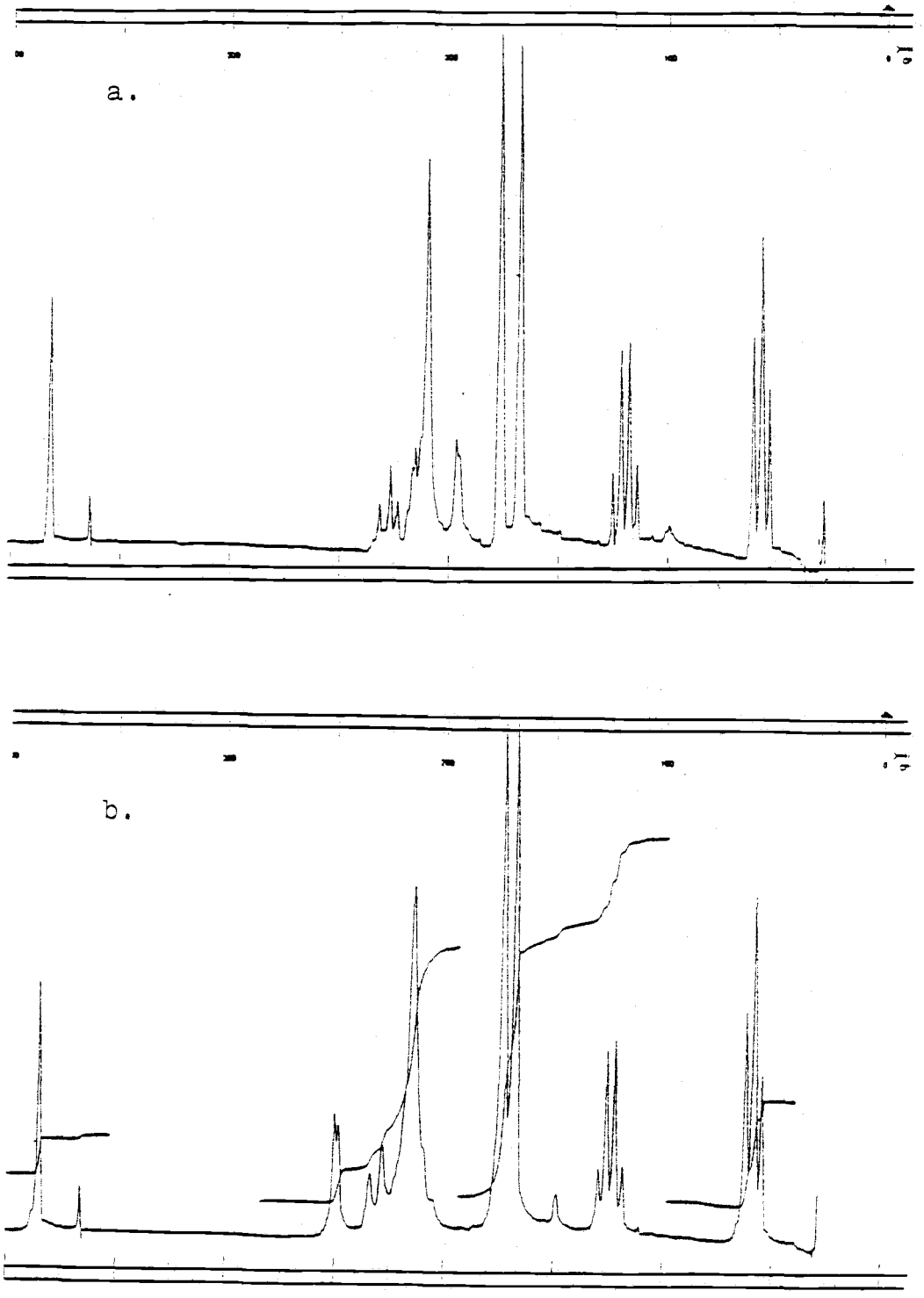

Figure 29. PMR Spectra of Primary Monopropionyl Dyphylline at Room Temperature (a), and -40°C (b)

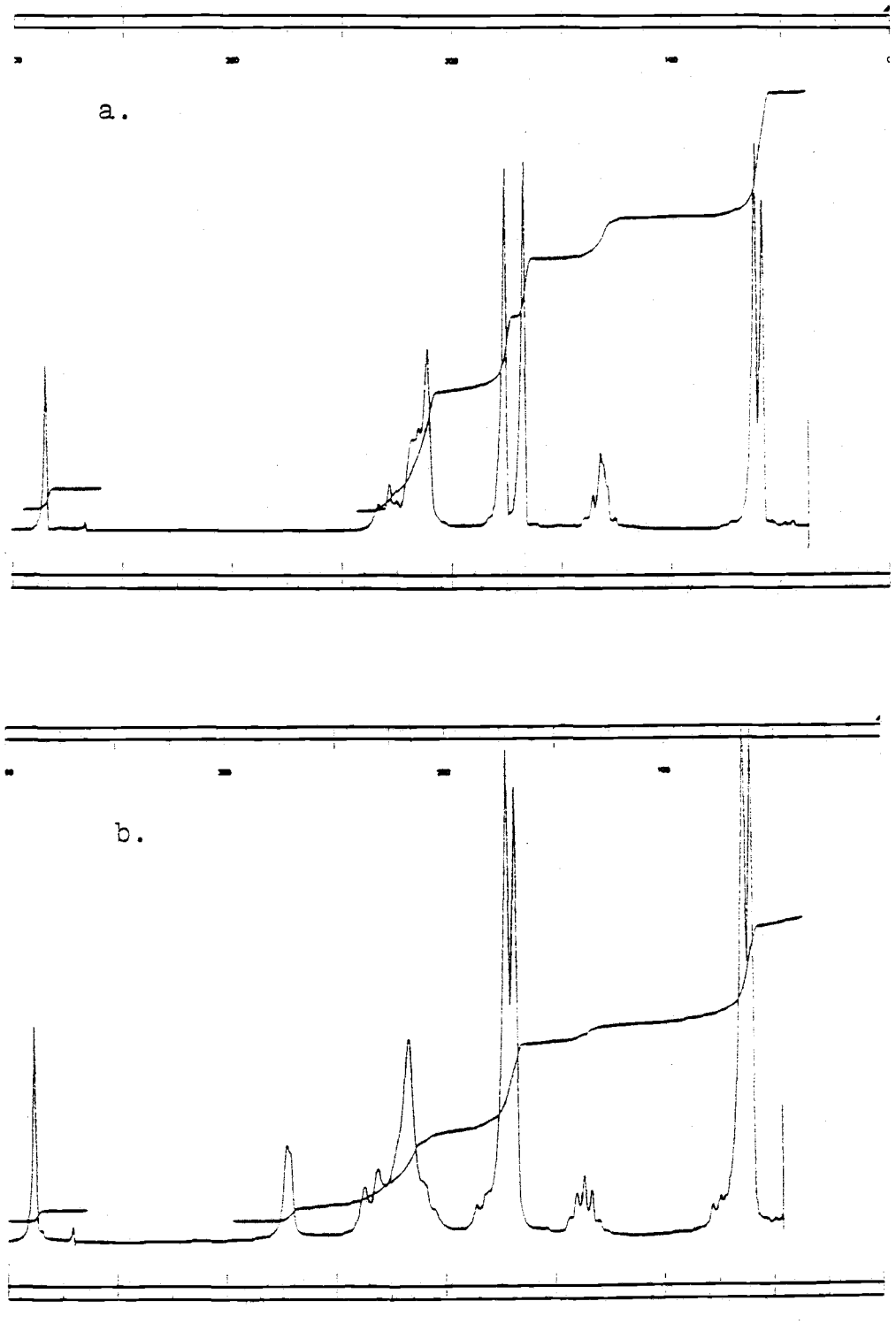

Figure 30. PMR Spectra of Primary Mono-isobutyryl Dyphylline at Room Temperature (a), and -55°C (b)

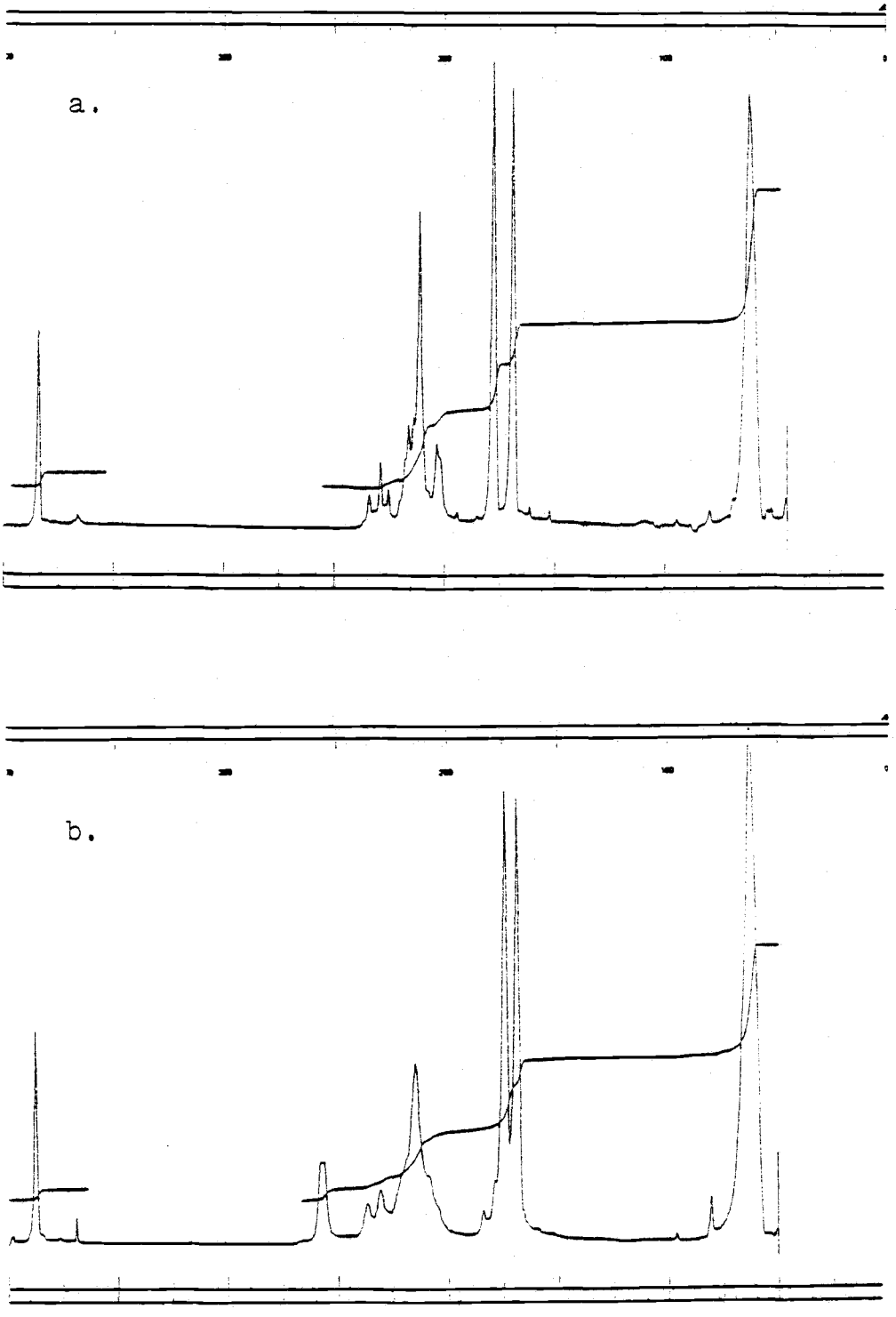

Figure 31. PMR Spectra of Primary Monopivaloyl Dyphylline at Room Temperature (a), and -55°C (b)

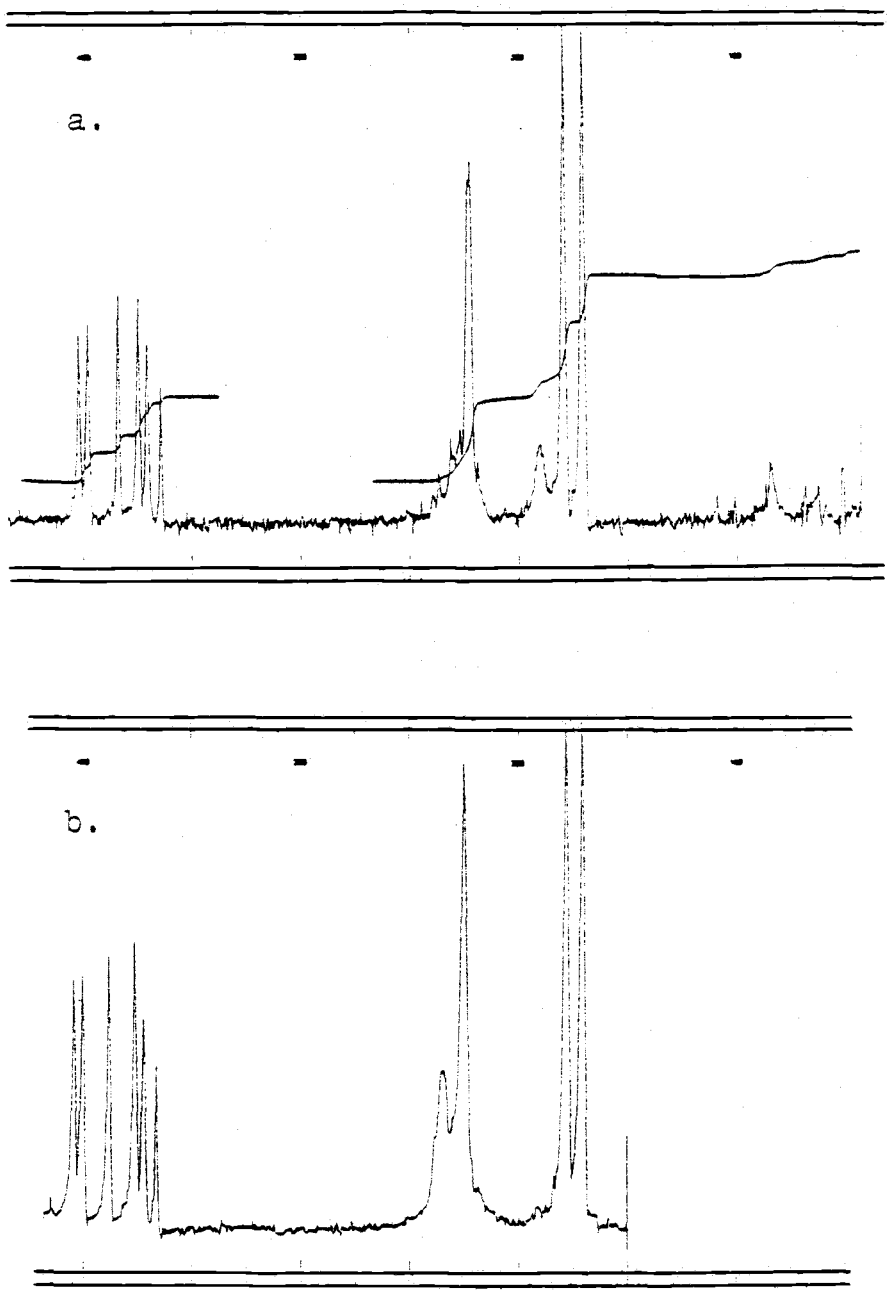

Figure 32. PMR Spectra of Primary Mono-p-Cl-benzoyl Dyphylline at Room Temperature (a), and -40°C (b)

obtained at room temperature (these hydroxy peaks can shift depending on concentration and temperature) (17). It was therefore impossible to tell whether the hydroxy group was at the α- or β- position. The PMR spectrum of the monopropionyl ester was then obtained at approximately -40°C using chloroform-d as the solvent and tetramethylsilane (TMS) as the internal standard. The hydroxy peak was shifted about 1 ppm (δ) downfield relative to the room temperature spectrum and appeared as a clear doublet (Figure 29). This spectrum confirmed that the hydroxy group of monopropionyl dyphylline was at the β-position as it should be a triplet if it were at the α-position. Thus, the monoester had formed at the α-position. Similar results but not quite as clear were obtained for all other monoesters reported here (Figures 30-32). Therefore, all four monoesters of dyphylline synthesized here were primary monoesters.

Solvent programming HPLC: The chromatographic conditions described in the experimental section produced the results summarized in Table IV and Figures 33 and 34. A good separation among dyphylline and its mono- and di- esters can be obtained for all ester derivatives synthesized here with total retention times of less than 15 minutes. The di-p-Cl-benzoyl dyphylline had the longest retention time which was 12.2 minutes and the peak was broadened somewhat.

Table IV. Summary of retention times of dyphylline and its mono- and di- hydroxy esters using HPLC chromatographic solvent programming conditions as follows: mobile phase for pump A = 10% acetonitrile in distilled water, mobile phase for pump B = 60% acetonitrile in distilled water, initial condition = 0% B, final condition = 100% B, programming time = 3 minutes, curve used = linear, solvent flow = 2 ml/min, chart flow = 0.5 inch/min.

Compound	Retention Time (minute)	Retention Distance (cm)
Dyphylline	4.75	6.00
Monopropionyl dyphylline	5.70	7.15
Dipropionyl dyphylline	6.70	8.30
Mono-isobutyryl dyphylline	5.80	7.45
Di-isobutyryl dyphylline	7.50	9.25
Monopivaloyl dyphylline	6.50	8.25
Dipivaloyl dyphylline	8.75	11.00
Mono-p-Cl-benzoyl dyphylline	6.70	8.45
Di-p-Cl-benzoyl dyphylline	12.20	15.30

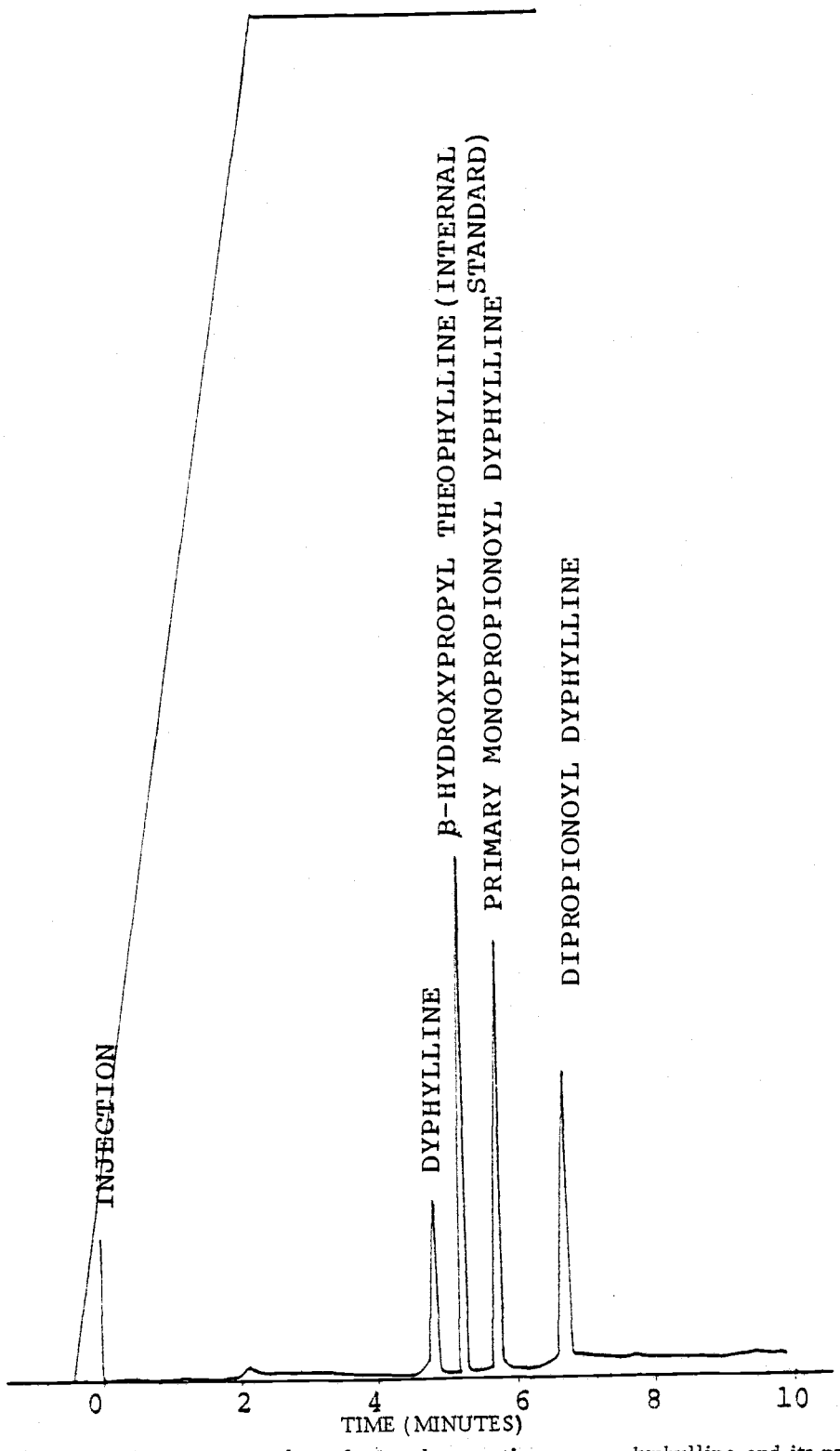

Figure 33. The HPLC chromatogram showed a good separation among dyphylline and its primary monopropionyl and dipropionyl esters using solvent programming

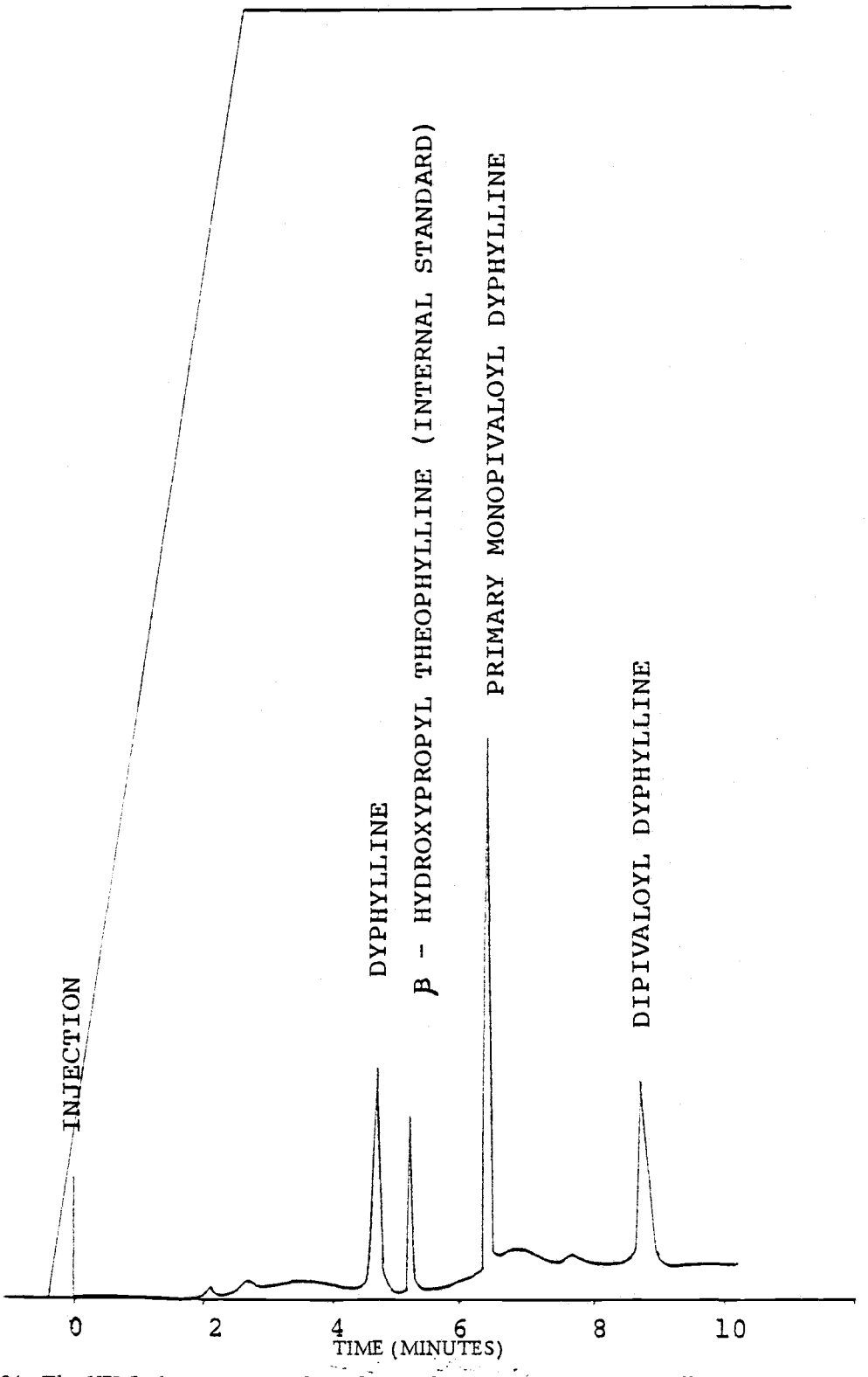

Figure 34. The HPLC chromatogram showed a good separation among dyphylline and its primary monopivaloyl and dipivaloyl esters using solvent programming

Secondary monoesters: An attempt was also made to synthesize the secondary monoesters as shown in Scheme II. Triphenyl pivaloyl dyphylline (X) was isolated as determined by PMR (Figure 35). However, after removal of the protecting group with glacial acetic acid as shown in scheme II the product isolated was the primary pivaloyl ester. The secondary ester may have shifted to the primary position after removal of the protecting group as shown in scheme III (19).

It has been determined that all four primary monoester derivatives of dyphylline synthesized as reported here do not remain only in the primary monoester form when dissolved in aqueous solvent. There was always a peak in the HPLC tracings prior to the appearance of the primary monoester peak. This unknown peak did not appear when the monoester derivative was dissolved in nonpolar organic solvents. Figure 36 shows a comparison of HPLC tracings for the primary monopropionyl ester of dyphylline after being dissolved in distilled water or in acetonitrile for 24 hours. The mobile phase used was 20% acetonitrile in distilled water. This system produced a good separation between the unknown and the primary monopropionyl ester. The retention times were 3.4 and 4.6 minutes for the unknown and the primary monopropionyl ester respectively. The unknown compound and the primary monopropionyl dyphylline were each collected from the outlet of the HPLC into two separate

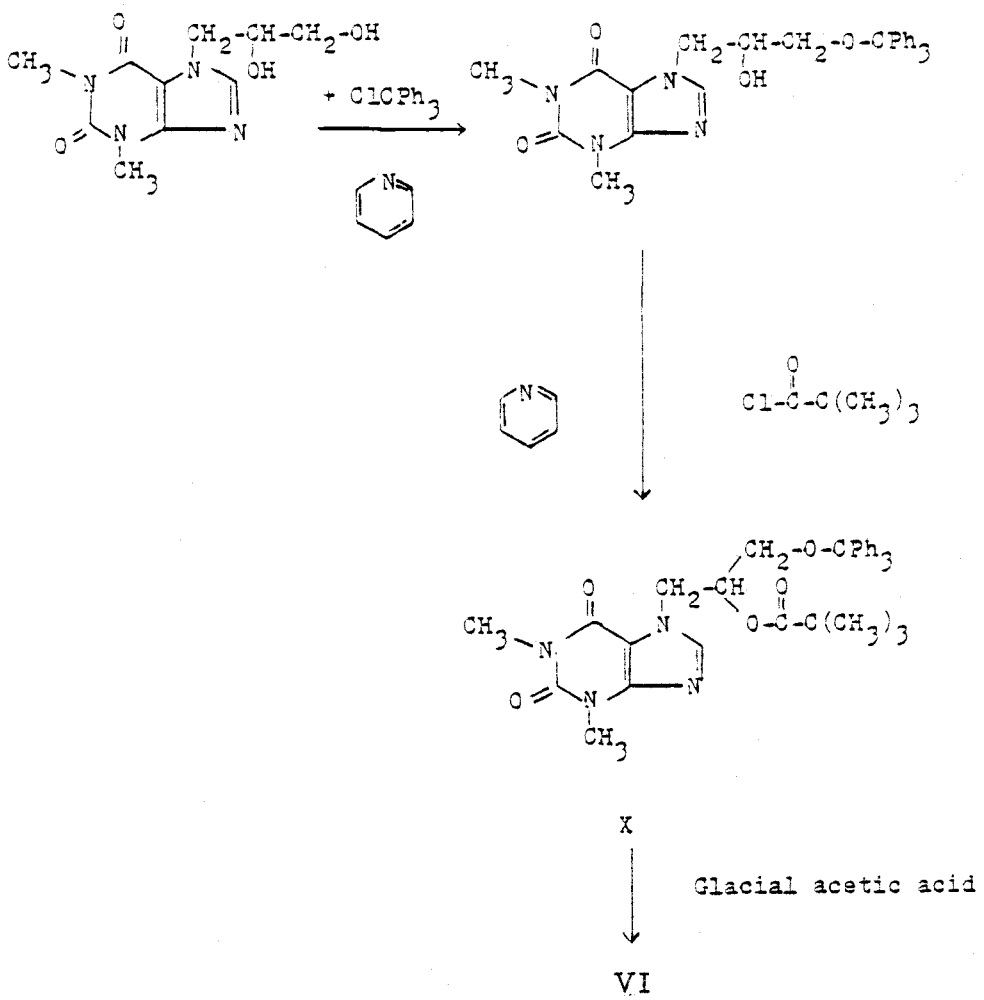

Scheme II. Pathway for the synthesis of secondary pivaloyl dyphylline

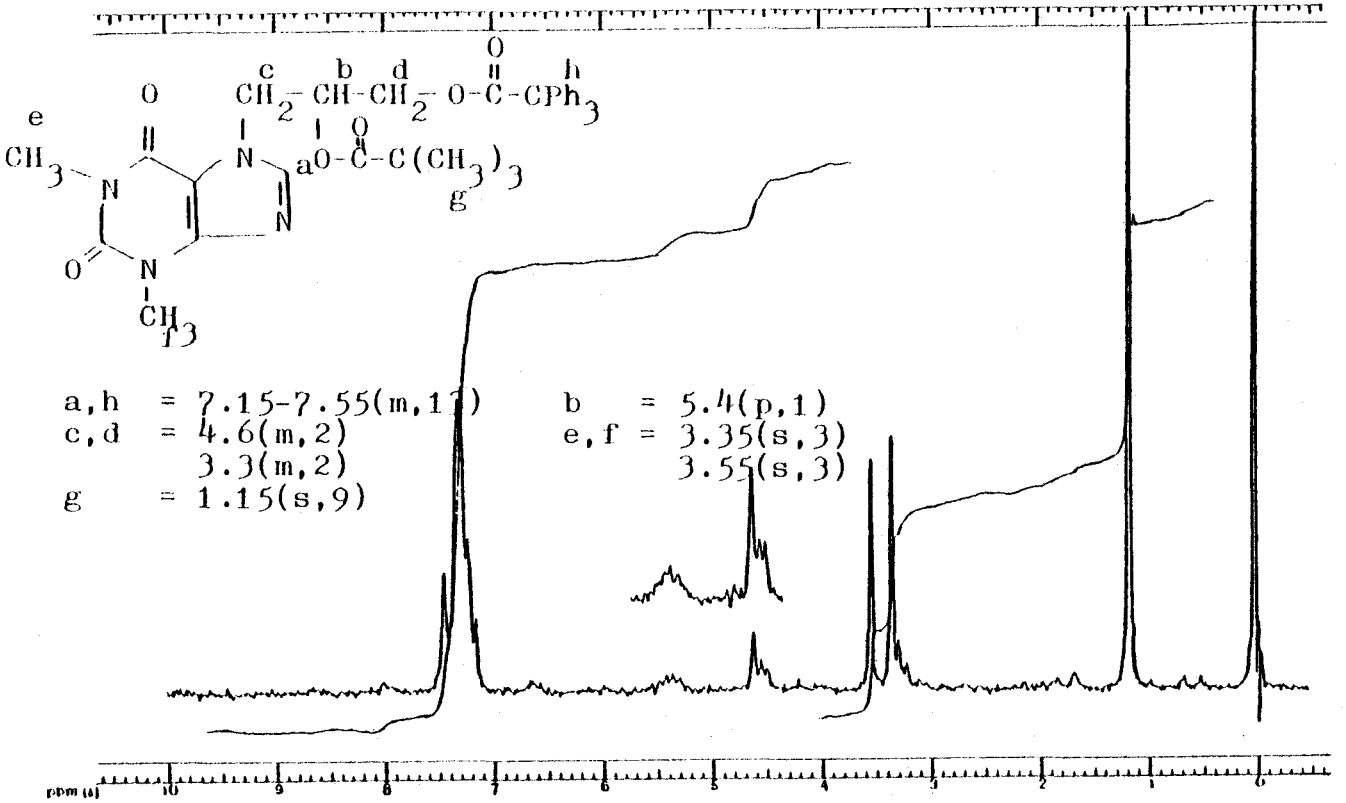

Figure 35. PMR Spectrum of Triphenylmethyl Pivaloyl Dyphylline (X)

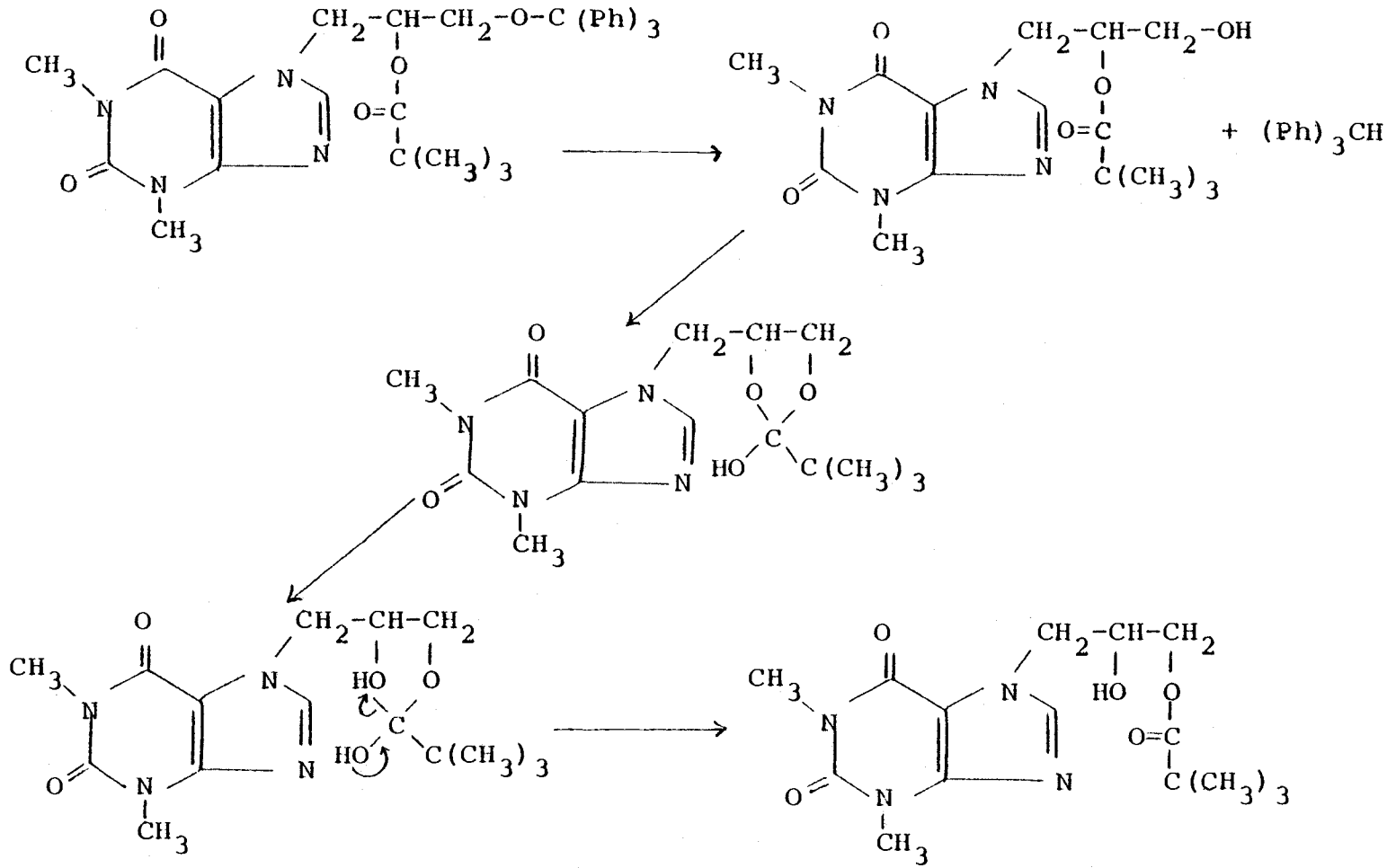

Scheme III. Pathway for the shifting of secondary pivaloyl dyphylline to the primary position during the removal of the protecting group with glacial acetic acid

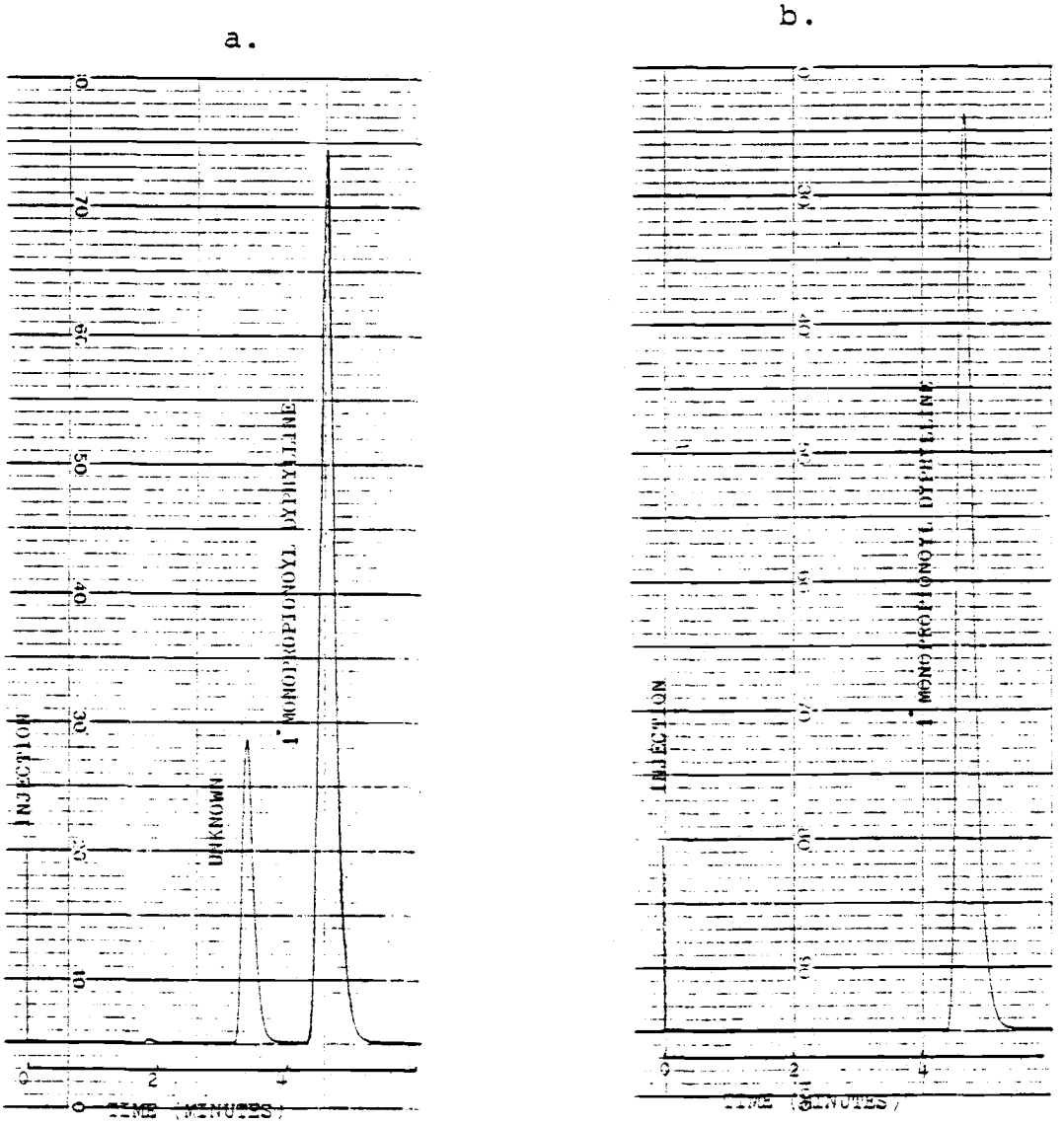

Figure 36. Comparison of HPLC chromatograms for primary monopropionyl dyphylline dissolved in distilled water (a) and in acetonitrile (b) after 24 hours. The mobile phase was 20% acetonitrile in distilled water and solvent flow was 2 ml/minute.

test tubes. The solution from each tube was injected back into the HPLC after standing for variable time periods at room temperature. The results (Figure 37) show that the peak height ratio of these two compounds was changing with time. The unknown compound and primary monopropionyl dephylline were shifting back and forth in aqueous solution until equilibrium was reached. The rate of conversion of the unknown to primary monopropionyl dyphylline is much faster than the rate of conversion of primary monopropionyl dephylline to the unknown. The equilibrium peak height ratio depended on the solvent conditions. For 100 percent distilled water, the peak height ratio of the unknown to the primary monopropionyl dyphylline after sitting at room temperature for several days was one to three (1:3). The unknown peak was then hypothesized to be the secondary monopropionyl dyphylline which was in equilibrium with the primary monopropionyl ester.

Further evidence to substantiate the assumption that the unknown peak is due to the presence of the secondary monoester was done by injecting the saturated solution of the primary monopropionyl dyphylline in distilled water into the HPLC. The unknown compound and the primary monopropionyl ester were each collected from the outlet of the HPLC as mentioned in detail in the experimental section. Insufficient drug was present to obtain PMR spectra but mass spectra were obtained as shown in Figure 38. The mass spectrum of the unknown when

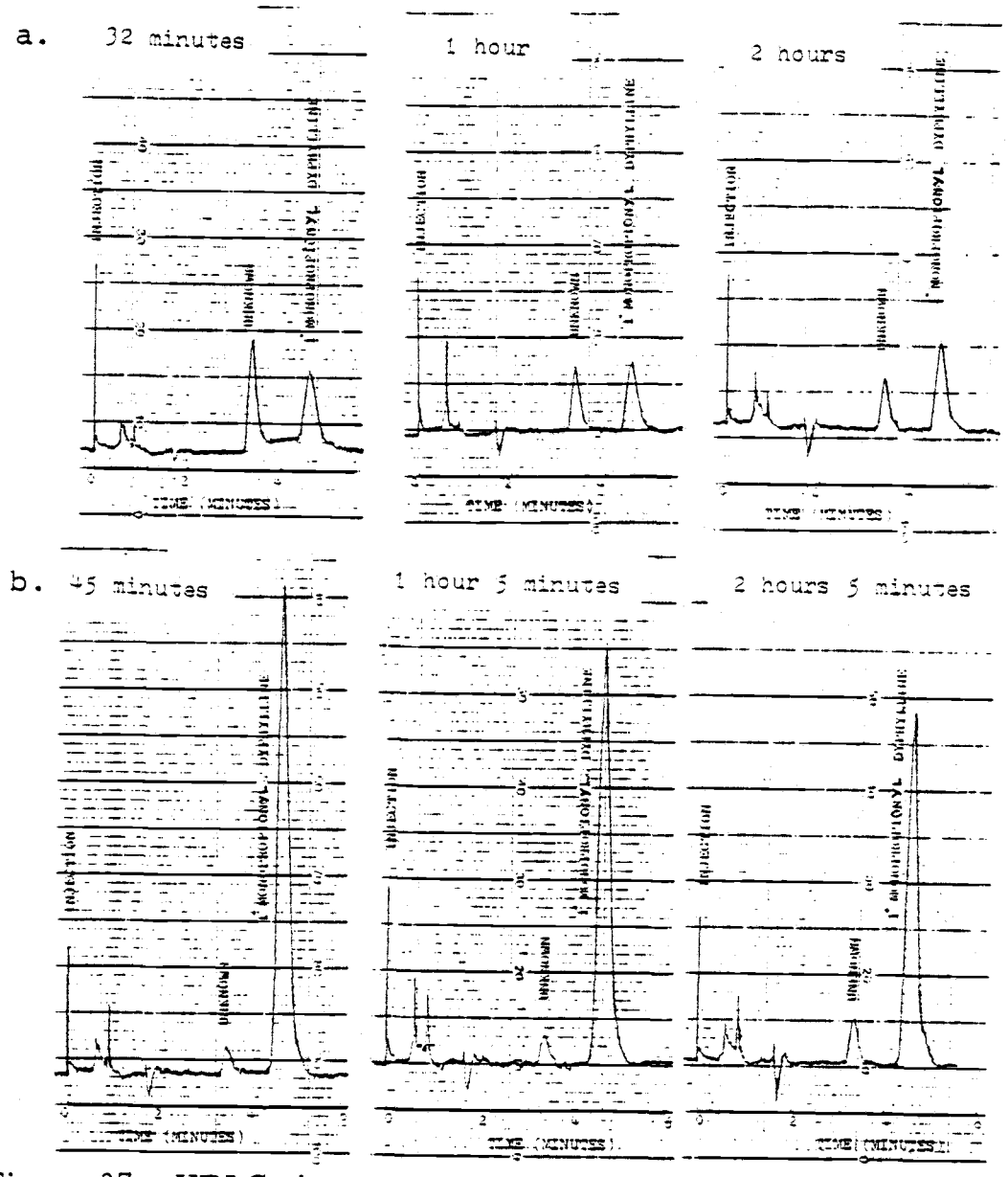

Figure 37. HPLC chromatograms of the "unknown" and primary monopropionyl dyphylline samples collected from the HPLC outlet and injected back into the HPLC after standing several different time periods at room temperature; a = the unknown samples, b = the primary monopropionyl dyphylline samples

a.

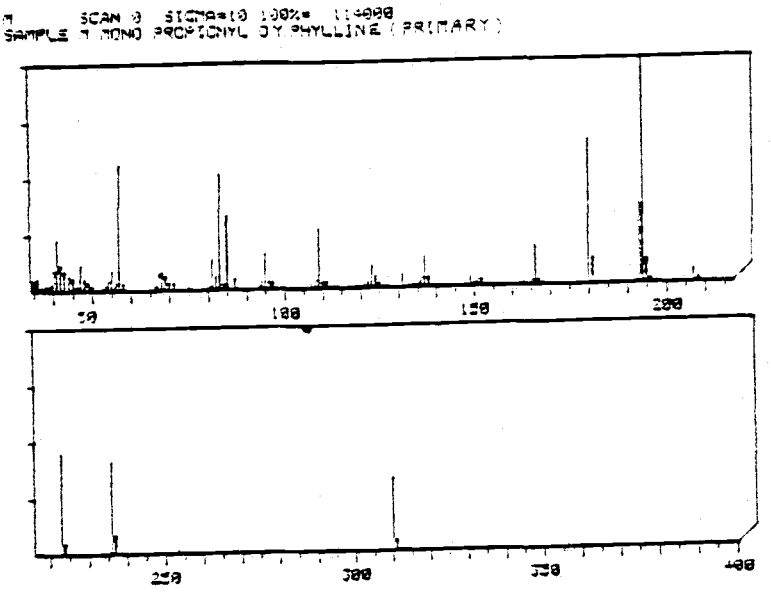

b.

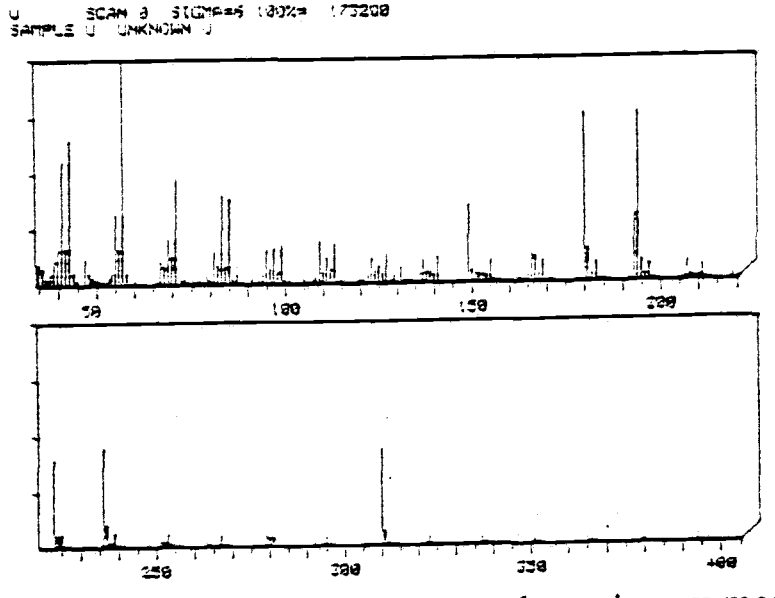

Figure 38. Comparison of mass spectra for primary monopropionyl dyphylline (a) and the "unknown" (b)

compared to that of the primary monopropionyl dyphylline indicates a high probability that the unknown is actually secondary monopropionyl dyphylline. Both compounds exhibited a molecular ion peak at 310 as would be expected. The entire spectra were similar, but not exactly the same. The m/e 180 and m/e 194, which were the two main peaks for all ester derivatives of dyphylline synthesized here, were nearly equal for the unknown but the m/e 194 was much higher than m/e 180 for the primary monopropionyl ester. Figure 39 compares the structures of the primary and the secondary monopropionyl esters of dyphylline and shows some of the possible fragment ions in the mass spectrum of the two compounds. When the ester was present at the secondary position the bond between the gamma carbon and the nitrogen might readily cleave to result in a higher fragment ion at m/e 180 compared to the primary ester. This was also true in the case of the diesters where the m/e 180 was usually the highest peak in the spectra. When the possible fragment ions for the primary monoesters and the secondary monoesters in figure 39 are compared, it can be seen that there should be two fragment ions at m/e 113 and at m/e 99 in the mass spectrum of the secondary monoester which should not appear in the mass spectrum of the primary monoester. These two peaks did appear in the spectrum of the unknown but not in the spectrum of the primary monopropionyl dyphylline. It can also be predicted that the secondary

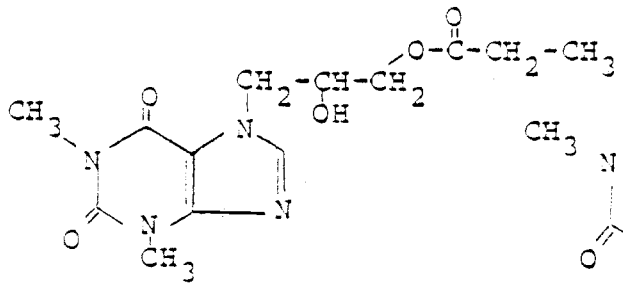

Primary Monopropionoyl Dyphylline (m/e = 310)

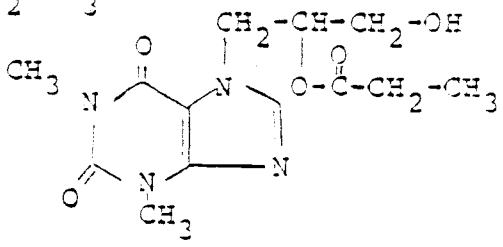

Secondary Monopropionoyl Dyphylline (m/e = 310)

Some Possible Fragment ions :

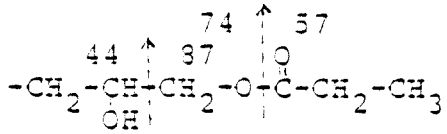

m/e = 131
74 = 44+CH_2-O
87 = 57+CH_2-O
87 = 58+CH_2-CH_3

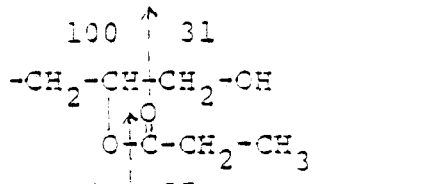

m/e = 131
131 = 113+H_2O
100 = 71+CH_2-CH_3
74 = 43+CH_2-OH

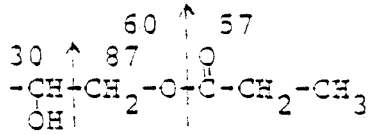

m/e = 117
60 = CH_2-O + CH-OH
87 = 57+CH_2-O
87 = 58+CH_2-CH_3

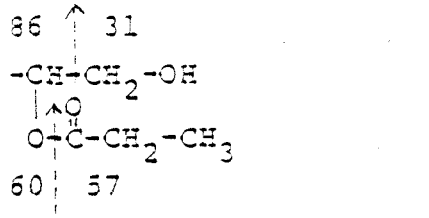

m/e = 117
117 = 99+H_2O
86 = 57+CH-O
60 = CH_2-OH+CH-O

Figure 39. Comparison between the structures of primary and secondary monopropionyl dyphylline and some of the fragment ions that could possibly be obtained from their mass spectra

propionyl ester should produce a high peak around m/e 70-71 and m/e 43, and these were present.

If the primary and secondary monoesters of dyphylline readily shift back and forth in aqueous media as is believed to occur, then there will be no special advantage in synthesizing the secondary monoester derivatives of dyphylline as a prodrug compared to the already prepared primary monoesters of dyphylline.

Footnotes, Chapter I:

1. Unimelt, Thomas Hoover Capillary Melting Point Apparatus, Arthur H. Thomas Company, Philadelphia, PA.
2. Silica Gel PF-254+366 E Merck Ag-Darmstadt, Germany or Elmsford, N. Y.
3. Perkin-Elmer Infrared Spectrophotometer 727, Norwalk, Connecticut.
4. Beckman Polystyrene Standard, Fullerton, California.
5. Varian MAT CH-7 Mass Spectrometer Equipped with a System Industries 150 data system, Palo Alto, California.
6. Varian Anaspect EM 360 NMR Spectrometer, Palo Alto, California.
7. SILANOR* C, MSD Canada Limited, Kirkland, Quebec, distributed in the United States by Merck and Co. Inc., Rahway, N. J.
8. Water Associates Chromatography Pumps, Milford, Mass.
9. Water Associates Model 660 Solvent Programmer, Milford, Mass.
10. Water Associates Model U6K Injector, Milford, Mass.
11. Water Associates μ BONDAPAK C_{18}, Milford, Mass.
12. Water Associates Model 440 Absorbance Detector, Milford, Mass.
13. SOLTEC, Encino, California.

14. Lemmon Pharmacal Company, Sellersville, PA.
15. Mallinckrodt Chemical Works (AR), St. Louis, Missouri, or 'Baker Analyzed' Reagent, J. T. Baker Chemical Co., Phillipsburg, N. J.
16. Aldrich Chemical Company, Milwaukee, Wisconsin.
17. Büchi Rotavapor-R, Brinkmann Instruments, Westbury, N. Y.
18. Baker Analyzed Reagent, J. T. Baker Chemical Co., Phillipsburg, N. J.
19. USP
20. Aldrich Chemical Company, Milwaukee, Wisconsin.
21. Aldrich Chemical Company, Milwaukee, Wisconsin, or Eastman Kodak Co., Rochester, N. Y.
22. Aldrich Chemical Company, Milwaukee, Wisconsin.
23. Mallinckrodt (AR), St. Louis, Missouri.

BIBLIOGRAPHY

1. P. V. Maney, J. W. Jones E. G. Gross and H. M. Korns, "Dihydroxypropyl Theophylline: Its Preparation and Pharmacological and Clinical Study," JAPhA (Sci. Ed.), Vol. 35, Sept 1946, p. 266-272.

2. L. D. Hudson, M. L. Tyler and T. L. Petty, "Oral Aminophylline and Dihydroxypropyl-theophylline in Reversible Obstructive Airway Disease: A Single-dose, Double-blind, Crossover Comparison," Curr Ther Res, Vol. 15, No. 7, Jul 1973, p. 367-372.

3. F. R. R. Simons, C. W. Bierman and A. C. Sprenkle, "Efficacy of Dyphylline (Dihydroxypropyltheophylline) in Exercise-induced Bronchospasm," Peds (Suppl), Vol. 56, Nov 1975, p. 916-918.

4. F. E. R. Simons, K. J. Simons and C. W. Bierman, "The Pharmacokinetics of Dihydroxypropyltheophylline: A Basis for Rational Therapy," J All Clin Immunol. Vol. 56, No. 5, Nov. 1975, p. 347-355.

5. K. J. Simons, F. E. R. Simons and C. W. Bierman, "Bioavailability of Sustained-release Dyphylline Formulation," J Clin Pharmacol, Vol. 17, No. 4, Apr 1977, p. 237-242.

6. V. C. Stephens and J. W. Conine, "Esters of Erythromycin III and Esters of Low Molecular Weight Alphatic Acids," Antibiot Ann, 1958-1959, p. 346-353.

7. A. B. A. Jansen and T. J. Russell, "Some Novel Penicillin Derivatives," J Chem Soc, 1965, p. 2127.

8. M. V. Daehne, E. Frederiksen, E. Gunderson, F. Lund, P. Morch, H. J. Peterson, K. Roholt, L. Tybring and W. O. Godtfredsen, "Acyloxymethyl Esters of Ampicilline," J Med Chem, Vol. 13, 1970, p. 607.

9. R. J. Baldessarini, N. S. Kula, K. G. Walton and R. J. Borgman, "Hydrolysis of Diester Prodrugs of Apomorphine," Biochem Pharmacol, Vol. 26, 1977, p. 1749-1756.

10. J. P. Clayton, M. Cole, S. W. Elson, K. D. Hardy, L. W. Mizen and R. Sutherland, "Preparation, Hydrolysis and Absorption of α-carboxy Esters of Carbenicilline," J Med Chem, Vol 18, No. 2, 1975, p. 172-177.

11. E. B. Roche, "Design of Biopharmaceutical Properties Through Prodrugs and Analogs," Am Pharm Assoc, Washington, D.C. 1977, p. 4.

12. F. Bischoff, Y. S. Yee, J. J. Moran and R. E. Katherman, "Enzymatic Hydrolysis of Steroid Hormone Esters by Blood Serum," J Biol Chem, Vol. 189, 1951, p. 729-738.

13. A. A. Sinkula and S. H. Yalkowsky, "Rational for Design of Biologically Reversible Drug Derivatives: Prodrugs," J Pharm Sci, Vol. 64, No. 2, 1975, p. 181.

14. M. M. Abdel-Monem and J. G. Henkel, "Essentials of Drug Product Quality," The CV Mosby Company, Saint Louis, 1978, p. 167.

15. S. Goenechea, "IR-Untersuchungen Sauer und Neutral Reagierender Arzneimittel III," Mikrochimica Acta (Wien), 1972, p. 286-287.

16. K. Kamei and A. Momose, "Gas Chromatography and Mass Spectrometry of Methylated Xantines," Chem Pharm Bull, Vol. 21, No. 6, 1973, p. 1228-1234.

17. J. R. Dyer, "Applications of Absorption Spectroscopy of Organic Compound," Prentice-Hall, N.J., 1965, p. 89.

18. J. F. W. McOmie, "Protective Groups in Organic Chemistry," Plenum Press, London and New York, 1973, p. 100.

19. B. W. Sands and A. T. Rowland, "Neighboring Group Participation Reaction in Steroids. Acetate Migration in the 5-Cholestane Series," Steroids, Vol. 4, No. 2, May 1964, p. 176.

CHAPTER II

STABILITY OF DIPROPIONYL DYPHYLLINE IN AQUEOUS SOLUTION

INTRODUCTION

The chemical action of solvent and other solutes present on a drug in solution is of prime importance in pre-formulation studies. Several hydroxyester derivatives of dyphylline were synthesized in this study with the objective of obtaining compounds which are converted to dyphylline at a controlled rate of enzyme esterases after the compounds have been absorbed into the body. The result will be prolongation of the duration of action of dyphylline. Knowledge of the kinetics of degradation of these ester derivatives of dyphylline under various pH and temperature conditions is required to provide information about the stability of these prodrugs prior to absorption. Such information provides a basis for predicting the stability of the prodrug in the gastrointestinal tract as well as for developing an optimum liquid or solid drug dosage formulation of these prodrugs.

In the present study, the stability of dipropionyl dyphylline was investigated when exposed to several pH values in aqueous buffered solutions. Accelerated stability studies were also employed in order to determine the degradation rate of the compound stored at a variety of temperatures. Solvent programming high pressure liquid chromatography (HPLC) was the analytical method used to determine the concentration of the intact diesters remaining as a function of time. The concentration of intact drug or a function of it was linearized

with respect to time and specific rate constants were determined from the slopes of these straight lines and utilized to generate Arrhenius plots.

EXPERIMENTAL

Chemicals and Materials

Dipropionyl dyphylline was synthesized as previously reported. The HPLC internal standard used was 7-(Beta-Hydroxypropyl)-theophylline[1] and was purchased commercially. Buffers of different pH used for the stability study of dipropionyl dyphylline were prepared according to published procedures and were used as such without further adjustment for any specific ionic strength (1). For HPLC the internal standard was dissolved in buffer pH 7.15 which was prepared using a described procedure (2). All chemicals used for preparing the buffers (citric acid,[2] phosphoric acid,[3] boric acid,[4] sodium hydroxide,[5] hydrochloric acid,[6] potassium dihydrogen phosphate,[7] and disodium hydrogen phosphate)[8] were analytical quality and were used without further purification. The pH values of the reaction solutions were measured at room temperature initially and at the end of each experiment with a pH meter[9] standardized at pH 4 and pH 7.[10] Samples were maintained at constant temperatures using a circulating water bath, and a magnetic stirrer[11] agitated the samples. At high temperatures, if the degradations were slow and the total sampling

time periods were longer than 12 hours, an oven[12] was usually used in place of the water bath.

Analytical

The high pressure liquid chromatograph (HPLC) employed was equipped with two mobile phase delivery pumps,[13] a programmer,[14] a sample injector apparatus,[15] a column,[16] a UV detector[17] set at 280 nm, a recorder[18] and an integrator.[19]

Since the retention times among dipropionyl dyphylline, monopropionyl dyphylline and dyphylline were either too divergent when the mobile phase was quite polar or too convergent when the mobile phase was quite nonpolar, solvent programming chromatographic conditions were developed to obtain good separation among dyphylline and its mono- and di- propionyl esters with a total retention time of less than ten minutes. The chromatographic mobile phases for pum A and pump B were 10% acetonitrile in distilled water (V/V) and 60% acetonitrile in distilled water (V/V) respectively. The initial condition of 0% B and the final condition was 100% B. The programming time was 3 minutes. The curve used was linear. The solvent flow rate was 2.0 ml/min. The UV detector was generally set at a sensitivity of 1.0. All samples were analyzed at room temperature.

Preparation of Standard Curves

Two sets of standard solutions with known concentrations of dipropionyl dyphylline, monopropionyl dyphylline, dyphylline, and a constant concentration of 7-(β-Hydroxypropyl)-theophylline (internal standard) in acetonitrile were accurately prepared. The concentrations of dyphylline and its mono- and di- esters ranged from 160 μg/ml to 8 μg/ml. The optimum concentration of the internal standard was 20 μg/ml. These standard solutions were analyzed using the solvent programming chromatographic condition described above. The area under the curve (AUC) ratios of dipropionyl dyphyllline, monopropionyl dyphylline and dyphylline were plotted versus their known concentrations and the intercepts, slopes and correlation coefficients (r^2) of these standard curves determined. The coefficients of variations (CV) were also calculated after inversely estimating the concentrations from the standard curves (3).

Stability Studies of Dipropionyl Dyphylline

All stock solutions for the buffers were prepared and stored in volumetric flasks at room temperature until used. Buffers needed were usually prepared from stock solutions one or two days before each experiment. The internal standard solution was prepared in a 500 ml volumetric flask and contained 40 μg of internal standard per

one ml of the buffer (pH 7.15). This internal standard solution was maintained at room temperature and used for all experiments.

Buffers and all glassware needed for each experiment were allowed to reach temperature equilibrium for at least 20 minutes before the zero time of the experiment. One ml of the internal standard solution was pipetted in advance into screw cap test tubes, capped, wrapped with parafilm and placed in a test tube rack packed in ice. Dipropionyl dyphylline (500 mg) was accurately weighed into a 100 ml volumetric flask. At zero time 100 ml of the temperature equilibrated buffer of the desired pH was transferred into the flask containing the drug. This mixture was shaken vigorously for 3-5 minutes and suction filtered into a 250 ml flask equilibrated and maintained with a water bath at the required temperature and the undissolved dipropionyl dyphylline collected on the filter was discarded. The top and side arm of the suction flask which contained the filtrate was then covered with parafilm or foil to prevent evaporation. At designated times, one ml samples were pipetted from the suction flask and placed into a test tube previously prepared which contained one ml of ice cold internal standard solution. This mixture was mixed well by vortexing, capped, wrapped with parafilm and kept in the ice bath. This procedure stopped all degradation as the drug was now in a cold, neutral solution. The samples were usually analyzed the same day or kept in the refrigerator and analyzed within 48 hours. The sampling times

of each experiment were variable based on preliminarily observed or predicted degradation rates. One 10 ml sample was taken at the beginning (shortly after filtration) and another 10 ml sample at the end of the experiment for determining pH. Two 5 ml samples were also removed at different time intervals, and mixed with an equal volume of internal standard solution, and the pH's measured to insure that neutralization was occurring. Stability studies were conducted at seven different pH values (1.75, 2.77, 3.60, 4.89, 6.35, 8.0 and 9.46) and at three different temperatures for each pH value.

RESULTS AND DISCUSSIONS

Figure 1 shows a typical HPLC tracing when solvent programming as described earlier was used. All compounds involved in this study separated nicely in less than 7 minutes.

The area under the curve (AUC) ratios of dipropionyl dyphylline, monopropionyl dyphylline and dyphylline were directly related to their concentrations. Linear regression of these AUC ratios on concentrations resulted in correlation coefficients (r^2) of 0.9964, 0.9924 and 0.9906 respectively. Figure 2 shows typical standard curves for dipropionyl dyphylline, monopropionyl dyphylline and dyphylline. Data used to establish these standard curves are summarized in Table I. Inversely estimated concentrations from each individual standard curve are shown in detail in Table II. When both

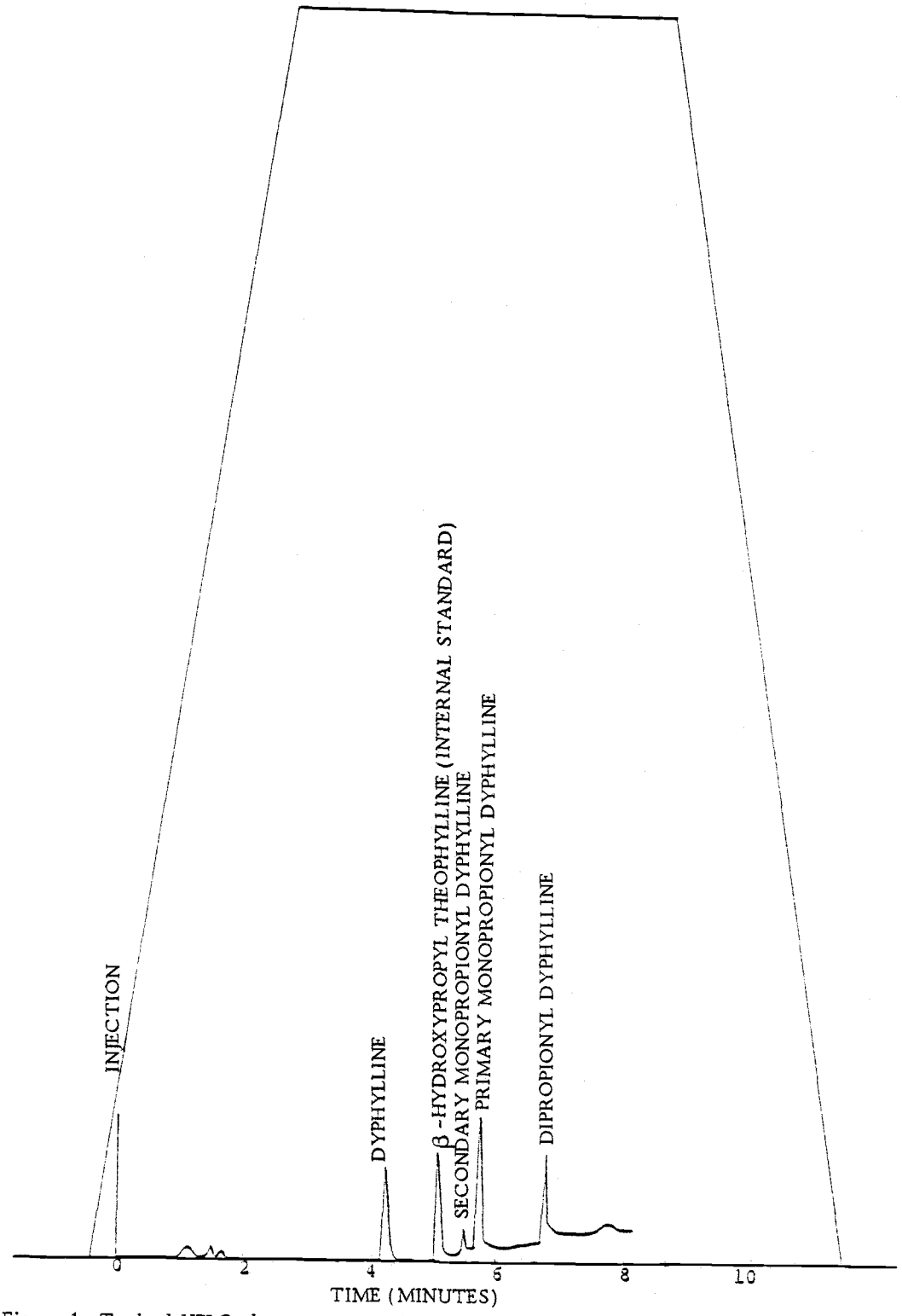

Figure 1. Typical HPLC chromatogram of degraded dipropionyl dyphylline using HPLC solvent programming

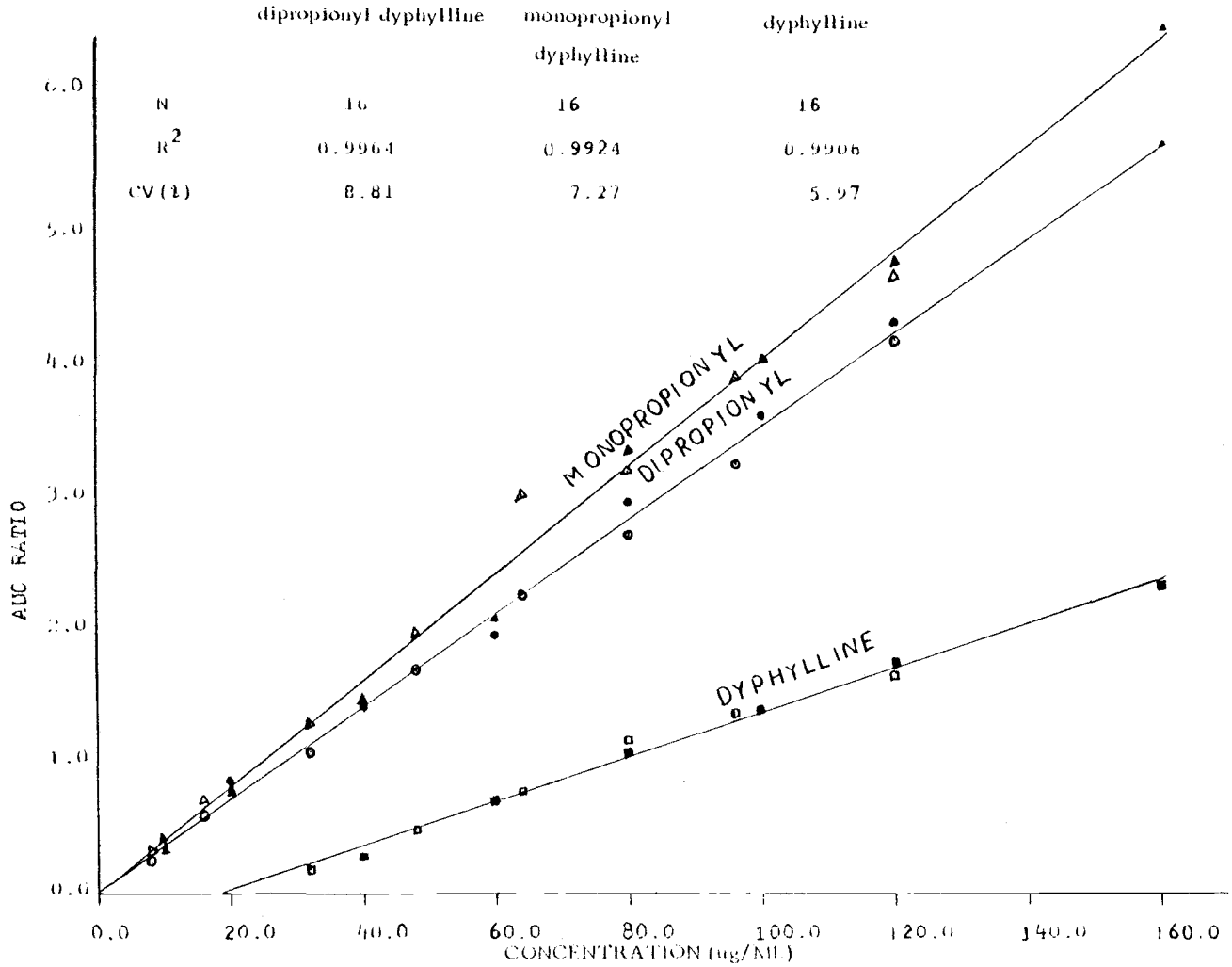

Figure 2. Typical standard curves for dipropionyl dyphylline (○ = trial 1, ● = trial 2), monopropionyl dyphylline (△ = trial 1, ▲ = trial 2) and dyphylline (□ = trial 1, ■ = trial 2)

Table I. Standard curves for dipropionyl dyphylline, monopropionyl dyphylline and dyphylline using 20 μg/ml β-hydroxypropyl theophylline as the internal standard. The solutions were prepared in acetonitrile.

Known Concentration (μg/ml)	Area under the curve (AUC) ratio					
	Dipropionyl Dyphylline		Monopropionyl Dyphylline		Dyphylline	
	Trial 1[a] 8/7/78	Trial 2[b] 8/24/78	Trial 1[a] 8/7/78	Trial 2[b] 8/24/78	Trial 1[a] 8/7/78	Trial 2[b] 8/24/78
8	-	0.2496	-	0.3194	-	-
10	0.4251	-	0.3632	-	-	-
16	-	0.5967	-	0.7161	-	-
20	0.8673	-	0.7910			
32	-	1.0798	-	1.2927	-	0.1787
40	1.4208	-	1.4661	-	0.2769	-
48	-	1.6759	-	1.9670	-	0.4848
60	1.9607	-	2.0888	-	0.7208	-
64	-	2.2586	-	2.9993	-	0.7836
80	2.9478	2.7069	3.3292	3.1820	1.0753	1.1534
96	-	3.2305	-	3.7938	-	1.3652
100	3.6155	-	4.0180	-	1.3914	-
120	4.3242	4.1598	4.7632	4.6449	1.7435	1.6265
160	5.6633	-	6.5270	-	2.3178	-
Number of Samples	16		16		12	
intercept[c]	0.0160		-0.0029		- 0.3078	
slope[c]	0.0350		0.0401		0.0168	
r^2[c]	0.9964		0.9924		0.9906	

[a]The total volume was qs. to 25 ml using volumetric flasks.

[b]The total volume was qs. to 10 ml in the test tube using pipettes.

[c]Results from linear regression of AUC ratios of both trials on concentrations.

Table II. Inversely estimated concentrations from individual standard curve data for dipropionyl dyphylline, monopropionyl dyphylline and dyphylline using solvent programming HPLC analysis

Concentration (µg/ml)	Dipropionyl Dyphylline		Monopropionyl Dyphylline		Dyphylline	
	Trial 1[a]	Trial 2[b]	Trial 1	Trial 2	Trial 1	Trial 2
8 c	-	6.67	-	8.03	-	-
d		83.36		100.36		
10 c	11.68	-	9.12	-	-	-
d	116.79		91.20			
16 c	-	16.58	-	17.91	-	-
d		103.61		111.95		
20 c	24.30	-	19.78	-	-	-
d	121.51		98.89			
32 c	-	30.37	-	32.28	-	28.94
d		94.90		100.86		90.44
40 c	40.10	-	36.60	-	34.78	-
d	100.25		91.49		86.95	
48 c	-	47.39	-	49.08	-	47.15
d		98.72		102.24		98.23
60 c	55.52	-	52.11	-	61.19	-
d	92.53		86.85		101.98	
64 c	-	64.02	-	74.79	-	64.92
d		100.03		116.86		101.44
80 c	83.69	76.82	85.01	79.34	82.28	86.92
d	104.62	96.02	103.76	99.18	102.85	108.65
96 c	-	91.76	-	94.59	-	-
d		95.59		98.53		
100 c	102.75	-	100.17	-	101.38	99.32
d	102.75		100.17		101.38	103.67
120 c	122.99	113.29	118.74	115.79	122.33	115.07
d	102.49	98.58	98.95	96.49	101.69	95.89
160 c	161.21	-	162.68	-	156.19	-
d	100.76		101.67		97.62	
Average	105.21	96.35	96.62	103.31	98.70	99.72
Standard Deviation	9.40	6.96	6.31	7.18	6.03	6.35
C.V. (%) e	8.94	6.18	6.22	6.95	6.11	6.16

a. The total volume was ca. to 15ml using volumetric flask.
b. The total volume was ca. to 10ml in the test tube using volumetric pipettes.
c. Inversely estimated concentration.
d. (Inversely estimated concentration/known concentration) (100).
e. Coefficient of variation = (Standard deviation/average)(100).

trials were combined for each drug the standard deviations for percent of theory by inverse estimation were 8.87, 7.27, 5.93 and the coefficient of variations were 8.81, 7.27, 5.97 for dipropionyl dyphylline, monopropionyl dyphylline and dyphylline respectively.

The molar extinction coefficients of dyphylline, monopropionyl dyphylline and dipropionyl dyphylline in water were determined and the results are summarized in Table III. The molar extinction coefficient of dyphylline is a little bit higher than those of the monopropionyl and dipropionyl esters. However, the standard curves in figure 2 show different slopes among dyphylline and its mono- and di- propionyl esters with dyphylline exhibiting the lowest slope. This is opposite to what would have been predicted and the cause is not known at the present time.

Rate Constant Determinations

The kinetics of dipropionyl dyphylline degradation were evaluated at various pH values and temperatures. Figures 3 and 4 are typical semilogarithmic plots of intact concentration of dipropionyl dyphylline in μg/ml vs. time for the hydrolysis of this compound at various pH values at room temperature and at 60°C respectively. It can be seen that the effects of pH are, in a relative sense, nearly the same for the different temperatures. Figures 5-7 and 9-11 show typical apparent first order plots for the hydrolysis of dipropionyl

Table III. Molar Extinction Coefficient of Dyphylline, Monopropionyl Dyphylline and Dipropionyl Dyphylline in Water.

Compound	Concentration (Molar)	Absorbance (λ =280)	Molar Extinction Coefficient (ε)
Dyphylline	0.0000393	0.340	8644.28
	0.0000590	0.505	8559.53
	0.0000787	0.700	8898.52
		Average =	8700.78
Monopropionyl dyphylline	0.0000322	0.275	8533.44
	0.0000483	0.420	8688.60
	0.0000645	0.555	8611.02
		Average =	8611.02
Dipropionyl dyphylline	0.0000273	0.232	8499.80
	0.0000409	0.345	8426.52
	0.0000546	0.458	8383.83
		Average =	8438.74

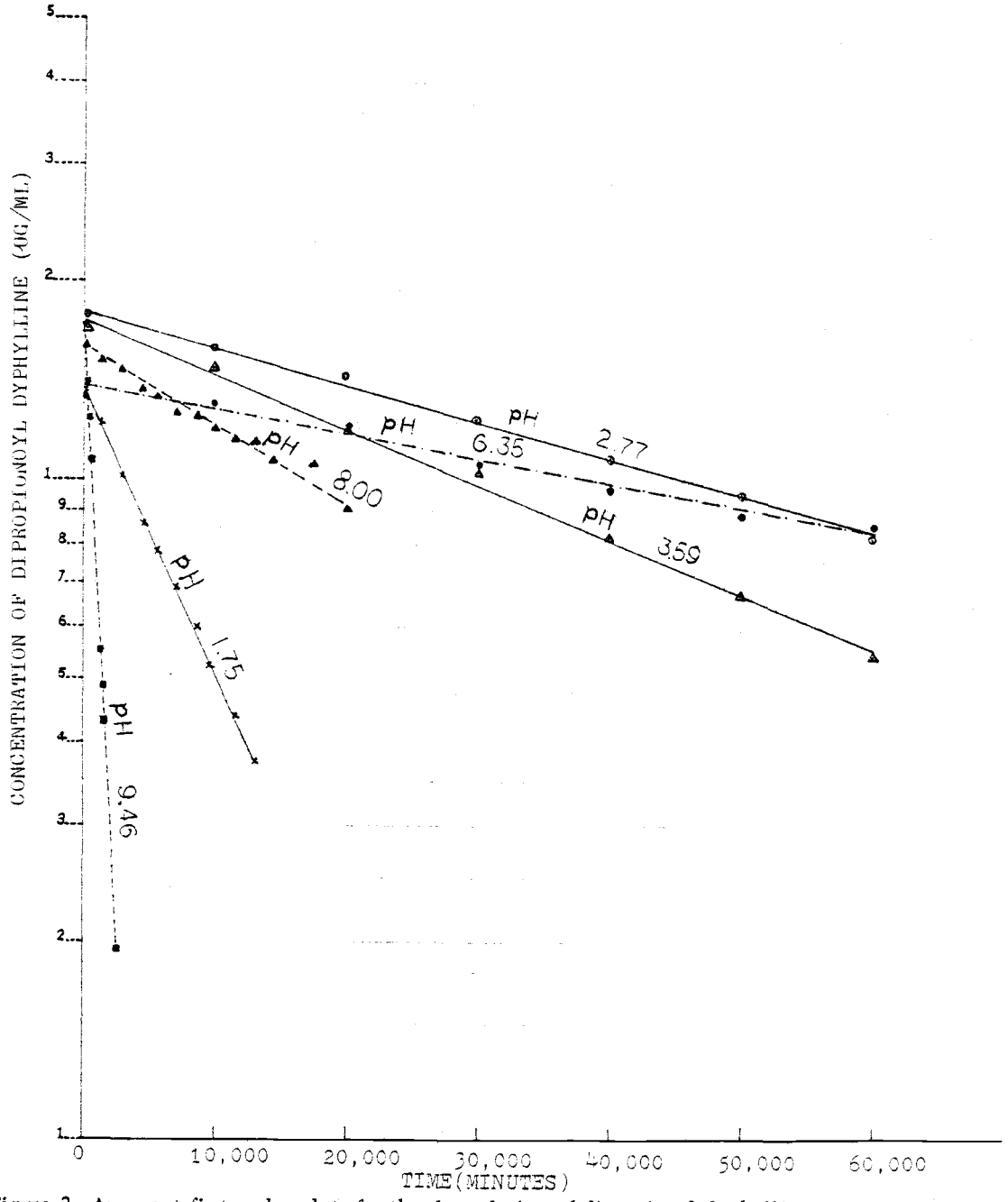

Figure 3. Apparent first-order plots for the degradation of dipropionyl dyphylline at room temperature at various pH values; pH 1.75 (x), pH 2.77 (○), pH 3.59 (△), pH 6.35 (●), pH 8.00 (▲), pH 9.46 (■).

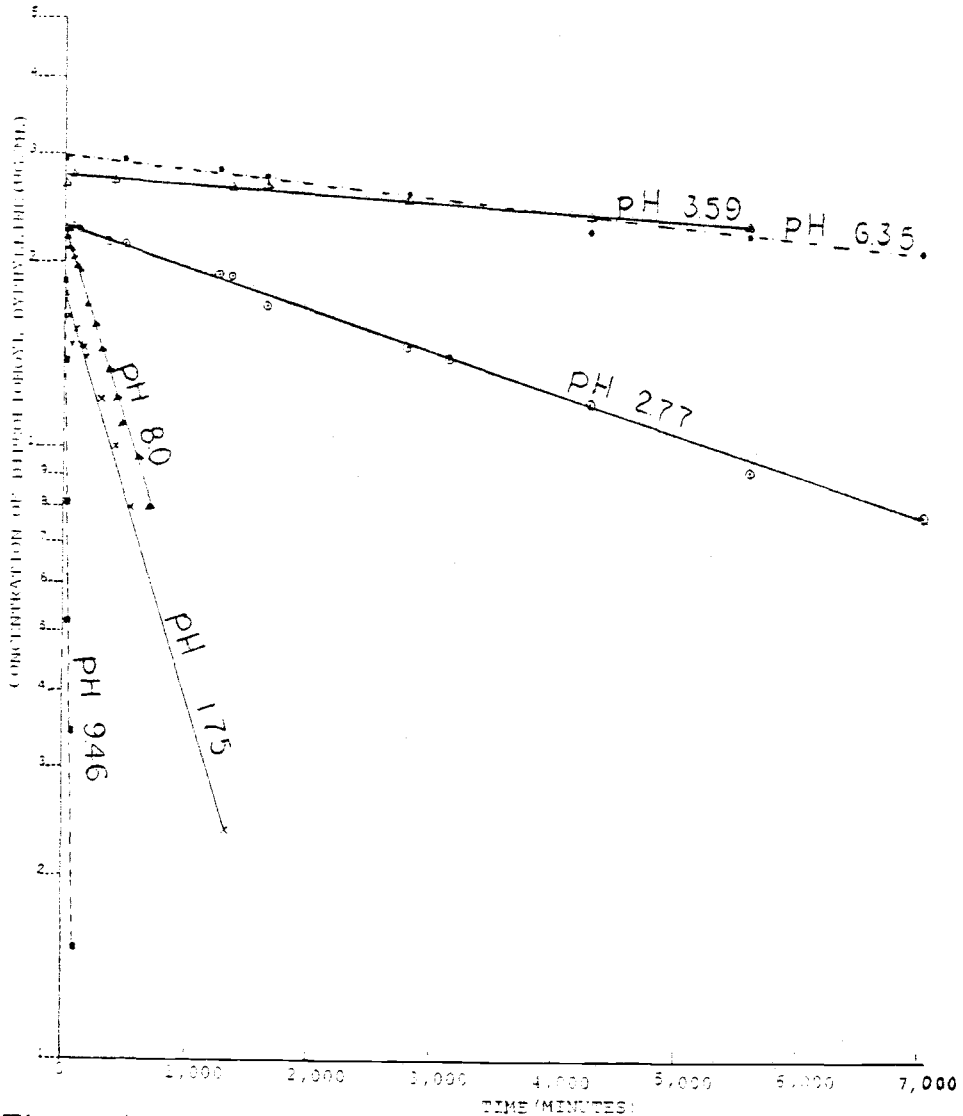

Figure 4. Apparent first-order plots for the degradation of dipropionyl dyphylline at 60°C at various pH values; pH 1.75 (x), pH 2.77 (o), pH 3.59 (Δ), pH 6.35 (●), pH 8.0 (▲), pH 9.46 (■)

dyphylline at three different temperatures in buffer pH 1.75, 2.77, 3.59, 6.35, 8.00 and 9.46 respectively. Figure 8 shows the degradation in pH 4.85 at two different temperatures.

Table IV summarizes the linear regression of ln concentration on time for each pH at each temperature studied. They all provided r^2 values higher than 0.94. For pH greater than 8.0 and lower than 3.0, the r^2 values were greater than 0.99. This highly linear relationship between ln concentration and time suggests an apparent first order degradation of dipropionyl dyphylline under the conditions studied, i.e. the rate of change per unit of time is proportional to the first power of the concentration of the compound being transformed.

$$-dc/dt = kc^1$$

$$\int_0^t \frac{dc}{c} = \int_0^t -kdt$$

$$\therefore \ln c = \ln c_o - kt$$

Preliminary studies have been conducted with a more dilute buffer solution. Figure 12 shows the results obtained from the degradation of dipropionyl dyphylline in aqueous buffer pH 11.8 which had been diluted to one-tenth of the full strength (1). The results show that dipropionyl dyphylline degradation in such dilute buffer exhibited second order rather than first order behavior.

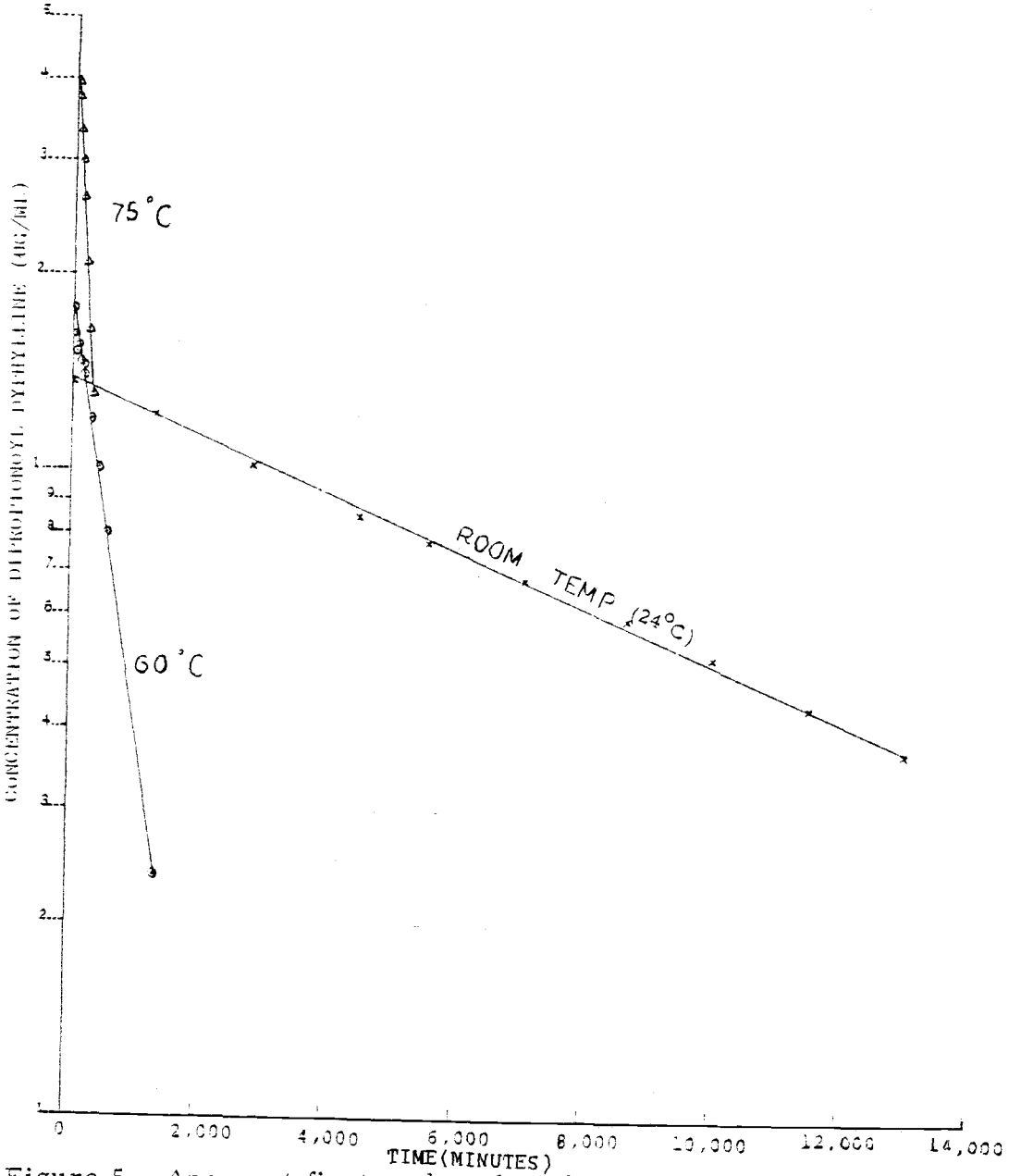

Figure 5. Apparent first-order plots for the degradation of dipropionyl dyphylline in buffered aqueous solution (pH 1.75) at three different temperatures; room temperature (24°C) (x), 60°C (o), 75°C (Δ)

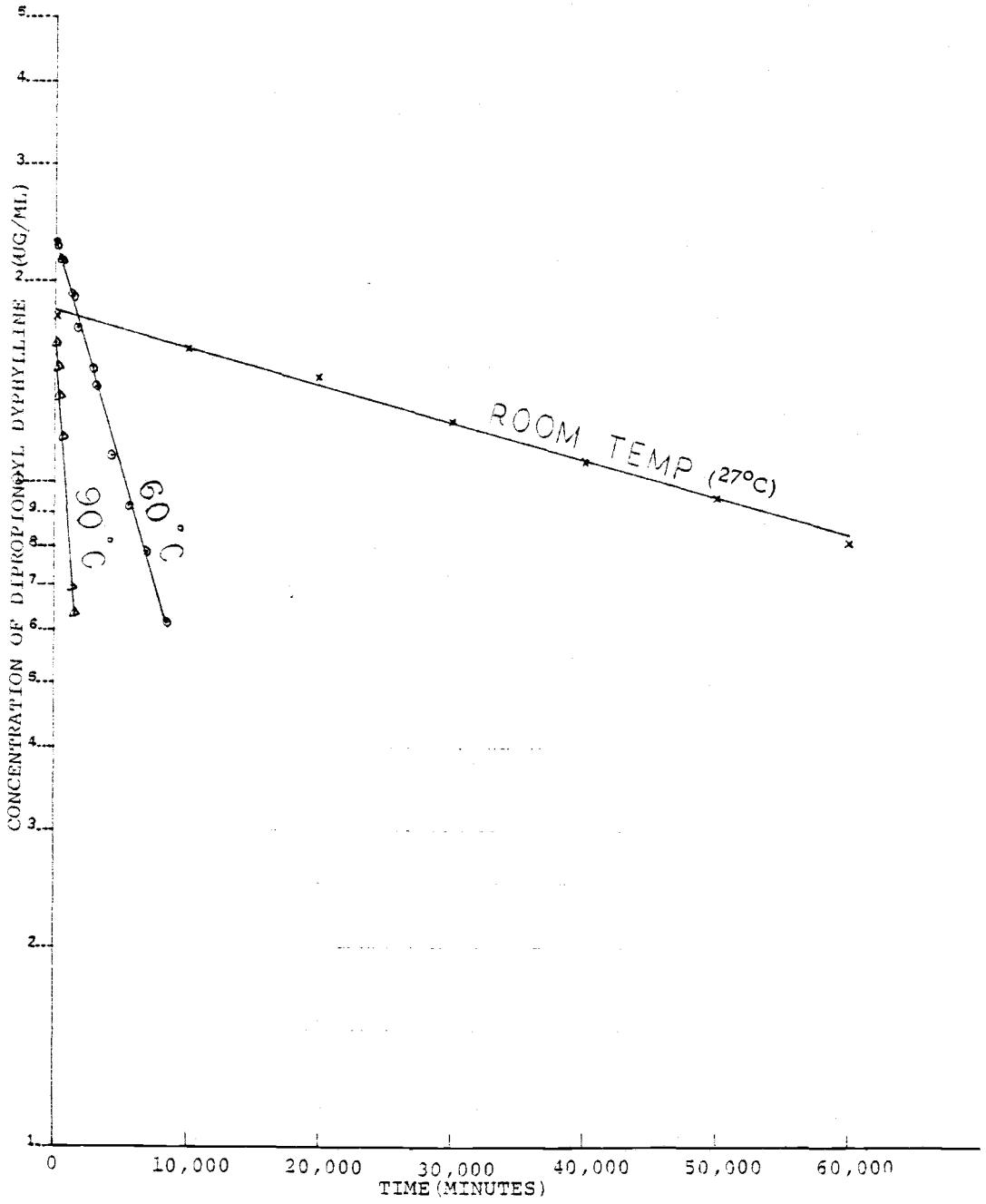

Figure 6. Apparent first-order plots for the degradation of dipropionyl dyphylline in buffered aqueous solution (pH 2.77) at three different temperatures; room temperature (27°C) (x), 60°C (o), 90°C (Δ)

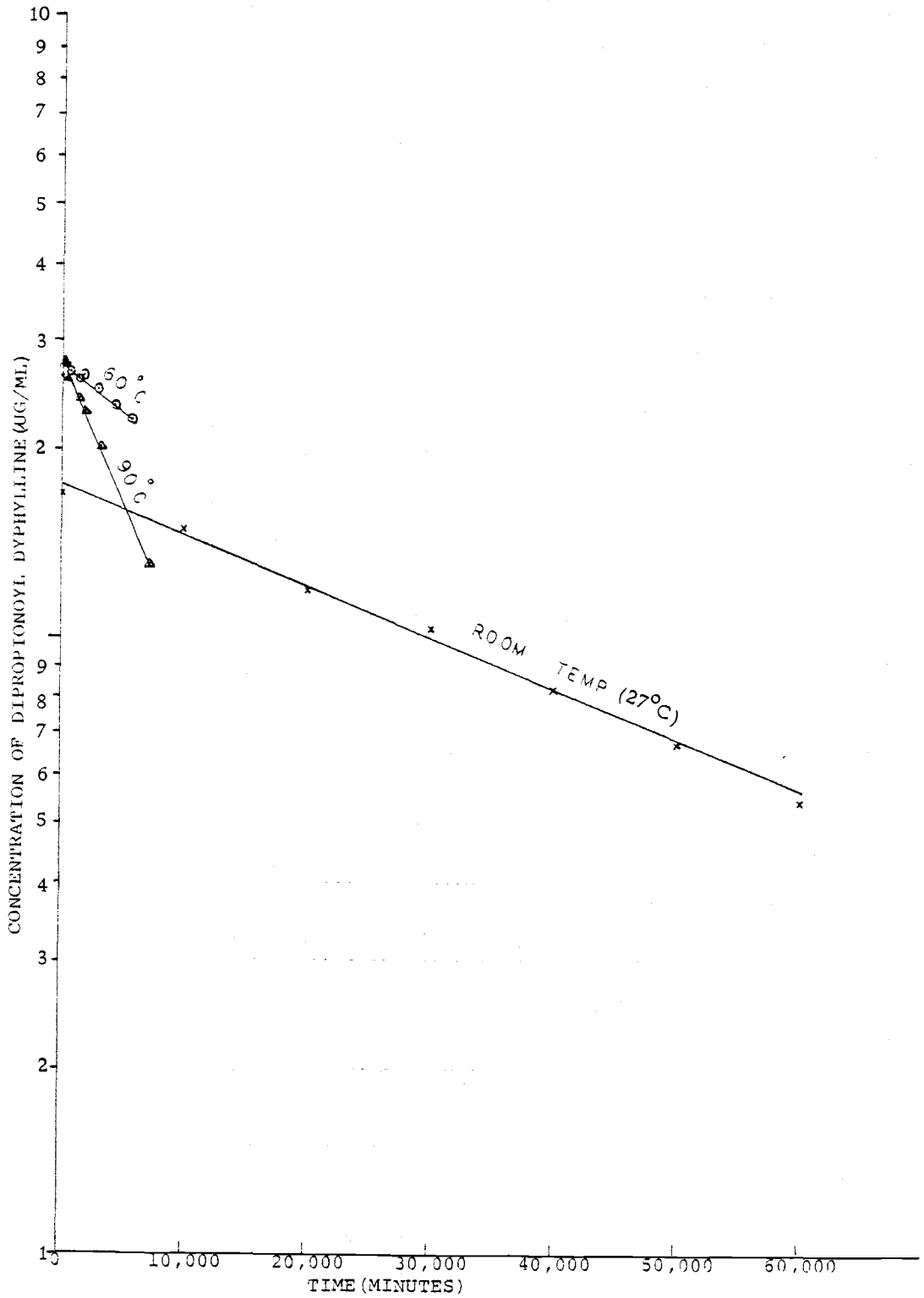

Figure 7. Apparent first-order plots for the degradation of dipropionyl dyphylline in buffered aqueous solution (pH 3.59) at three different temperatures; room temperature (27°C) (x), 60°C (o), 90°C (Δ)

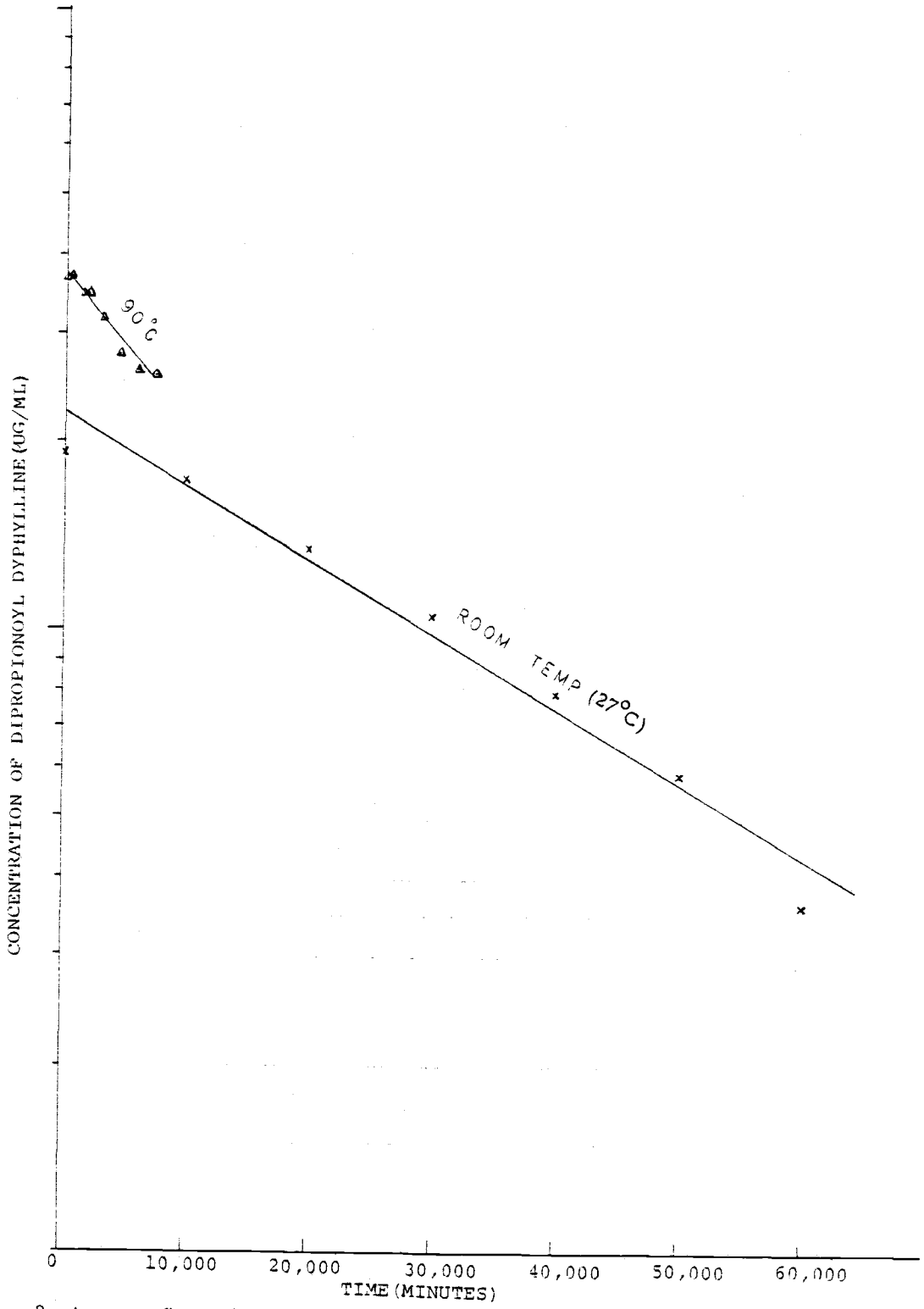

Figure 8. Apparent first-order plots for the degradation of dipropionyl dyphylline in buffered aqueous solution (pH 4. 89) in two different temperatures; room temperature (27°C) (x), 90 °C (Δ)

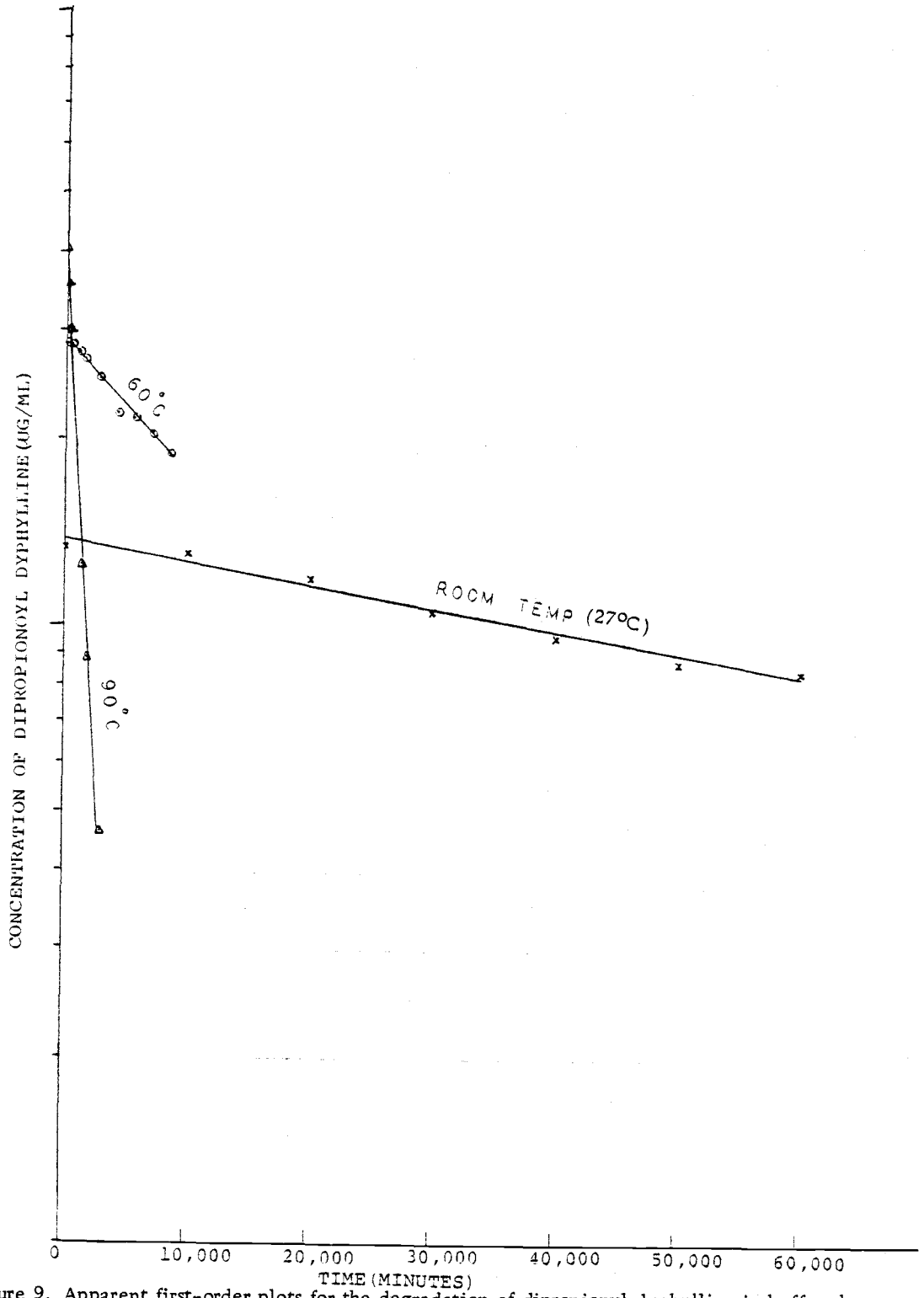

Figure 9. Apparent first-order plots for the degradation of dipropionyl dyphylline in buffered aqueous solution (pH 6.35) at three different temperatures; room temperature (27°C) (x), 60°C (o), 90°C (△)

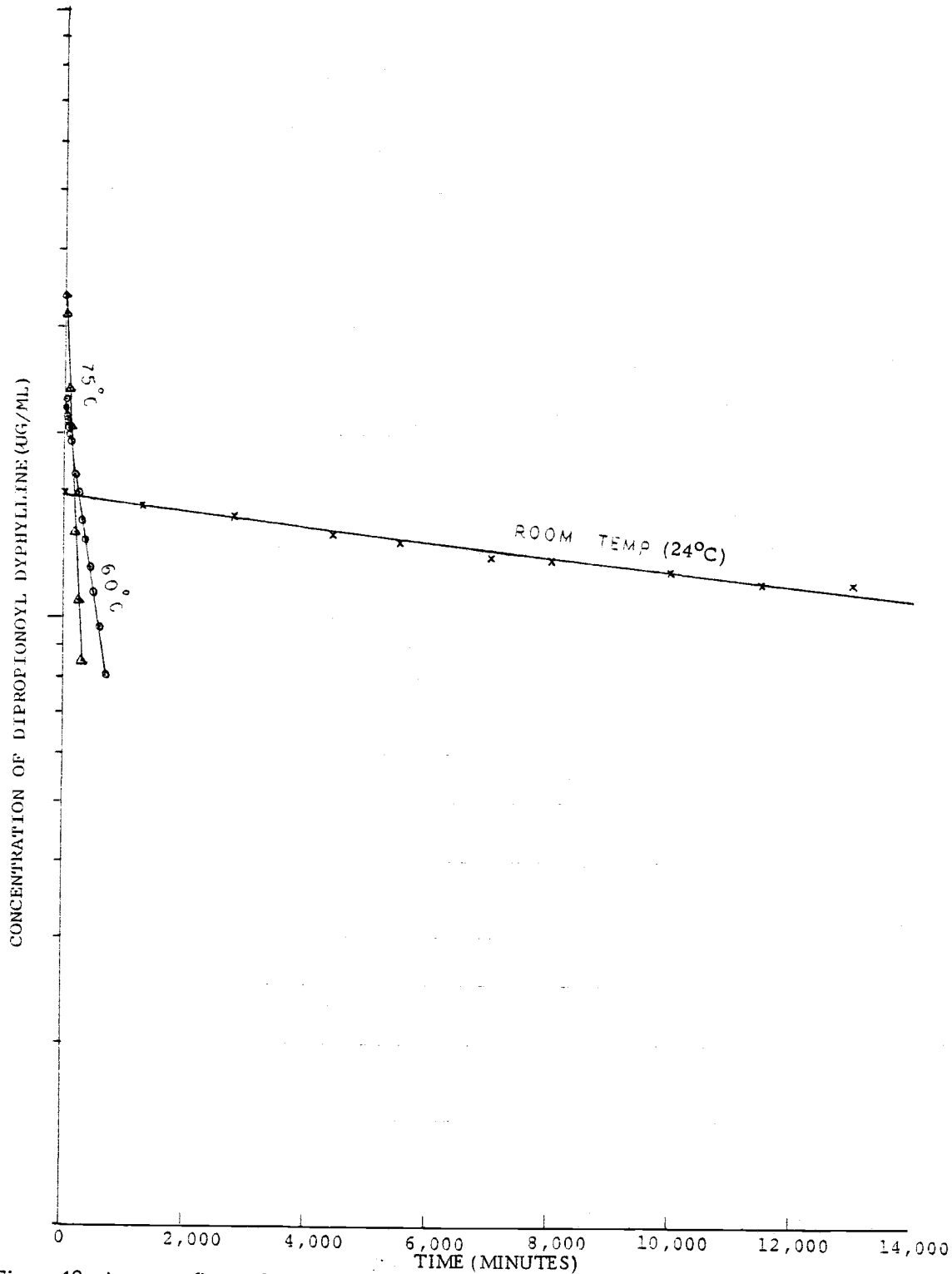

Figure 10. Apparent first-order plots for the degradation of dipropionyl dyphylline in buffered aqueous solution (pH 8.00) at three different temperatures; room temperature (24°C) (x), 60°C (⊙), 75°C (△)

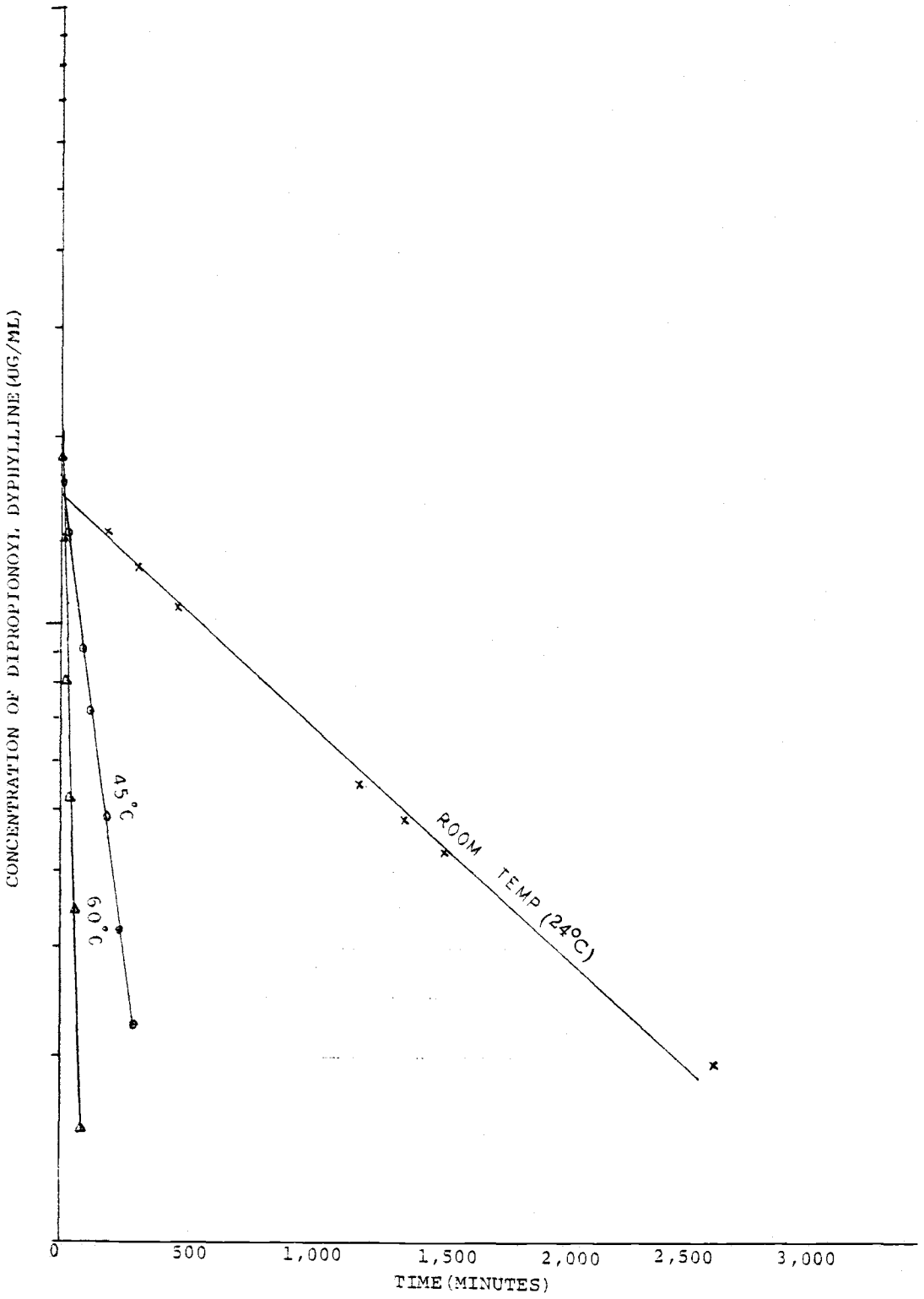

Figure 11. Apparent first-order plots for the degradation of dipropionyl dyphylline in buffered aqueous solution (pH 9.46) at three different temperatures; room temperature (24°C) (x), 45°C (⊙), 60°C (△)

Table IV. Summary of results of linear regression of ln concentration of dipropionyl dyphylline on time for the degradation of dipropionyl dyphylline in various pH buffers at specific temperatures.

pH	Temperature °C	Number of Samples	Intercept (μg/ml) (S. E.)	-slope = k (10^6 min^{-1}) (S. E.)	r^2	t 1/2 = ln2/k (min)
1.75	24	10	136.57 (1.01)	98.36 (1.51)	0.9981	7047.04
	60	11	177.25 (1.02)	1489.39 (39.95)	0.9936	465.39
	75	8	416.98 (1.01)	3850.98 (44.65)	0.9992	179.99
2.77	27	7	180.36 (1.01)	12.85 (0.36)	0.9961	53941.41
	60	14	228.69 (1.01)	155.16 (2.16)	0.9977	4467.31
	90	6	163.00 (1.00)	624.80 (3.95)	0.9998	1109.39
3.59	27	7	174.46 (1.02)	19.02 (0.57)	0.9955	36443.07
	60	8	268.72 (1.01)	29.90 (3.06)	0.9407	23182.18
	90	7	272.69 (1.01)	103.24 (2.65)	0.9967	6713.94
4.89	27	7	222.92 (1.08)	27.52 (2.18)	0.9697	25187.03
	60	-	-	-	-	-
	90	8	375.70 (1.02)	56.63 (4.68)	0.9606	12239.93
6.35	27	7	137.85 (1.02)	8.34 (0.56)	0.9776	83111.17
	60	9	290.28 (1.01)	50.89 (2.74)	0.9801	13620.50
	90	7	348.20 (1.08)	630.41 (26.51)	0.9912	1099.52
8.00	24	13	156.14 (1.01)	25.65 (1.25)	0.9745	27023.28
	60	15	224.32 (1.01)	1464.00 (21.25)	0.9973	473.46
	75	7	337.75 (1.02)	4733.14 (108.88)	0.9974	146.45
9.46	24	8	160.73 (1.03)	823.03 (24.33)	0.9948	842.19
	45	7	171.48 (1.02)	6916.45 (112.83)	0.9987	100.22
	60	6	204.46 (1.03)	29319.50 (649.43)	0.9980	23.64

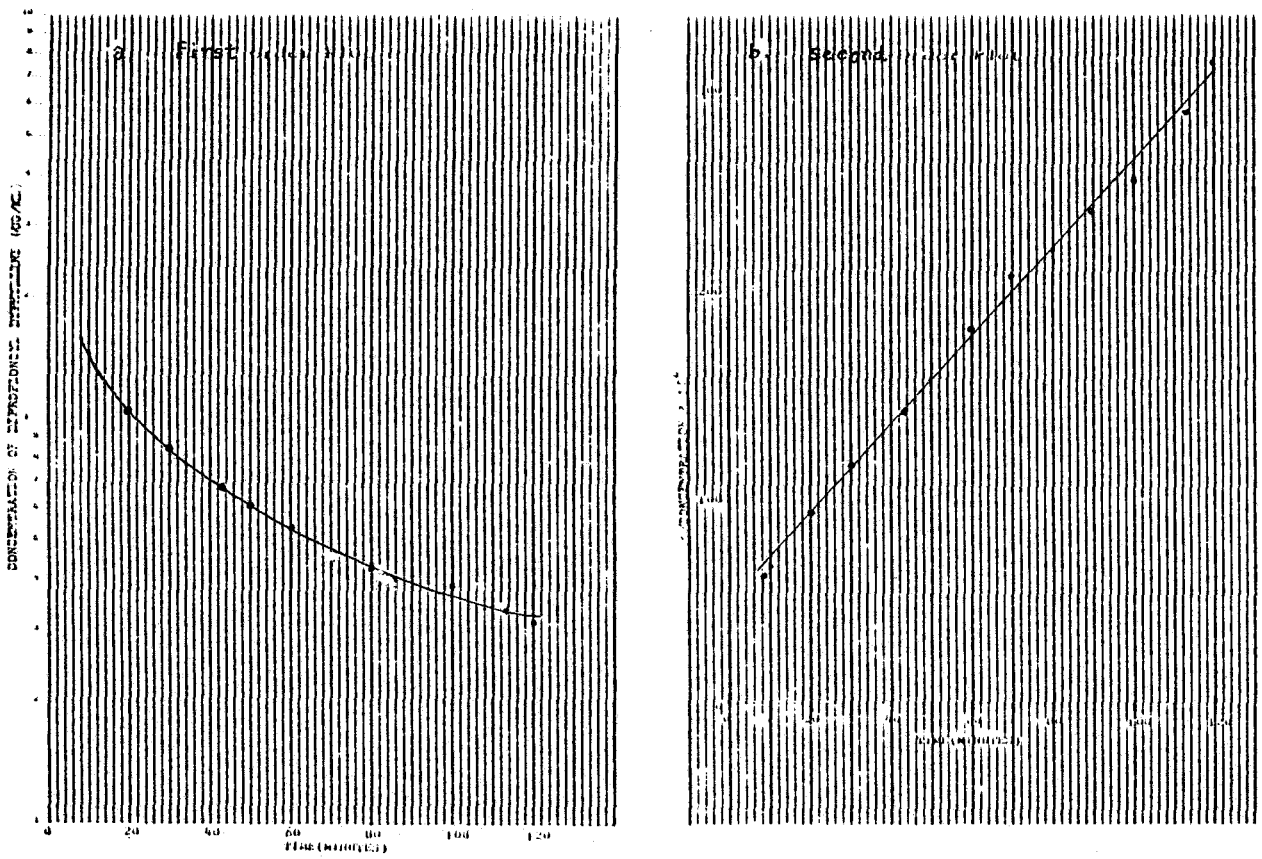

Figure 12. Comparison of first-order (a) and second-order (b) plots for dipropionyl dyphylline degradation at 50°C in buffered aqueous solution (pH 11.8) which had been diluted to one-tenth of the full strength.

$$-dc/dt = kc^2$$

$$\int_o^t c^{-2}\, dc = \int_o^t -k\,dt$$

$$\frac{1}{c} = \frac{1}{c_o} + kt$$

Thus, the plot of 1/c vs. time was linear.

For the hydrolysis of esters, hydrogen ions and hydroxide ions are generally the sole effective acid and base catalysts respectively, i.e. specific acid-base catalysis are occurring when general acid and base catalysis are not important (4). If catalysis is effected simultaneously by hydrogen and hydroxide ions and the reaction may also occur spontaneously, i.e. without a catalyst, then the rate of reaction may be written as (4)

$$v = k_o[S] + k_{H^+}[H^+][S] + k_{OH^-}[OH^-][S]$$

The apparent first-order rate constant is therefore given by

$$k = k_o + k_{H^+}[H^+] + k_{OH^-}[OH^-]$$

or

$$k = k_o + k_{H^+}[H^+] + \frac{k_{OH^-} k_w}{[H^+]}$$

k_o = rate constant of the spontaneous reaction

k_{H^+} and k_{OH^-} = catalytic constants for H^+ and OH^- respectively

k_w = ionic product of water = 10^{-14}

At pH 11.8, the concentration of hydrogen ions should be reduced to such an extent that these ions do not have any appreciable catalytic action; the hydroxide ions are then the only effective catalysts, and the velocity constant k can be written as

$$k = k_{OH^-} [OH^-]$$

or $$v = k_{OH^-} [OH^-] [S]$$

In high concentrations of buffers, the hydroxide ion concentration could be assumed to remain constant, therefore

$$v = k'_{OH^-} [S]$$

which is typical first-order kinetics and $k'_{OH^-} = k_{OH^-} [OH]$. On the other hand, when the buffer strength was low the hydroxide ions concentration could change as the reaction occurred, especially in the case presented here where one of the products of the hydrolysis of dipropionyl esters was propionic acid and thus the rate of reaction became dependent on both the hydroxide ions and substrate (dipropionyl dyphylline) concentrations, i.e. the reaction rate followed the second-order law (5-8). A downward deviation (Figure 12) indicates that the reaction is proceeding more slowly than would be expected for first-order reaction kinetics which reflects the decrease of hydroxide ions concentration with time and the occurrence of a second-order degradation.

Pseudo first-order rate constants, obtained in the presence of an excess of buffer provides a particularly useful method for evaluation of reaction mechanisms because they make possible a separation of the variables involved and the reaction occurs in a controlled manner, which is often difficult or impossible if the reaction occurs with the reactants at similar or equal concentrations (5). Moreover,

the most important reason for evaluating degradation in excess buffer is that the gastrointestinal tract in the body contains sufficient buffer strength to allow apparent first-order degradation to occur. Therefore, full strength buffers were used throughout this study.

Log k_{pH}-pH Profiles - For the degradation of dipropionyl dyphylline in aqueous buffer, a pH- rate profile (Figure 13) was constructed from first-order rate constants and pH values at 60°C and room temperature. There was a range where hydrolysis was catalyzed appreciably by hydrogen ion and catalysis by hydroxide ions was unimportant (pH below 3), and a range at which catalysis by hydroxide was predominate and catalysis by hydrogen ions was unimportant (pH above 8). These ranges were separated by a fluctuating region, extending from approximately pH 3.0 to pH 8.0, in which the amount of hydrogen or hydroxide ion catalysis may have been unimportant in comparison with a spontaneous reaction (4). Within regions of catalysis by hydrogen and hydroxide ions the rates were linear functions of $[H^+]$ and $[OH^-]$ respectively. The slope of the plots of log k versus pH were sufficiently close to -1 and +1 for the left-hand and right-hand limb respectively to confirm specific acid and base catalysis of the dipropionyl ester of dyphylline in the aqueous buffer solutions studied.

For acid $\log k = \log k_{H^+} + \log [H^+]$

or $\log k = \log k_{H^+} - pH$

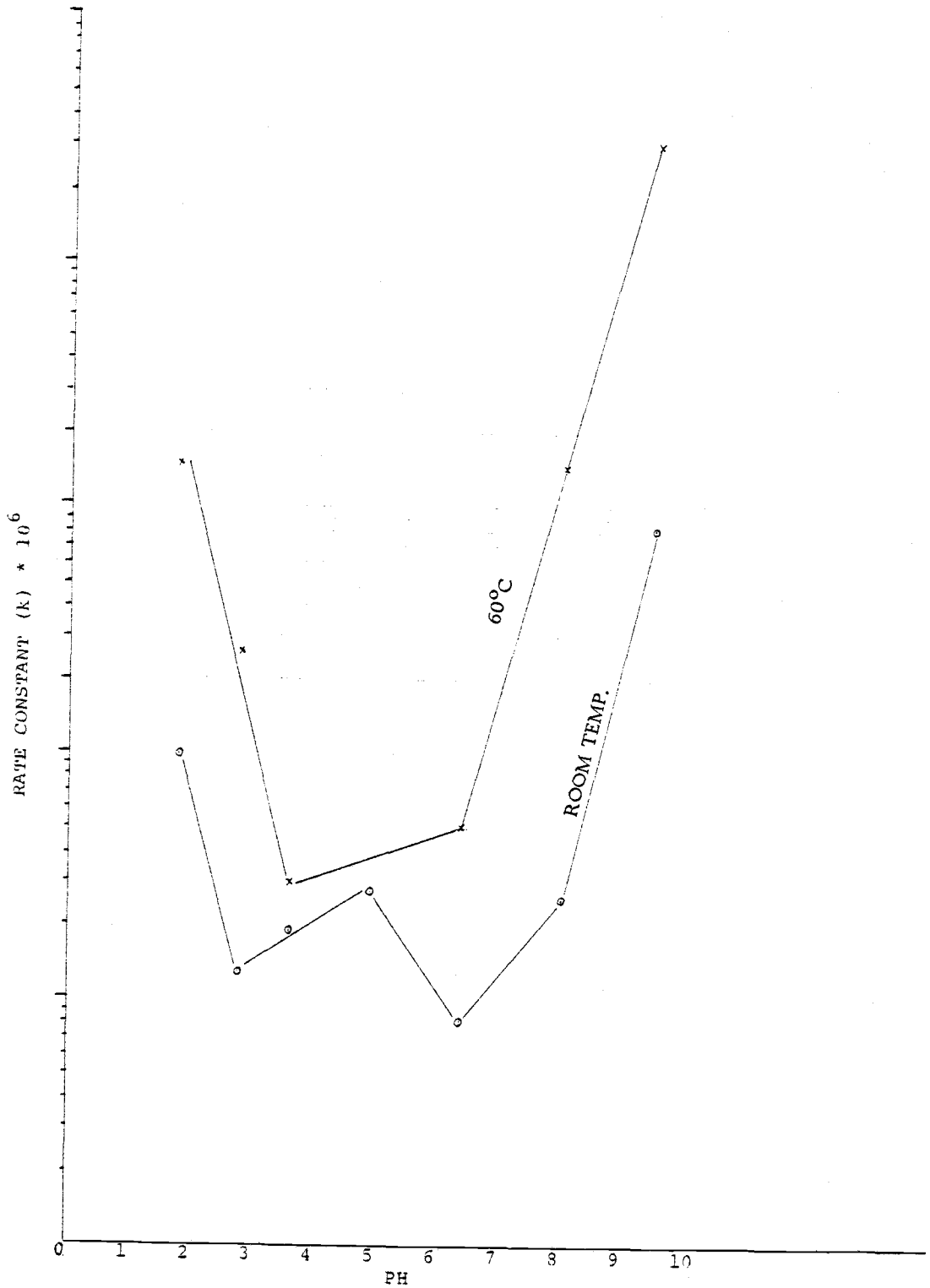

Figure 13. Logarithm of Rate Constant (k) vs. pH Profile for degradation of dipropionyl dyphylline in buffered aqueous solution at room temperature (24-27°C) and 60°C

For base $\log k = \log k_{OH^-} + \log k_w - \log [H^+]$

or $\log k = \log k_{OH^-} + \log k_w + pH$

The essence of an acid catalysis is the possibility of adding a proton to the reacting system on one side of a bond being made or broken, and the essence of a base catalysis to the possibility of removing a proton from the opposite side of that bond. In the case of dipropionyl dyphylline both possibilities existed. When the reactant was simultaneously less acidic and less basic than the solvent the pH rate profile exhibited a minimum similar to the inverted bell which is the common case for typical ester hydrolysis (9). However, it is not very common to find a reaction which shows a water reaction, together with specific catalysis by hydrogen or hydroxide ions (10).

In both acid-catalyzed and base-catalyzed hydrolyses of esters in aqueous solution, there is generally a nucleophilic attack on the carbonyl carbon atom and an electrophilic attack on the alcoholic oxygen atom (11, 12). In alkaline solution the nucleophilic attack is brought about by hydroxide ion and electrophilic attack (actually a proton transfer) by a water molecule; the mechanism therefore can be written as

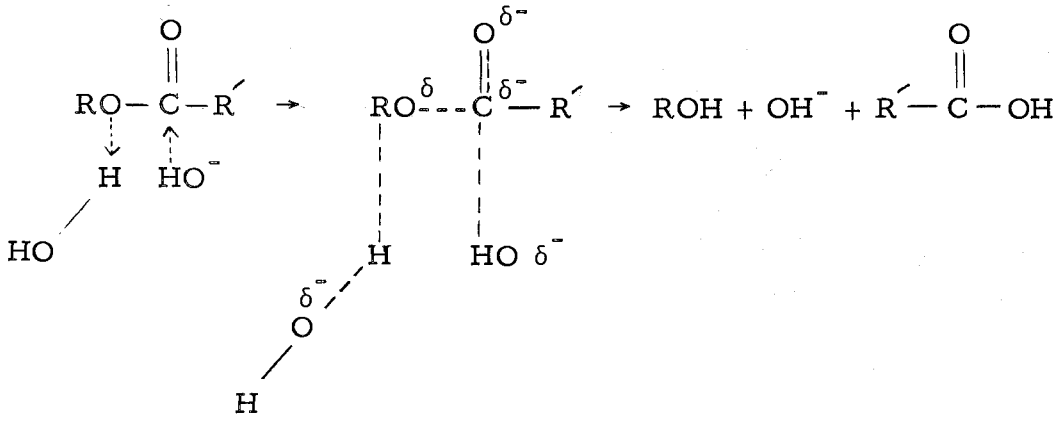

In acid solution, the nucleophilic attack is brought about by a water molecule on the carbonyl carbon atom and there will be proton transfer from the hydrogen ion to the alcoholic oxygen atom; the mechanism for the acid-catalyzed hydrolysis of an ordinary ester is therefore

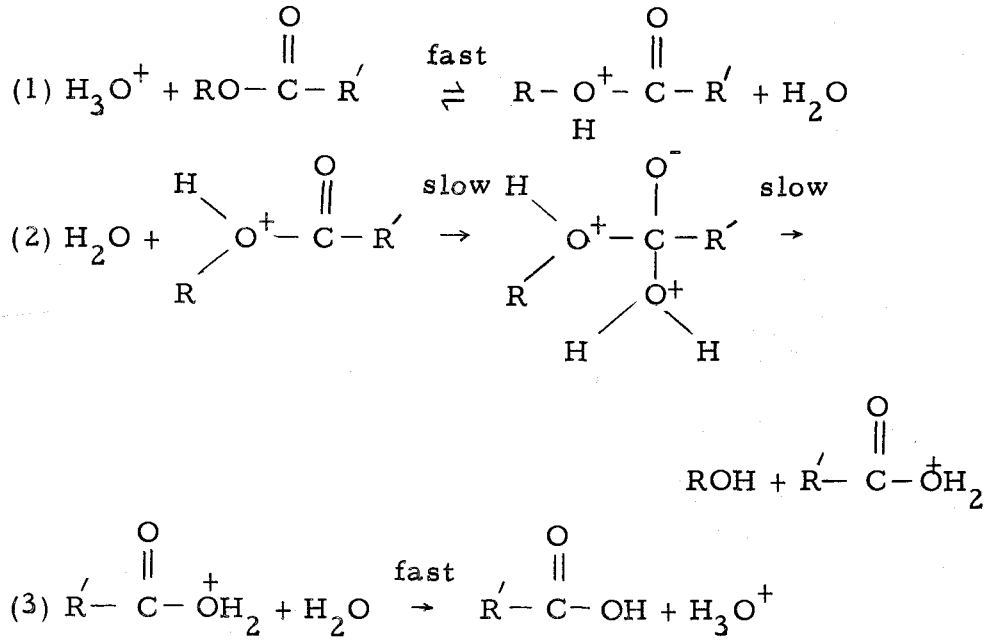

The distinction between the stages is not necessarily as clear cut as represented above.

The hydrolysis of dipropionyl dyphylline was accounted for over the entire pH range by considering all possible bimolecular reactions between the diesters and the H_3O^+, OH^-, and H_2O species. The pH-independent hydrolysis of dipropionyl dyphylline as represented by the fluctuation of rate versus pH over pH range 3-8 in figure 13 might be attributed to attack of water on the compound and might imply general acid-base catalysis (13, 10). The hydrolysis of aspirin in the pH-independent range has been reported (14, 15, 16) and Cephalosporins have also been reported to undergo pH-independent hydrolysis (17). However, the actual cause of the shape of Figure 13 in this study is still not completely explained.

Dependence of Rate on Temperature

An increase in temperature usually causes a marked increase in the rate of a reaction; for reaction in solution a rough generalization is that the rate is doubled by a rise in temperature of 10°C (18, 19). However, in order to increase accuracy of prediction, the Arrhenius relationship is widely used (20, 21). The Arrhenius equation may be written as

$$k = Ae^{-Ea/RT}$$

A is a constant known as the frequency or collision factor, Ea is the activation energy, and the factor $e^{-Ea/RT}$ is the fraction of systems having energy in excess of the value Ea, i. e. there may be

many collision complexes in existence at a given time, but only those with the energy Ea or higher are capable of forming products directly. The plot of ln k vs. the reciprocal of the absolute temperature should result in a straight line with the slope equal to -Ea/R and the intercept equal to ln A if the above equation describes a reaction. Figure 14 is a plot of ln k for degradation of dipropionyl dyphylline vs. the reciprocal of the absolute temperature at the several pH's studied. The results of these Arrhenius plots are summarized in table V. For pH range below 3.0 where specific acid catalysis was predominate and for pH range above 8.0 where specific base catalysis was most important the degradation of dipropionyl dyphylline at different temperatures followed Arrhenius predictions quite closely, i.e. the linear regression of ln k on the reciprocal of absolute temperature for each pH in these regions resulted in r^2 values greater than 0.99. However, the degradation of this compound was not predicted as well by the Arrhenius relationship in the pH range where spontaneous reaction was predominate. Reactions with small or zero activation energies may show a nonlinear temperature dependence since the A factor in the Arrhenius equation of such reactions may become a function of temperature itself (22). However, the dependency of factor A on temperature might still be inadequate to explain the nonlinearity (23). The real cause in this case may be some complicity of the reactions which are not explicable at this time.

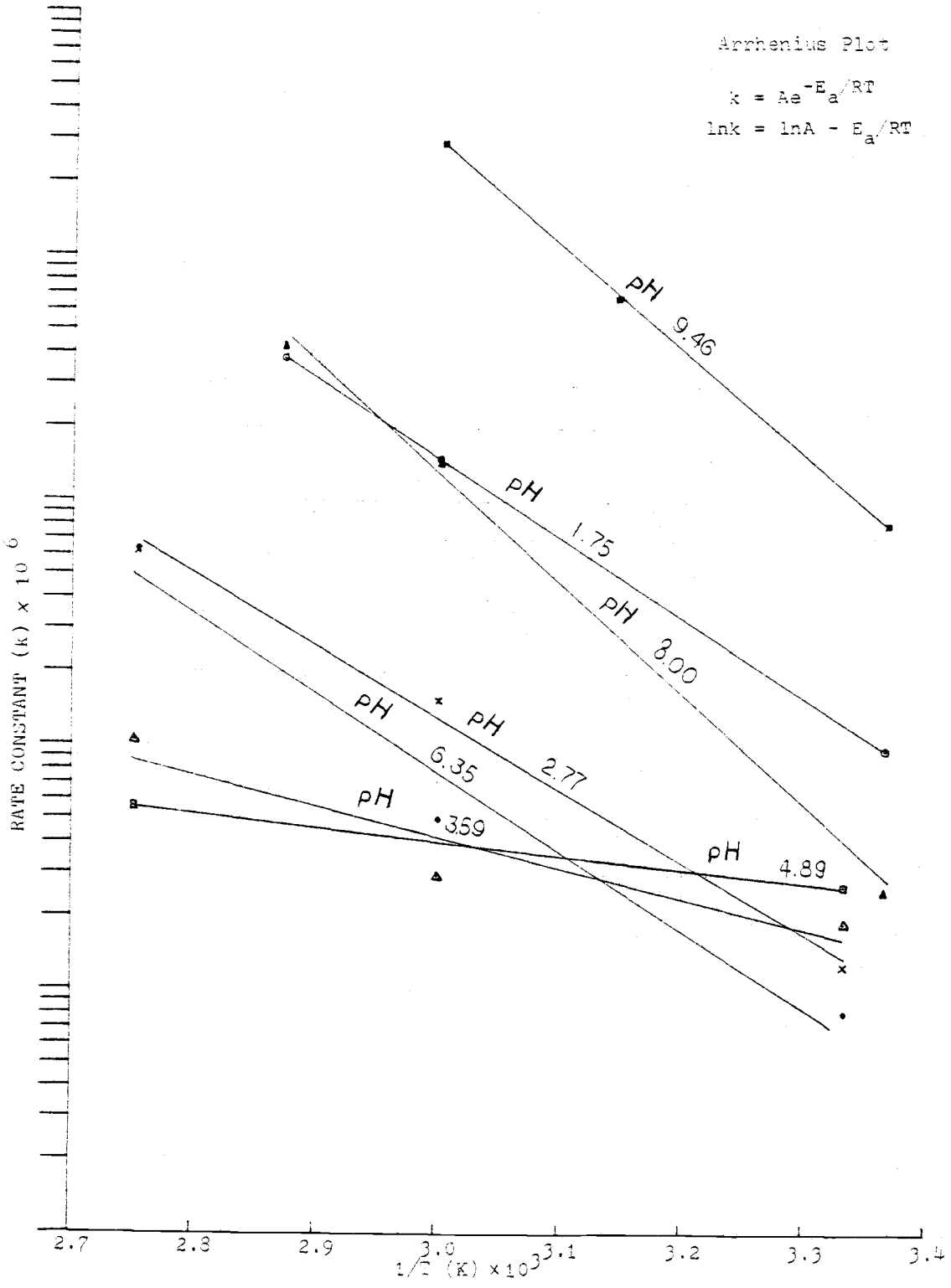

Figure 14. Arrhenius plots of apparent first-order rate constants for degradation of dipropionyl dyphylline in buffered aqueous (pH 1. 75 (⊙), 2. 77 (×), 3. 59 (△), 4. 89 (▣), 6. 35 (●), 8. 00 (▲) and 9. 46 (■))

Table V. Summary of Results of Arrhenius Plots.

pH	Intercept (S.E.)	-slope = Ea/R (S.E.)	Ea kcal/mole	r^2
1.75	7.1530×10^{6} (1.14)	7430.87 (43.79)	14.76	0.99997
2.77	8.5320×10^{4} (5.29)	6764.65 (548.48)	13.44	0.99347
3.59	4.6436 (22.20)	2845.67 (1020.30)	5.65	0.88610
4.89	*1.7636×10^{-3}	*1248.71	2.48	-
6.35	3.2607×10^{5} (53.68)	7376.88 (1310.90)	14.66	0.96939
8.00	1.1539×10^{11} (3.74)	10700.50 (427.14)	21.26	0.99841
9.46	1.730×10^{11} (1.75)	9804.13 (176.59)	19.48	0.99968

*generated from two points instead of three points as for other pH values.

Once the frequency factor and activation energy for any given pH were determined, the specific rate of the reaction at that specific pH condition could be obtained for any temperature of interest. Table VI and figure 15 show an example of the use of frequency factors and activation energies previously obtained from the data in Table IV to generate predicted degradation constants for dipropionyl dyphylline at various pH values at body temperature (37°C). The results from Arrhenius plots (table V) and the plot of energy of activation and ln frequency factor against pH in figure 16 and figure 17 show that both the experimental activation energies and the frequency factors vary markedly with pH. Some of this variation might be explained by determining the free energy of activation of the reactions (12). According to the theory of absolute reaction rates, the specific reaction rate may be related to $\triangle F^{\ddagger}$, $\triangle H^{\ddagger}$ and $\triangle S^{\ddagger}$, the standard free-energy, heat-content and entropy changes, respectively (24, 35) and can be written in the form:

$$k = Be^{-\triangle F\ddagger/RT}$$

or

$$k = Be^{-\triangle H\ddagger/RT}e^{\triangle S\ddagger R}$$

or

$$k = \frac{k'T}{h} e^{-\triangle H\ddagger/RT}e^{\triangle S\ddagger/R}$$

where $\frac{k'T}{h}$ is the effective velocity of the activated complexes to

Table VI. Estimated rate constants and half-life values for dipropionyl dyphylline at body temperature (37°C=310.15K) for each pH studied using the frequency factory and activation energy constants obtained from Arrhenius plots.

pH	Rate Constant $k = Ae^{-Ea/Rt}$ (min^{-1})	Half-life $t\ 1/2 = \ln 2/k$ (min)
1.75	2.8145×10^{-4}	2462.77
2.77	2.8756×10^{-5}	24104.44
3.59	2.2313×10^{-5}	31064.72
4.89	3.1468×10^{-5}	22027.05
6.35	1.5263×10^{-5}	45413.56
8.00	1.1982×10^{-4}	5784.90
9.46	3.2342×10^{-3}	214.32

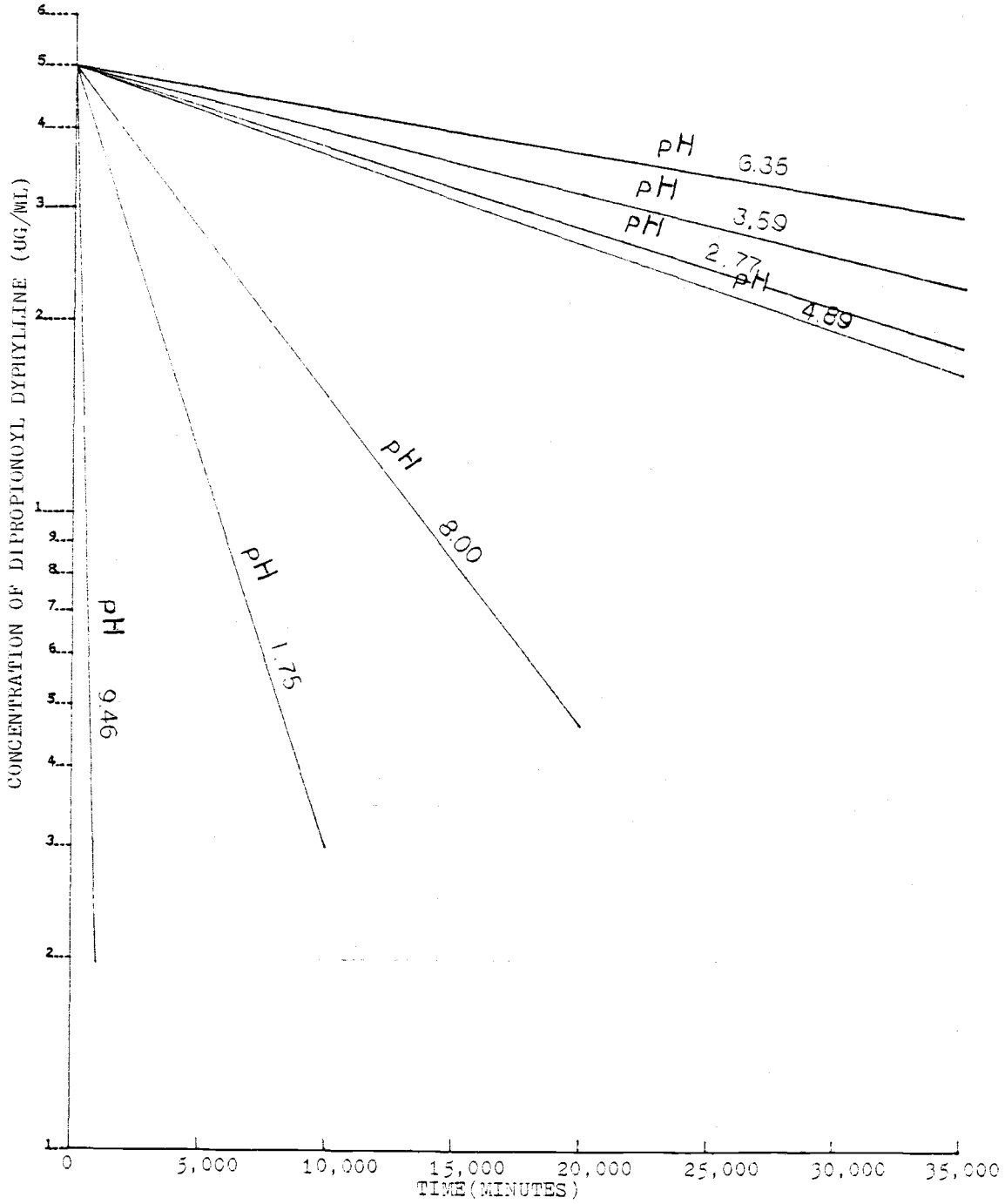

Figure 15. Estimated concentration-time curves for the degradation of dipropionyl dyphylline at 37°C from previously obtained frequency factors and activation energies of buffered aqueous systems

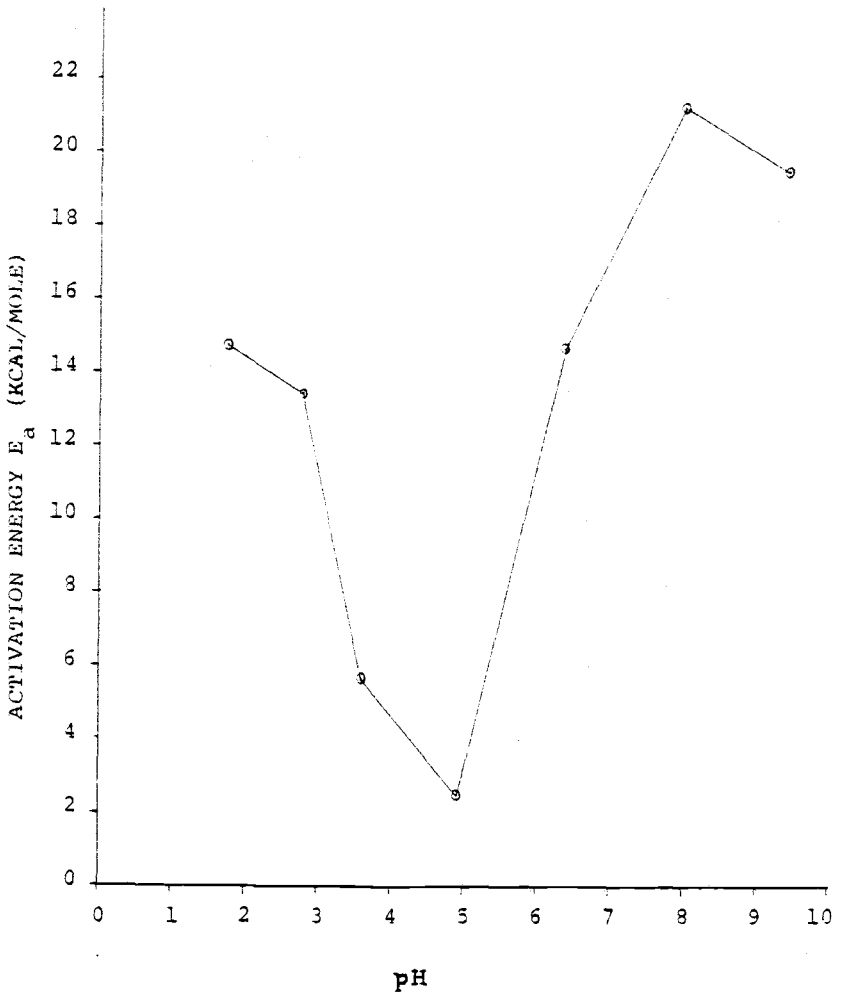

Figure 16. Activation Energy-pH Profile for the degradation of dipropionyl dyphylline in buffered aqueous systems

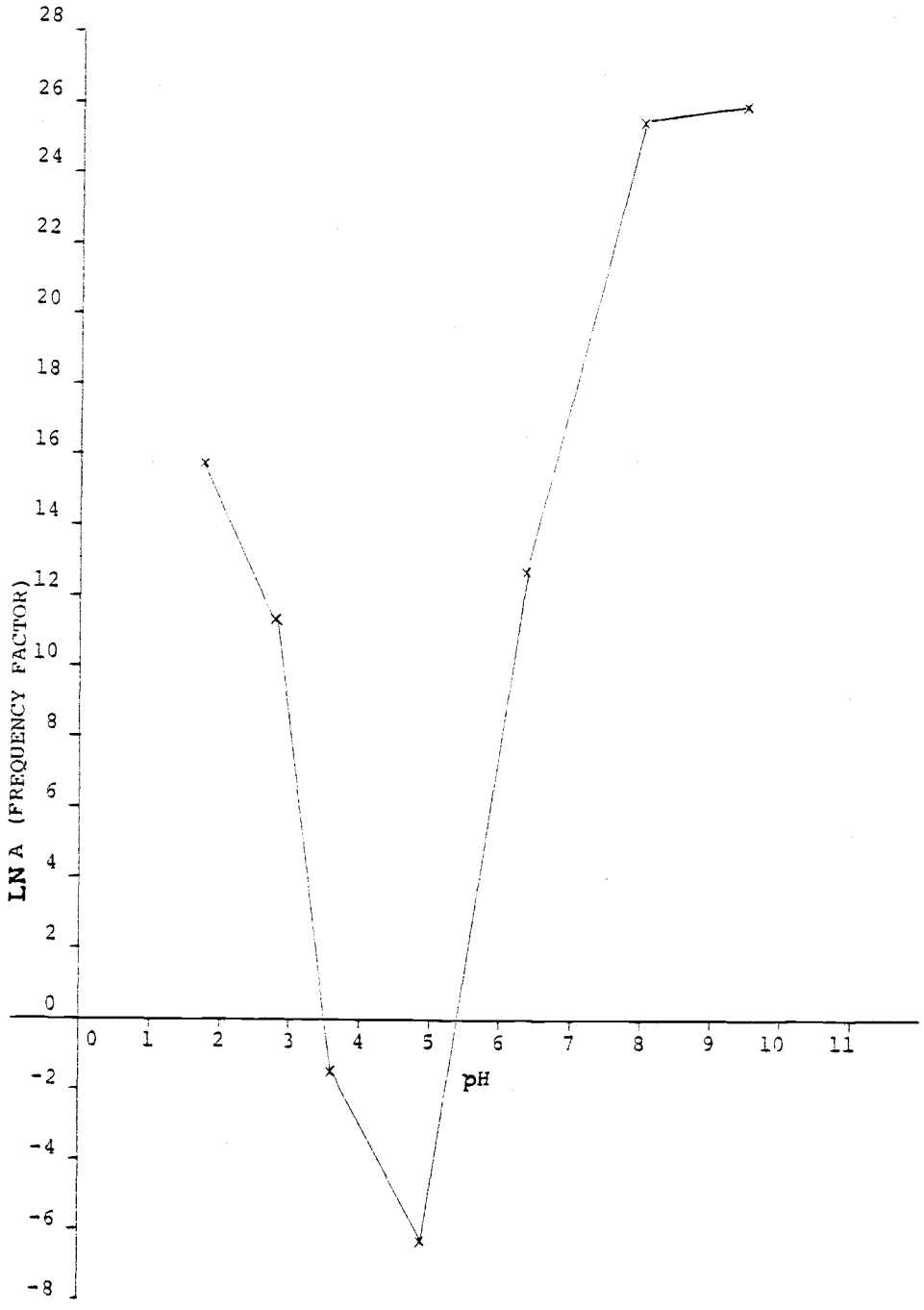

Figure 17. Logarithm of Frequency Factor-pH Profile for the degradation of dipropionyl dyphylline in buffered aqueous systems

cross the energy barrier, called the universal frequency, which is dependent only on temperature and independent of the nature of the reactants and the type of reaction. The above equations are consistent with a requirement that the reaction rate is determined by the free energy of activation and, additionally, gives a precise and simple significance to the frequency factor. The frequency factor can now be expressed as

$$A = \frac{kT}{h} e^{\triangle S^{\ddagger}/R}$$

The heat of activation $\triangle H^{\ddagger}$ can be derived from the slope of a plot of ln k/(kT/h) against 1/T. This $\triangle H^{\ddagger}$ differs only by a small amount from the experimental activation energy of the reaction. It is also possible to obtain the value of $\triangle S^{\ddagger}$ from the intercept of the regression of ln k/(kT/h) on 1/T and thus $\triangle F^{\ddagger}$ can be calculated by means of the common thermodynamic relationship.

$$\triangle F^{\ddagger} = \triangle H^{\ddagger} - T\triangle S^{\ddagger}$$

Table VII shows the data used to generate plots using the above equation and table VIII shows the thermodynamic values obtained from the degradation of dipropionyl dyphylline at 60°C. It is seen that in spite of the variation of $\triangle H^{\ddagger}$ between 1.83 and 20.63 kcal and the experimental activation energy (Ea) variation between 2.48 and 21.26

Table VII. Data used to generated modified Arrhenius plots based on the theory of absolute reaction rates.

pH	Temperature (^{o}C)	1/T ($\times 10^{3}$ Kelvin^{-1})	k/(kt/h)	Regression ln k/(kt/h)** on 1/T
1.75	24	3.3653	2.6460×10^{-19}	a* = -18.84 (0.15)
	60	3.0017	3.5734×10^{-18}	b^{+} = -7110.96 (48.85)
	75	2.8723	8.7538×10^{-18}	r^2 = 0.99995
2.77	27	3.3317	3.4224×10^{-20}	a* = -23.30 (1.69)
	60	3.0017	3.7332×10^{-19}	b^{+} = -6435.77 (557.14)
	90	2.7537	1.3753×10^{-18}	r^2 = 0.99286
3.59	27	3.3317	5.0639×10^{-20}	a* = -36.19 (3.07)
	60	3.0017	7.1730×10^{-20}	b^{+} = -2516.81 (1011.40)
	90	2.7537	2.2754×10^{-19}	r^2 = 0.86095
4.89	27	3.3317	7.3281×10^{-20}	a* = -41.00 (-)
	60	3.0017	-	b_2^{+} = -919.18 (-)
	90	2.7537	1.2466×10^{-19}	r^2 = -
6.35	27	3.3317	2.2198×10^{-20}	a* = -21.96 (3.96)
	60	3.0017	1.2210×10^{-19}	b_2^{+} = -7048.02 (1302.10)
	90	2.7537	1.3877×10^{-18}	r^2 = 0.96699
8.00	24	3.3653	6.9021×10^{-20}	a* = -9.15 (1.33)
	60	3.0017	3.5125×10^{-18}	b_2^{+} = -10380.54 (432.21)
	75	2.8723	1.0868×10^{-17}	r^2 = 0.99827
9.46	24	3.3653	2.2142×10^{-18}	a* = -8.73 (0.54)
	45	3.1432	1.7333×10^{-17}	b_2^{+} = -9489.88 (171.47)
	60	3.0017	7.0343×10^{-17}	r^2 = 0.99967

*a = intercept = $\Delta S^{\ddagger}/R$ (S.E.)

$^{+}$b = slope = $-\Delta H^{\ddagger}$ (S.E.)

**k = Boltzmann constant = 1.381×10^{-23} JK^{-1} = $1.381 \times 10^{-23}/4.184$ cal K^{-1}, h = Planck constant = 6.626×10^{-34} Js = $6.626 \times 10^{-34}/4.184 \times 60$ cal min

Table VIII. Thermodynamic values obtained from the degradation of dipropionyl dyphylline in aqueous buffers at various pH values at 60°C (333.15K)

pH	$\triangle H^{\ddagger}$ Kcal $mole^{-1}$	$\triangle S^{\ddagger}$ cal $mole^{-1} k^{-1}$	$\triangle F^{\ddagger}$ Kcal $mole^{-1}$
1.75	14.13	-37.44	26.60
2.77	12.79	-46.30	28.21
3.59	5.00	-71.91	28.96
4.89	1.83	-81.46	28.97
6.35	14.00	-43.63	28.54
8.00	20.63	-18.18	26.69
9.46	18.86	-17.35	24.64

kcal (Table V), the free energy of activation ($\triangle F\ddagger$) remains almost constant. It can also be observed that the exceptionally low energies of activation at pH 3.59 and pH 4.89 were compensated to a great extent by large decreases of entropy accompanying activation. A large negative entropy of activation is consistent with a slow reaction. The activation energy decreased to some extent simultaneously, but this is insufficient to compensate for the observed change in the entropy of activation. This could be an explanation of why the reaction rates in the regions of acid and base catalysis dominance were faster than the spontaneous degradation region even though the experimental activation energies were higher in the acid-base catalysis regions than in the spontaneous region. The acid catalyzed hydrolysis of p-methoxy-biphenylyl benzoate has also been reported as having a higher energy of activation than the uncatalyzed hydrolysis and the greater rate for the catalysis reaction was said to be due to the much larger value of the frequency factor A (19). One of the fundamental bases of the theory of absolute reaction rates states that the velocity of a reaction is determined primarily by the free energy, not by the heat of activation (12).

The hydrolysis of dipropionyl dyphylline occurs in stages. The diester was converted into the monoester which was further converted into dyphylline

$$\underset{[A]}{\text{Dipropionyl Dyphylline}} \xrightarrow{k_1} \underset{[B]}{\text{Monopropionoyl Dyphylline}}$$

$$\downarrow k_2$$

$$\underset{[C]}{\text{Dyphylline}}$$

The differential equations can be written as follows:

$$\frac{d[A]^t}{dt} = -k_1[A]^t$$

$$\frac{d[B]^t}{dt} = k_1[A]^t - k_2[B]^t$$

$$\frac{d[C]^t}{dt} = k_2[B]^t$$

These equations can be solved by applying Laplace transforms:

$$s[A]^s - [A]^o = [A]^o = -k[A]^s$$

$$[A]^s = \frac{[A]^o}{(s+k_1)} \quad \text{(1)}$$

$$s[B]^s - [B]^o = k_1[A]^s - k_2[B]^s = o$$

$$[B]^s = \frac{k[A]^s}{(s+k_2)} \text{ since } [B]^o = o$$

$$[B]^s = \frac{k[A]^o}{(s+k_1)(s+k_2)} \quad \text{(2)}$$

$$s[C]^s - [C]^o = k_2[B]^s$$

$$[C]^s = \frac{k_2[B]^s}{s} \quad \text{since } [C]^o = o$$

$$[C]^s = \frac{k_1k_2[A]^o}{s(s+k_1)(s+k_2)} \quad \text{(3)}$$

Inverse Laplace transforms for equations (1), (2), and (3) are:

$$[A]^t = [A]^o e^{-k_1 t} \qquad \text{(4)}$$

$$[B]^t = \frac{k_1 [A]^o}{(k_2 - k_1)} \left(e^{-k_1 t} - e^{-k_2 t}\right) \qquad \text{(5)}$$

$$[C]^t = [A]^o \left[1 + \frac{k_2 e^{-k_1 t}}{(k_1 - k_2)} - \frac{k_1 e^{-k_2 t}}{(k_1 - k_2)} \right] \qquad \text{(6)}$$

The degradation of monopropionyl dyphylline has also been studied at 60°C in aqueous buffer pH 1.75 and pH 9.46. The results are shown in figure 18 and table IX. Since the degradation rate of dipropionyl dyphylline to primary monopropionyl dyphylline and the degradation rate of monopropionyl dyphylline to dyphylline (corresponding to k_1 and k_2 in equations 4, 5 and 6) are now known, equations 4, 5 and 6 can be used to predict the concentrations of dipropionyl dyphylline, primary monopropionyl dyphylline and dyphylline at various times during the degradation of dipropionyl dyphylline at these specific pH's and temperature. Figures 19 and 20 show the predicted and experimental concentration-time curves of monopropionyl dyphylline from degradation of dipropionyl dyphylline at 60°C in aqueous buffer pH 1.75 and pH 9.45 respectively. The k_1 was calculated to be 1.4894×10^{-3} min^{-1} and k_2 was calculated to be 1.1341×10^{-3} min^{-1} for pH 1.75 while k_1 was calculated to be 0.02932 min^{-1} and k_2 was calculated to be 0.01871 min^{-1} for pH 9.45. The deviation of the experimental curve from the predicted curve could be due partly to the occurrence of a more complex degradation involving

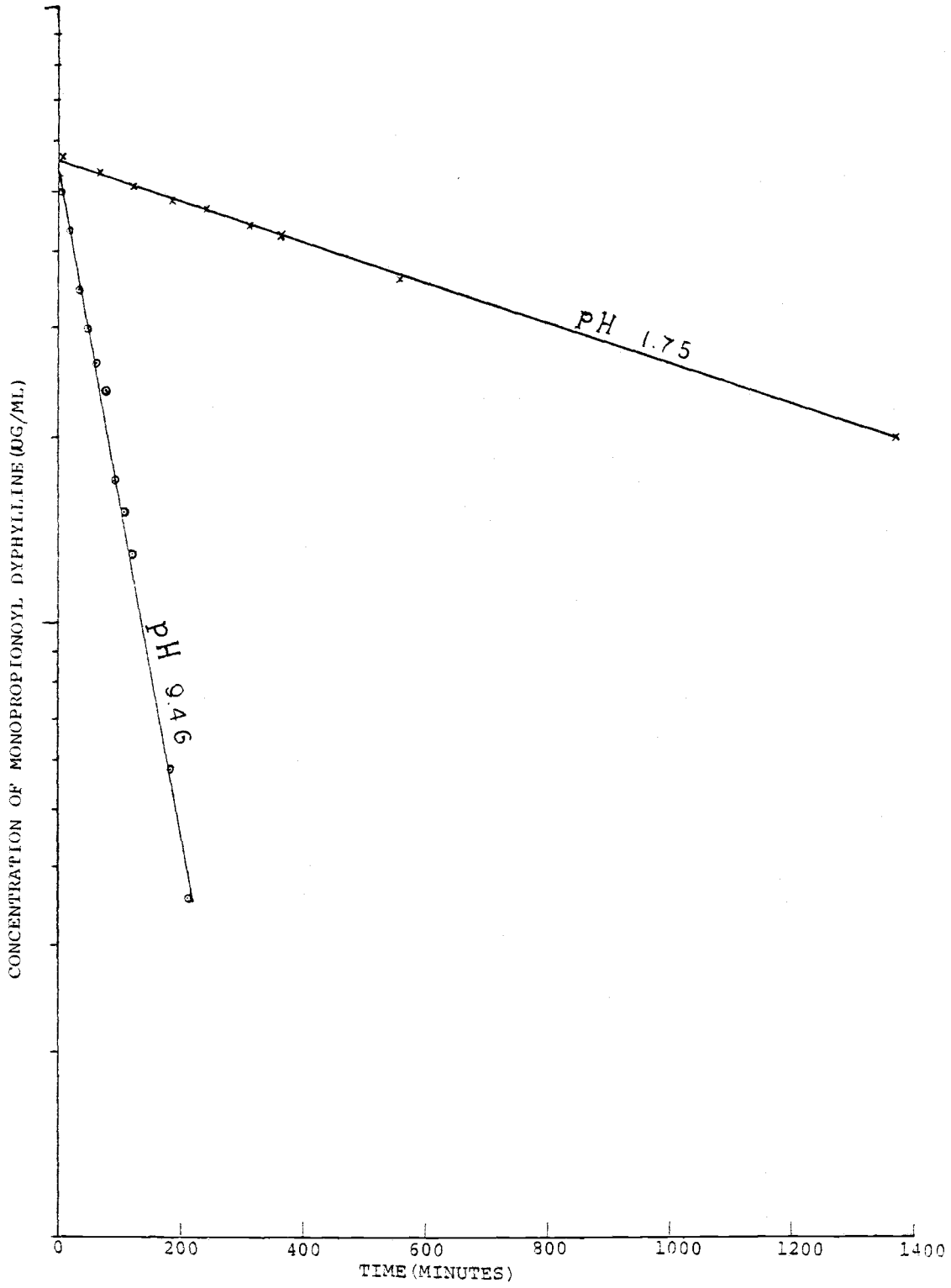

Figure 18. Degradation of primary monopropionyl dyphylline at 60°C in aqueous buffer solutions (pH 1.75 (×) and pH 9.46 (○))

Table IX. Results from the linear regression of ln concentration of primary monopropionyl dyphylline on time for the degradation of primary monopropionyl dyphylline in buffer pH 1.75 and pH 9.46 at 60°C

pH	Number of samples	Intercept (μg/ml)(S.E.)	-slope = k (10^3 min^{-1})(S.E.)	r^2
1.75	9	421.05 (1.01)	1.13 (0.01)	0.99886
9.46	11	398.11 (1.05)	18.71 (0.48)	0.99406

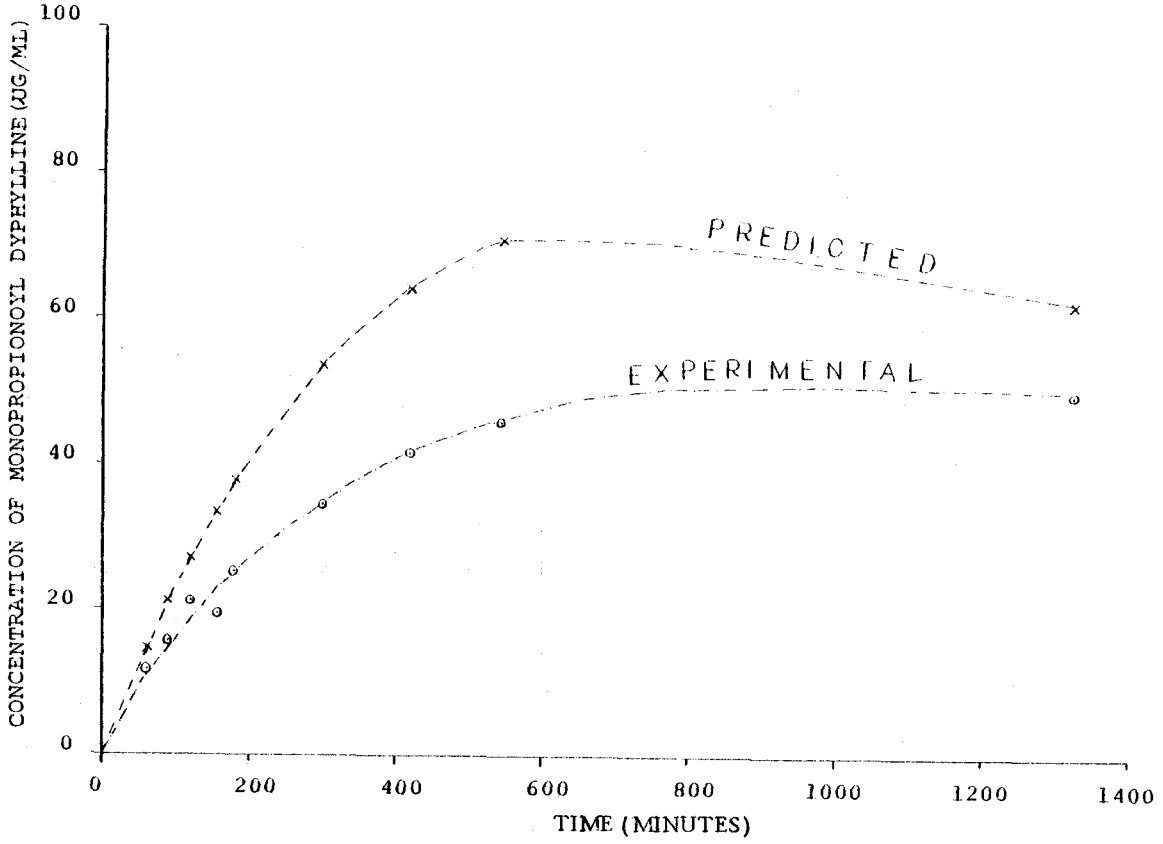

Figure 19. Predicted and experimental concentration-time curves of monopropionyl dyphylline generated from degradation of dipropionyl dyphylline at 60°C in aqueous buffer (pH 1.75)

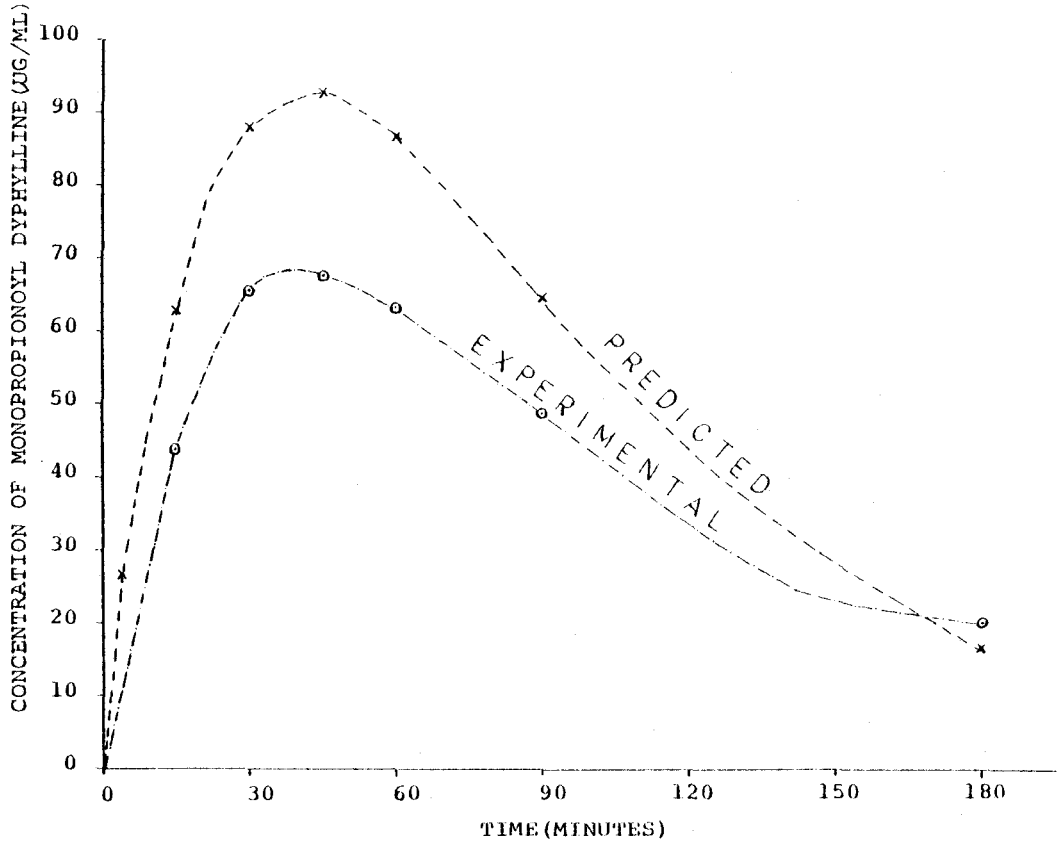

Figure 20. Predicted and experimental concentration-time curves of monopropionyl dyphylline generated from the degradation of dipropionyl dyphylline at 60°C in aqueous buffer (pH 9.46)

the secondary monopropionyl dhphylline as explained in the previous chapter. The secondary mono-ester was present whenever an aqueous solution of primary monopropionyl ester was investigated. This more complicated reaction would result in deviations between predicted and observed dyphylline concentrations. Therefore, no useful results can be obtained by comparing experimental values to predicted concentrations of dyphylline until further studies which quantify the secondary mono-ester have been done in detail.

Footnctes, Chapter II:

1. Alfred Bader Library of Rare Chemicals (Division of Aldrich Chemical Company), Milwaukee, Wisconsin.
2. Reagent, A.C.S., Granular, Matheson Coleman and Bell, Norwood, Ohio.
3. Acid Phosphoric Merck 85%, Rahway, N. J.
4. USP, Powder, Matheson Coleman and Bell, Norwood, Ohio.
5. 'Baker Analyzed' Reagent, J. T. Baker Chemical Co., Phillipsburg, N. J.
6. 0.1 N USP
7. 'Baker Analyzed' Reagent, J. T. Baker Chemical Co., Phillipsburg, N. J.
8. 'Baker Analyzed' Reagent, J. T. Baker Chemical Co., Phillipsburg, N. J.
9. Sargent-Welch, Anaheim, California, or Corning Scientific Instruments, Corning, N. Y.
10. VAN-LAB, VWR Scientific, Portland, Oregon.
11. PORTA TEMP, Precision Scientific Co., Chicago, Illinois.
12. Lab-line Instruments, Melrose Park, Illinois.
13. Water Associates Chromatography Pumps, Milford, Mass.
14. Water Associates Model 660 Solvent Programmer, Milford, Mass.
15. Water Associates Model U6k Injector, Milford, Mass.

16. Water Associates u BONDAPAK C_{18}, Milford, Mass.

17. Water Associates Model 440 Absorbance Detector, Milford, Mass.

18. SOLTEC, Encino, California.

19. 3373B Integretor, Hewlett Packard.

BIBLIOGRAPHY

1. K. Kiem and C. Lemliner, "Documenta Geigy-Scientific Tables," 7th edition, Geigy Pharmaceuticals, Ardsley, New York, 1970, p. 281-282.

2. C. Long, "Biochemist' Handbook," D. Van Nostrand Company, Princeton, New Jersey, 1961, p. 32.

3. D. C. Garg, J. W. Ayres and J. G. Wagner, "Determination of Methylprednisolone and Hydrocortisone in plasma using High Pressure Liquid Chromatography," Research Communications in Chemical Pathology and Pharmacology, Vol. 18, No. 1, 137-146 (1977).

4. K. J. Laidler, "Chemical Kinetics," 2nd Edition, McGraw-Hill Book Company, New York, 1965, p. 450-474.

5. W. P. Jencks, "Catalysis in Chemistry and Enzymology," McGraw-Hill Book Company, New York, 1969, p. 564-569.

6. S. W. Benson, "The Foundations of Chemical Kinetics," McGraw-Hill Book Company, New York, 1960, p. 17-21.

7. K. J. Laidler, "Chemical Kinetics," 2nd Edition, McGraw-Hill Book Company, New York, 1965, p. 5-8.

8. F. Daniels and R. A. Alberty, "Physical Chemistry," 4th edition, John Wiley and Sons, New York, 1975, p. 5-8.

9. L. P. Hammett, "Physical Organic Chemistry," 2nd edition, McGraw-Hill Book Company, New York, 1970, p. 332-333.

10. R. P. Bell, "Acid-Base Catalysis," Oxford University Press, London, 1941, Chapter V.

11. S. W. Benson, "The Foundations of Chemical Kinetics," McGraw-Hill Book Company, New York, 1960, p. 493-501.

12. S. Glasstone, K. J. Laidler and H. Eyring, "The Theory of Rate Processes," McGraw-Hill Book Company, New York, 1941. p. 442-452.

13. W. P. Jencks, "Calalysis in Chemistry and Enzymology," McGraw-Hill Book Company, New York, 1965, p. 578-585.

14. E. R. Garrett, "The Kinetics of Solvolyis of Acyl Esters of Salicylic Acid," J. Am. Chem. Soc., 79, 3401-3408 (1957).

15. C. A. Kelly, "Determination of the Decomposition of Aspirin," J. Pharm. Sci., vol. 59, No. 8, 1053-1078 (1970).

16. J. A. Mollica, S. Ahuja and J. Cohen, "Stability of Pharmaceuticals," J. Pharm. Sci., Vol. 67, No. 4, April 1978. p. 445-446.

17. T. Yamana and A. Ysuji, "Comparative Stability of Cephalosporins in Aqueous Solution: Kinetics and Mechanisms of Degradation," J. Pharm. Sci., Vol. 65, No. 11, 1563-1574, (1976).

18. N. S. Isaacs, "Experiments in Physical Organic Chemistry," The Macmillan Company, London, 1969, p. 37-41.

19. J. G. Morris, "A Biologist's Physical Chemistry," Addison-Wesley Publishing, California, 1968, p. 253-255.

20. K. J. Laidler, "Chemical Kinetics," 2nd edition, McGraw-Hill Book Company, New York, 1965, p. 50-54.

21. S. Glasslone, K. J. Laidler and H. Egring, "The Theory of Rate Processes," McGraw-Hill Book Company, New York, 1941, Chapter I.

22. C. Capellos and H. H. J. Bielski, "Kinetic Systems: Mathematical Description of Chemical Kinetics in Solution," Wiley-Interscience, a division of John Will and Sons, New York, 1972, p. 115.

23. E. A. Molluyn-Hughes, "The Kinetics of Reactions in Solution," 2nd edition, Oxford University Press, Amen House, London, 1947, Chapter I, II.

24. S. Glasstone, K. J. Laidler and H. Eyring, "The Theory of Rate Processes," McGraw-Hill Book Company, New York, 1941, p. 195-199.

25. K. J. Laidler, "Chemical Kinetics," 2nd edition, McGraw-Hill Book Company, New York, 1965, p. 238.

CHAPTER III

THE PHARMACOKINETICS OF DYPHYLLINE PRODRUGS: A SIMULATION STUDY

INTRODUCTION

A series of dyphylline hydroxy esters has been synthesized with the goal of controlling the input and subsequent conversion of prodrug to drug and thus increasing the duration of action of dyphylline (1). Absolute selectivity for control of only one function is unlikely since each process of pharmacokinetics is influenced by the physical-chemical characteristics of the drug; the elimination and distribution processes are unavoidably altered when the chemical structure of a compound is modified. A compromise of these overall pharmacokinetic processes is thus required in order to obtain successful results. Before an optimum set of rate processes can be obtained, some information about the influence of each rate process on the dyphylline blood concentration distribution over time is needed. Pharmacokinetic patterns for dyphylline prodrugs were therefore developed using computer simulations to gain some understanding of the potential behavior of these prodrugs from a pharmacokinetic point of view. The pharmacokinetic microconstants were chosen based on information known for dyphylline, theophylline and the ratios of the apparent partition coefficients of these compounds and the mono- and di- propionyl dyphylline esters. Hopefully, the information gained from this study, together with some simple experiments, can provide an idea of which compounds synthesized as reported in

the preceding chapter should be chosen for pharmacokinetic study in animals and/or humans.

THEORETICAL

Based on information from the previous chapter the hydrolysis rates of propionyl dyphylline proceeded so slowly at 37°C in the pH range of the G-I tract (including pH 1-2 of the stomach) that the assumption was made that no degradation of the propionyl esters will occur prior to absorption. This also requires the assumption that no enzyme esterase will contribute to degradation in the G-I tract. It was also assumed that no elimination occurred in any peripheral compartment for the di- and mono- esters of dyphylline. A pharmacokinetic diagram for the diesters of dyphylline can then be presented as shown in scheme I. However, these assumptions could easily be relaxed if the required additional pharmacokinetic information were available.

Mass Balance Equations from Scheme I:-

$$\frac{dM_1}{dt} = -R_{12}C_1$$

$$= -k_{12}M_1$$

$$= -K_1 M_1 \qquad (1)$$

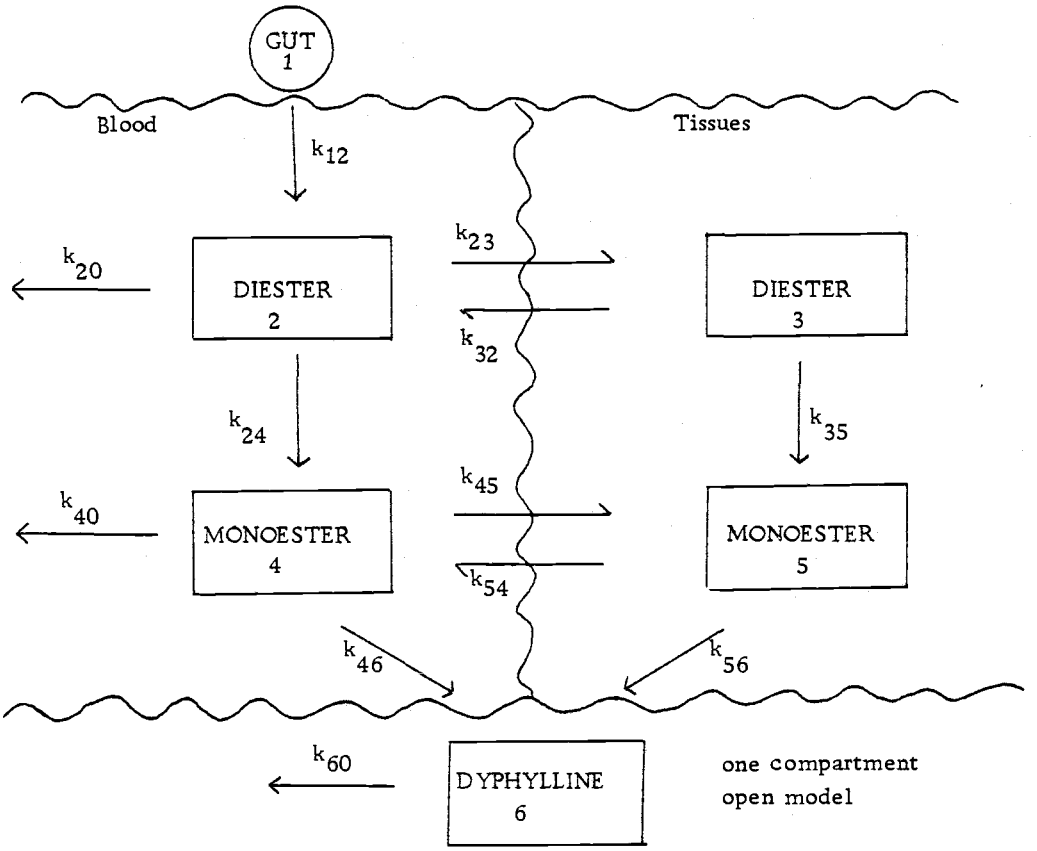

Scheme I. General Pharmacokinetic Pattern for Diester Prodrugs of Dyphylline:

Compartment 1 = Gut

Compartment 2 = Central compartment for the diester

Compartment 3 = Peripheral compartment for the diester

Compartment 4 = Central compartment for the monoester

Compartment 5 = Peripheral compartment for the monoester

Compartment 6 = Compartment for dyphylline. The Pharmacokinetics of dyphylline were reported to be compatible with a one compartment open model[1] as a first approximation.

$$\frac{dM_2}{dt} = R_{12}C_1-(R_{20}+R_{23}+R_{24})C_2+R_{32}C_3$$

$$= k_{12}M_1-(k_{20}+k_{23}+k_{24})M_2+k_{32}M_3$$

$$= k_{12}M_1-K_2M_2+k_{32}M_3 \qquad (2)$$

$$\frac{dM_3}{dt} = R_{23}C_2-(R_{32}+R_{35})C_3$$

$$= k_{23}M_2-(k_{32}+k_{35})M_3$$

$$= k_{23}M_2-K_3M_3 \qquad (3)$$

$$\frac{dM_4}{dt} = R_{24}C_2-(R_{40}+R_{45}+R_{46})C_4+R_{54}C_5$$

$$= k_{24}M_2-(k_{40}+k_{45}+k_{46})M_4+k_{54}M_5$$

$$= k_{24}M_2-K_4M_4+k_{54}M_5 \qquad (4)$$

$$\frac{dM_5}{dt} = R_{35}C_3+R_{45}C_4-(R_{54}+R_{56})C_5$$

$$= k_{35}M_3+k_{45}M_4-(k_{54}+k_{56})M_5$$

$$= k_{35}M_3+k_{45}M_4-K_5M_5 \qquad (5)$$

$$\frac{dM_6}{dt} = R_{46}C_4+R_{56}C_5-R_{60}C6$$

$$= k_{46}M_4+k_{56}M_5-k_{60}M_6$$

$$= k_{46}M_4+k_{56}M_5-K_6M_6 \qquad (6)$$

in which

M_i = Mass in compartment i.

C_i = Concentration in compartment i.

R_{ij} = Rate constant for the flow or the conversion of compound from compartment i to compartment j with the units equal to volume-time^{-1}.

k_{ij} = Rate constant for the flow or the conversion of compound from compartment i to compartment j with the units equal to time^{-1}.

$K_i = \sum_{j=1}^{n} k_{ij}$

Apply Laplace Transform to solve the Mass Balance Equations:

From (1) $sM_1(s) - M_1(0) = -K_1 M_1(s)$

$(s+K_1) M_1(s) = M_1(0)$ (7)

From (2) $-k_{12}M_1(s) + (s+K_2)M_2(s) - k_{32}M_3(s) = M_2(0)$ (8)

From (3) $-k_{23}M_2(s) + (s+K_3)M_3(s) = M_3(0)$ (9)

From (4) $-k_{24}M_2(s) + (s+K_4)M_4(s) - k_{54}M_5(s) = M_4(0)$ (10)

From (5) $-k_{35}M_3(s) - k_{45}M_4(s) + (s+K_5)M_5(s) = M_5(0)$ (11)

From (6) $-k_{46}M_4(s) - k_{56}M_5(s) + (s+K_6)M_6(s) = M_6(0)$ (12)

The determinant ($\triangle$) of equation (7) to equation (12) can be solved as follows:

$$\triangle = \begin{vmatrix} (s+K_1) & 0 & 0 & 0 & 0 & 0 \\ -k_{12} & (s+K_2) & -k_{32} & 0 & 0 & 0 \\ 0 & -k_{23} & (s+K_3) & 0 & 0 & 0 \\ 0 & -k_{24} & 0 & (s+K_4) & -k_{54} & 0 \\ 0 & 0 & -k_{35} & -k_{45} & (s+K_5) & 0 \\ 0 & 0 & 0 & -k_{46} & -k_{56} & (s+K_6) \end{vmatrix}$$

$$= (s+K_1)\begin{vmatrix} (s+K_2) & -k_{32} & 0 & 0 & 0 \\ -k_{23} & (s+K_3) & 0 & 0 & 0 \\ -k_{24} & 0 & (s+K_4) & -k_{54} & 0 \\ 0 & -k_{35} & -k_{45} & (s+K_5) & 0 \\ 0 & 0 & -k_{46} & -k_{56} & (s+K_6) \end{vmatrix}$$

$$= (s+K_1)(-1)^2(s+K_2)\begin{vmatrix} (s+K_3) & 0 & 0 & 0 \\ 0 & (s+K_4) & -k_{54} & 0 \\ -k_{35} & -k_{45} & (s+K_5) & 0 \\ 0 & -k_{46} & -k_{56} & (s+K_6) \end{vmatrix}$$

$$+(s+K_1)(-1)^3(-k_{32})\begin{vmatrix} -k_{23} & 0 & 0 & 0 \\ -k_{24} & (s+K_4) & -k_{54} & 0 \\ 0 & -k_{45} & (s+K_5) & 0 \\ 0 & -k_{46} & -k_{56} & (s+K_6) \end{vmatrix}$$

$$= (s+K_1)(s+K_2)(-1)^2(s+K_3)\begin{vmatrix} (s+K_4) & -k_{54} & 0 \\ -k_{45} & (s+K_5) & 0 \\ -k_{46} & -k_{56} & (s+K_6) \end{vmatrix}$$

$$+ (s+K_1)k_{32})(-1)^2(-k_{23})\begin{vmatrix} (s+K_4) & -k_{54} & 0 \\ -k_{45} & (s+K_5) & 0 \\ -k_{46} & -k_{56} & (s+K_6) \end{vmatrix}$$

$$= (s+K_1)(s+K_2)(s+K_3)(-1)^6(s+K_6)\left[(s+K_4)(s+K_5)-k_{45}k_{54}\right]$$

$$-(s+K_1)(k_{32})(k_{23})(-1)^6(s+K_6)\left[(s+K_4)(s+K_5)-k_{45}k_{54}\right]$$

$$= (s+K_1)(s+K_6)\,[(s+K_2)(s+K_3)(s+K_4)(s+K_5) - k_{45}k_{54}(s+K_2)(s+K_3) - k_{23}k_{32}(s+K_4)(s+K_5) + k_{23}k_{32}k_{45}k_{54}]$$

$$= (s+K_1)(s+K_6)\,[s^4 + (K_2+K_3+K_4+K_5)s^3 + (K_2K_3+K_2K_4+K_2K_5+K_3K_4+K_3K_5)s^2 + (K_2K_3K_4+K_2K_3K_5+K_2K_4K_5+K_3K_4K_5)s + K_2K_3K_4K_5 - k_{45}k_{54}s^2 - k_{45}k_{54}(K_2+K_3)s - k_{45}k_{54}K_2K_3 - k_{23}k_{32}s^2 - k_{23}k_{32}(K_4+K_5)s - k_{23}k_{32}K_4K_5 + k_{23}k_{32}k_{45}k_{54}]$$

$$= (s+K_1)(s+K_6)\,[(s+\alpha)(s+\beta)(s+\gamma)(s+\delta)]$$

where

$$\alpha + \beta + \gamma + \delta = K_2+K_3+K_4+K_5$$

$$\alpha\beta + \alpha\gamma + \alpha\delta + \beta\gamma + \beta\delta + \gamma\delta = K_2K_3+K_2K_4+K_2K_5+K_3K_4+K_3K_5+K_4K_5 - k_{45}k_{54} - k_{23}k_{32}$$

$$\alpha\beta\gamma + \alpha\beta\delta + \alpha\gamma\delta + \beta\gamma\delta = K_2K_3K_4+K_2K_3K_5+K_2K_4K_5+K_3K_4K_5 - k_{45}k_{54}(K_2+K_3) - k_{23}k_{32}(K_4+K_5)$$

$$\alpha\beta\gamma\delta = K_2K_3K_4K_5 - k_{45}k_{54}K_2K_3 - k_{23}k_{32}K_4K_5 + k_{23}k_{32}k_{45}k_{54}$$

The mass in each compartment can now be obtained by means of Cramer's rule (2)

$$\frac{M_i(s)}{M(0)} = (-1)^{i+1}\frac{\Delta_{1;i}}{\Delta}$$

in which $\Delta_{1;i}$ corresponds to the determinant obtained from Δ by

suppressing the first row and the ith column. For example, the mass in the dyphylline compartment, i.e. compartment 6 can be calculated as follows:-

$$\frac{M_6(s)}{M(0)} = (-1)^7 \begin{vmatrix} -k_{12} & (s+K_2) & -k_{32} & 0 & 0 \\ 0 & -k_{23} & (s+K_3) & 0 & 0 \\ 0 & -k_{24} & 0 & (s+K_4) & -k_{54} \\ 0 & 0 & -k_{35} & -k_{45} & (s+K_5) \\ 0 & 0 & 0 & -k_{46} & -k_{56} \end{vmatrix} \Big/ \triangle$$

$$= -(-1)^2(-k_{12}) \begin{vmatrix} -k_{23} & (s+K_3) & 0 & 0 \\ -k_{24} & 0 & (s+K_4) & -k_{54} \\ 0 & -k_{35} & -k_{45} & (s+K_5) \\ 0 & 0 & -k_{46} & -k_{56} \end{vmatrix} \Big/ \triangle$$

$$= k_{12}(-1)^2(-k_{23}) \begin{vmatrix} 0 & (s+K_4) & -k_{54} \\ -k_{35} & -k_{45} & (s+K_5) \\ 0 & -k_{46} & -k_{56} \end{vmatrix}$$

$$+k_{12}(-1)^3(-k_{24}) \begin{vmatrix} (s+K_3) & 0 & 0 \\ -k_{35} & -k_{45} & (s+K_5) \\ 0 & -k_{46} & -k_{56} \end{vmatrix} \Big/ \triangle$$

$$= -k_{12}k_{23}(-1)^3(-k_{35})\left[(s+K_4)(-k_{56})-k_{46}-k_{54}\right]$$
$$+k_{12}k_{24}(-1)^2(s+K_3)\left[k_{45}k_{56}+k_{46}(s+K_5)\right]$$
$$\frac{}{\Delta}$$

$$= k_{12}k_{23}k_{35}k_{56}(s+K_4)+k_{12}k_{23}k_{35}k_{46}k_{54}$$
$$+k_{12}k_{24}k_{45}k_{56}(s+K_3)+k_{12}k_{24}k_{46}(s+K_3)(s+K_5)$$
$$\frac{}{\Delta}$$

$$= \frac{A_1(s+K_3)+A_2(s+K_4)+A_3(s+K_3)(s+K_5)+A_4}{(s+K_1)(s+K_6)(s+\alpha)(s+\beta)(s+\gamma)(s+\delta)}$$

where

$$A_1 = k_{12}k_{24}k_{45}k_{56}$$

$$A_2 = k_{12}k_{23}k_{35}k_{56}$$

$$A_3 = k_{12}k_{24}k_{46}$$

$$A_4 = k_{12}k_{23}k_{35}k_{46}k_{54}$$

Assuming $M_1(0)$ = Dose = D, $M_2(0) = 0$, $M_3(0) = 0$, $M_4(0) = 0$, $M_5(0) = 0$ and $M_6(0) = 0$

$$M_6(s) = D\left[\frac{A_1(s+K_3)+A_2(s+K_4)+A_3(s+K_3)(s+K_5)+A_4}{(s+K_1)(s+K_6)(s+\alpha)(s+\beta)(s+\gamma)(s+\delta)}\right]$$

Use the general partial fraction theorem for obtaining the inverse Laplace Transform (3):-

$$L^{-1}\left\{\frac{P(s)}{Q(s)}\right\} = \sum_{j=1}^{n} \frac{P(\lambda_i)}{Q(\lambda_i)} e^{\lambda_i t}$$

$$M_6(t) = D\left[\frac{A_1(K_3-K_1)+A_2(K_4-K_1)+A_3(K_3-K_1)(K_5-K_1)+A_4}{(K_6-K_1)(\alpha-K_1)(\beta-K_1)(\gamma-K_1)(\delta-K_1)}\right] e^{-K_1 t}$$

$$+ D\left[\frac{A_1(K_3-K_6)+A_2(K_4-K_6)+A_3(K_3-K_6)(K_5-K_6)+A_4}{(K_1-K_6)(\alpha-K_6)(\beta-K_6)(\gamma-K_6)(\delta-K_6)}\right] e^{-K_6 t}$$

$$+ D\left[\frac{A_1(K_3-\alpha)+A_2(K_4-\alpha)+A_3(K_3-\alpha)(K_5-\alpha)+A_4}{(K_1-\alpha)(K_6-\alpha)(\beta-\alpha)(\gamma-\alpha)(\delta-\alpha)}\right] e^{-\alpha t}$$

$$+ D\left[\frac{A_1(K_3-\beta)+A_2(K_4-\beta)+A_3(K_3-\beta)(K_5-\beta)+A_4}{(K_1-\beta)(K_6-\beta)(\alpha-\beta)(\gamma-\beta)(\delta-\beta)}\right] e^{-\beta t}$$

$$+ D\left[\frac{A_1(K_3-\gamma)+A_2(K_4-\gamma)+A_3(K_3-\gamma(K_5-\gamma)+A_4}{(K_1-\gamma)(K_6-\gamma)(\alpha-\gamma)(\beta-\gamma)(\delta-\gamma)}\right] e^{-\gamma t}$$

$$+ D\left[\frac{A_1(K_3-\delta)+A_2(K_4-\delta)+A_3(K_3-\delta)(K_5-\delta)+A_4}{(K_1-\delta)(K_6-\delta)(\alpha-\delta)(\beta-\delta)(\gamma-\delta)}\right] e^{-\delta t}$$

The mathematical procedures are so complex and arduous that simulation provides a simpler method of solution. The numerical method Runge-Kutta III (4) was used to solve the mass balance differential equations.

RK III method

$$dX_i/dt = f_i(X_1, X_2, \ldots\ldots, X_N; t_n)$$

$$i = 1, 2, \ldots\ldots, N$$

$$X_i^{(n+1)} = X_i^n + \Delta t/6\,(F_{0i} + 2F_{1i} + 2F_{2i} + F_{3i})$$

$$i = 1, 2, \ldots\ldots, N$$

$$F_{0i} = f_i(X_1, X_2, \ldots\ldots, X_N; t_n)$$

$$i = 1, 2, \ldots\ldots, N$$

$$F_{1i} = f_i(X_1+(\Delta t/2)F_{01}, X_2+(\Delta t/2)F_{02}, \ldots\ldots, X_N +(\Delta t/2)F_0N; t_n+\Delta t/2)$$

$$i = 1, 2, \ldots\ldots\ldots, N$$

$$F_{2i} = f_i(X_1+(\Delta t/2)F_{11}, X_2+(\Delta t/2)F_{12}, \ldots\ldots, X_N +(\Delta t/2)F_{1N}; t_n+\Delta t/2)$$

$$F_{3i} = f_i(X_1+\Delta t\, F_{21}, X_2+\Delta t\, F_{22}, \ldots\ldots, X_N+\Delta t\, F_{2N}; t_{n+1})$$

$$i = 1, 2, \ldots\ldots\ldots, N$$

n = index in time

i = index for the row equation number in the differential system

EXPERIMENTAL

Simulations were performed using the Oregon State University CDC 6400 Cyber 70 model 73-16, 64 bit word size computer. The computer progam used (c.f. Appendix I) consists of a modified version of the program SIMMOD.[2] The program employed to simulate behavior of the diester prodrugs according to the pharmacokinetic pattern in scheme I is shown in Appendix I. With slight modification of the program and/or careful input of the data, this program can also be used to generate simulation curves for pharmacokinetic patterns of the monoesters and dyphylline. The original program

SIMMOD was written such that it can evaluate up to a ten compartment model and can also be applied to Michaelis-Menton type processes besides general first order rate processes. However, due to the unobtainable volume of distribution in most compartments and the unavailable data required for Michaelis-Menton type rate processes at the present time, the assumption was made that only first order rate processes were occurring in the pharmacokinetic behavior of the prodrugs and output was designed to be the mass of drug in each compartment instead of drug concentration.

In order to obtain approximate numbers which could represent the system microconstants, the apparent partition coefficients of dyphylline, monopropionyl dyphylline and dipropionyl dyphylline were first determined. Dyphylline, monopropionyl dyphylline and dipropionyl dyphylline (5 mg each) were accurately weighed and placed into three separated 25 ml volumetric flasks. They were then thoroughly dissolved in 25 ml of octanol saturated water. These solutions (6 ml each) were accurately pipetted into three different 25 ml ampules and 6 ml of water saturated octanol was added into each ampule. The ampules were sealed and were placed on a mechanical rotator[3] overnight. The next day the ampules were opened and the water and octanol layers were separated. After suitable dilution, the UV

absorption in each layer was determined with a spectrophotometer.[4] The absorption of the undiluted solution could then be calculated and ratio of the absorbance of the octanol layer compared to the absorbance of the water layer from each ampule was taken as the apparent partition coefficient of the compound in that particular ampule. The assumption being made is that the medium (octanol or water) does not markedly influence the absorption. Another set of samples was performed in the same way with the exception that the compounds were initially dissolved in the octanol phase into which the water phase was then added. The apparent partition coefficients used to calculate the appropriate microconstant for the simulation experiments were taken from the average of the first and second sets of samples. Table I is a summary of data used for calculation of apparent partition coefficients. From a partition coefficient data base (5) the log p of theophylline is -0.02 which corresponds to a partition coefficient of 0.955. Table II summarizes the ratios of the apparent partition coefficients of monopropionyl dyphylline and dipropionyl dyphylline compared to dyphylline and theophylline. The square roots of these ratios were used as factors to multiply or divide reported pharmacokinetic microconstants of dyphylline and theophylline to provide estimates of the microconstants of propionyl dyphylline prodrugs.

Table I. Data used for calculating the apparent partition coefficients of dyphylline, monopropionyl dyphylline and dipropionyl dyphylline.

Compound	Initial Phase	Absorbance		Ratio	Apparent Partition Coefficient
		Octanol Phase	Water Phase		
Dyphylline	Water	0.860	8.300	0.104	0.112
	Octanol	0.925	7.760	0.119	
Monopropionyl Dyphylline	Water	2.350	1.130	2.080	2.031
	Octanol	2.180	1.100	1.982	
Dipropionyl Dyphylline	Water	3.340	1.190	2.807	3.070
	Octanol	3.600	1.080	3.333	

Consider the following two compartment model:

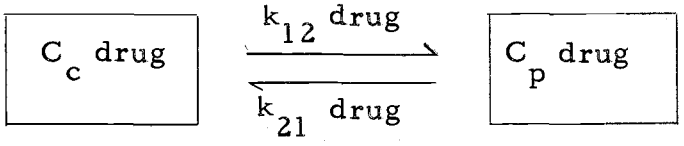

(Central Compartment) (Peripheral Compartment)

$$\frac{dC_c \text{ drug}}{dt} = -k_{12} \text{ drug } C_c \text{ drug} + k_{21} \text{ drug } C_p \text{ drug}$$

At equilibrium $\frac{dC_c \text{ drug}}{dt} = 0$

therefore k_{12} drug C_c drug = k_{21} drug C_p drug

$$= \frac{k_{12} \text{ drug}}{k_{21} \text{ drug}} = \frac{C_p \text{ drug}}{C_c \text{ drug}} = \text{Partition Coefficient of drug } (P_D) \quad (1)$$

and

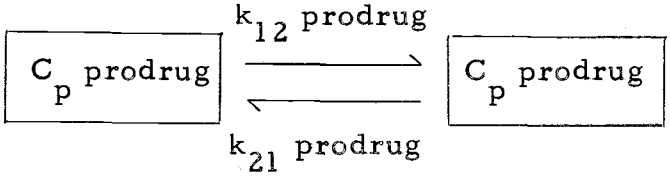

(Central Compartment) (Peripheral Compartment)

At equilibrium

$$= \frac{k_{12} \text{ prodrug}}{k_{21} \text{ prodrug}} = \frac{C_p \text{ prodrug}}{C_c \text{ prodrug}} = \text{Partitition coefficient of Prodrug } (P_P) \quad (2)$$

$$\frac{(2)}{(1)} \quad \frac{k_{12} \text{ prodrug}}{k_{12} \text{ drug}} \cdot \frac{k_{21} \text{ drug}}{k_{21} \text{ prodrug}} = \frac{P_P}{P_D} = \text{Partition Coefficient ratio}$$

Assuming that the increase in the transfer rate of the prodrug from central compartment to peripheral compartment is equal to the decrease in the transfer rate of the prodrug from peripheral

compartment to central compartment, i.e. percent increase in k_{12} = percent decrease in k_{21}, then:

$$k_{12}\ \text{prodrug}/k_{12}\ \text{drug} = k_{21}\ \text{drug}/k_{21}\ \text{prodrug},$$

therefore

$$\frac{k_{12}\ \text{prodrug}}{k_{12}\ \text{drug}} = \frac{k_{21}\ \text{drug}}{k_{21}\ \text{prodrug}} = \sqrt{\text{partition coefficient ratio}}$$

Table II. Apparent partition coefficient ratios of propionyl dyphylline compared to dyphylline and theophylline.

Compound	The Apparent Partition Coefficient Ratio	Square root of the ratio
Monopropionyl Dyphylline / Dyphylline	$\frac{2.031}{0.112} = 18.134$	4.258
Monopropionyl Dyphylline / Theophylline	$\frac{2.031}{0.955} = 2.127$	1.458
Dipropionyl Dyphylline / Dyphylline	$\frac{3.070}{0.112} = 27.411$	5.236
Dipropionyl Dyphylline / Theophylline	$\frac{3.070}{0.955} = 3.215$	1.793

The first step of the simulation experiments was carried out to observe the sensitivity of dyphylline blood concentrations to each unknown microconstant and was initiated with the pharmacokinetic model for a dyphylline monoester given intravenously, i.e. three compartment open model with the first three compartments in scheme I neglected. The intravenous route of administration was chosen for

simplicity. The numbers representing the mean value of each microconstant involved are summarized in table III. The number representing k_{60} is the known value for dyphylline[5] and was fixed throughout all simulation experiments. k_{46} and k_{56} were assumed to be equal and arbitrarily chosen to be equal to 90% conversion in 10 hours. k_{45} and k_{54} were modified from the distribution rate constants of theophylline. The modification was based on the square root of the partition coefficient ratio of monopropionyl dyphylline compared to theophylline, i.e. the distribution rate of monopropionyl dyphylline from the central compartment to the peripheral compartment was 1.458 times (table II) faster than that of theophylline which was equal to 0.0641 min^{-1} (6) and in contrast, the distribution rate from the peripheral compartment back to the central compartment was 1.458 times slower for monopropionyl dyphylline compared to that of theophylline which was equal to 0.0369 min^{-1} (6). The number representing k_{40} was calculated based on the assumption that the elimination rate of monopropionyl dyphylline was 4.258 times (table II) slower than that of dyphylline. There were five microconstants, k_{46}, k_{56}, k_{45}, k_{54} and k_{40} which were varied using the standard Yedts factorial design. The high and low values were 10 times different, i.e. the high values were the square root of 10 times higher than the mean values and the low values were the square root of 10 times lower than the mean values. Since k_{46} and k_{56} were assumed to be

Table III. Mean pharmacokinetic microconstants and the high-low values used for simulation experiments involving monopropionyl dyphylline - IV route of administration.

Microconstant	Mean (min^{-1})	High (min^{-1})	Low (min^{-1})
k_{60}	0.0058	0.0058*	0.0058*
$k_{46}=k_{56}$	0.0038	0.0120	0.0012
k_{45}	0.0934	0.2954	0.0295
k_{54}	0.0253	0.0800	0.0800
k_{40}	0.0014	0.0044	0.0004

*Fixed to be equal to mean value

equal, there were 16 possible combinations of these high-low rate constants. These 16 high-low combination patterns are shown in table IV.

The second step of the simulation experiments was to determine the sensitivity of dyphylline blood concentrations to the conversion rate constant of monopropionyl dyphylline to dyphylline. The rate of conversion was varied to be 10, 30, 50 and 70 percent conversion in one hour, while the other rate constants were kept constant using the mean values in table III. The computer program was also modified so that it was able to perform multiple dose simulations as well as single dose simulations.

In the third step of the simulation experiments, compartment 2 and 3 were added in order to perform simulations for the diesters.

Table IV. Standard Yedts 2^4 Factorial Design for Four Variables of Interest.[6]

Combination Number (Run No.)	Parameter Values			
	k_{40}	k_{54}	k_{45}	$k_{46} = k_{56}$
1	-	-	-	-
2	+	-	-	-
3	-	+	-	-
4	+	+	-	-
5	-	-	+	-
6	+	-	+	-
7	-	+	+	-
8	+	+	+	-
9	-	-	-	+
10	+	-	-	+
11	-	+	-	+
12	+	+	-	+
13	-	-	+	+
14	+	-	+	+
15	-	+	+	+
16	+	+	+	+

"+" = high value while "-" = low value.

Note:- In this format the following "empirical model" may be built up with ease.[6]

$$\underset{\sim}{y} = \underset{\text{(grand mean)}}{\eta} + \text{main effects } (4\ k\text{'s}) + \text{2nd order interaction effects } (k_{40} \text{ by } k_{54},\ k_{40} \text{ by } k_{45},\ \text{etc.}) + \text{3rd order interaction effects} + \text{4th order interaction effects} + \underset{\sim}{\varepsilon}$$

The conversion rates of the diesters to monoesters in the central and peripheral compartments, k_{24} and k_{35}, were again assumed to be equal and were varied as equal to the conversion rates of monoesters to dyphylline (0.0038 min^{-1}), two times faster (0.0077 min^{-1}) and two times slower (0.0019 min^{-1}) than the conversion rates of monoesters to dyphylline respectively, while the other microconstants were kept constant. The distribution rates of the dipropionyl esters, k_{23} and k_{32}, were calculated based on the distribution rates of theophylline (6) and the square root of the apparent partition coefficient ratio of dipropionyl dyphylline compare to the theophylline (table II). The numbers used were 0.1149 min^{-1} for k_{23} and 0.0206 min^{-1} for k_{32} respectively. The elimination rate of dipropionyl dyphylline, k_{20}, was taken as 0.0011 min^{-1}. This number was calculated based on the assumption that the elimination rate of dipropionyl dyphylline was 5.236 times (table II) slower than that of dyphylline.

In the fourth step of the simulation experiments, dyphylline blood concentrations versus time curves resulting from simulation of administering equal doses of dipropionyl dyphylline, monopropionyl dyphylline and dyphylline were compared to determine the predicted effect of mono- and di- propionyl prodrugs.

Since the absorption rate would be altered changing from dyphylline to prodrugs, in the fifth step, compartment 1 in scheme I was added and simulations were performed to observed the affect of

absorption rate of prodrugs on dyphylline blood concentrations, i.e. to compare dyphylline blood concentrations between intravenous and oral routes of administration of prodrugs. The absorption rates were varied to be equal to that of theophylline ($0.0233\ min^{-1}$)(7), square root of partition coefficient ratio times slower than theophylline ($0.0160\ min^{-1}$ for monopropionyl dyphylline and $0.0130\ min^{-1}$ for dipropionyl dyphylline), and one-tenth of the absorption rate of theophylline ($0.0023\ min^{-1}$). These comparison simulations were performed with both the mono- and di- propionyl dyphylline prodrugs.

All simulation curves were plotted with the aid of a Tektronix 4004 graphics terminal and a Gerber model 1022 flatbed plotter, using the program TEKPLOT[7] listed in Appendix II. This program can plot up to eight curves on the same graph.

RESULTS AND DISCUSSIONS

Figures 1, 2 and 3 show the results of the first step of the simulation experiments. They were generated according to the standard Yedts 2^4 factorial design shown in Table IV. Figure 1 shows combination number 1, 2, 3, 5 and 9; figure 2 shows combination number 4, 6, 7, 10, 11 and 13; figure 3 shows combination number 8, 12, 14, 15 and 16. From these results, it is obvious that predicted dyphylline blood concentrations are highly sensitive to variation in the conversion rate of monoester to dyphylline (k_{46}, k_{56}), i.e. predicted dyphylline blood concentrations were high when these rate constants were high and predicted dyphylline blood concentrations were low when these rate constants were low, independent of the other rate constants. The high value of the elimination rate constant of monoester (k_{40}) and the high distribution rate of the monoester from the peripheral compartment back to the central compartment (k_{54}) both caused some relatively small decrease in predicted dyphylline blood concentrations. In contrast, the high distribution rate of the monoester from the central compartment to the peripheral compartment (k_{45}) resulted in a small increase in predicted dyphylline blood concentrations. These results were not too surprising since the assumption had been made that no elimination of the monoesters would occur in the peripheral compartment. In order to observe

Figure 1. Dyphylline mass versus time curves generated from simulation of a three compartment open pharmacokinetic model with intravenous dosing of 1.5 g of monopropionyl dyphylline using the high-low combination number 1, 2, 3, 5 and 9 in table IV:-

+ - k_{40}, k_{54}, k_{45}, $k_{46} = k_{56}$ = low;

o - k_{40} = high while k_{54}, k_{45}, $k_{46} = k_{56}$ = low;

□ - k_{54} = high while k_{40}, k_{45}, $k_{46} = k_{56}$ = low;

△ - k_{45} = high while k_{40}, k_{54}, $k_{46} = k_{56}$ = low;

* - $k_{46} = k_{56}$ = high while k_{40}, k_{54}, k_{45} = low.

Predicted dyphylline blood concentrations could be obtained by dividing the values on the Y-axis by the volume of distribution.

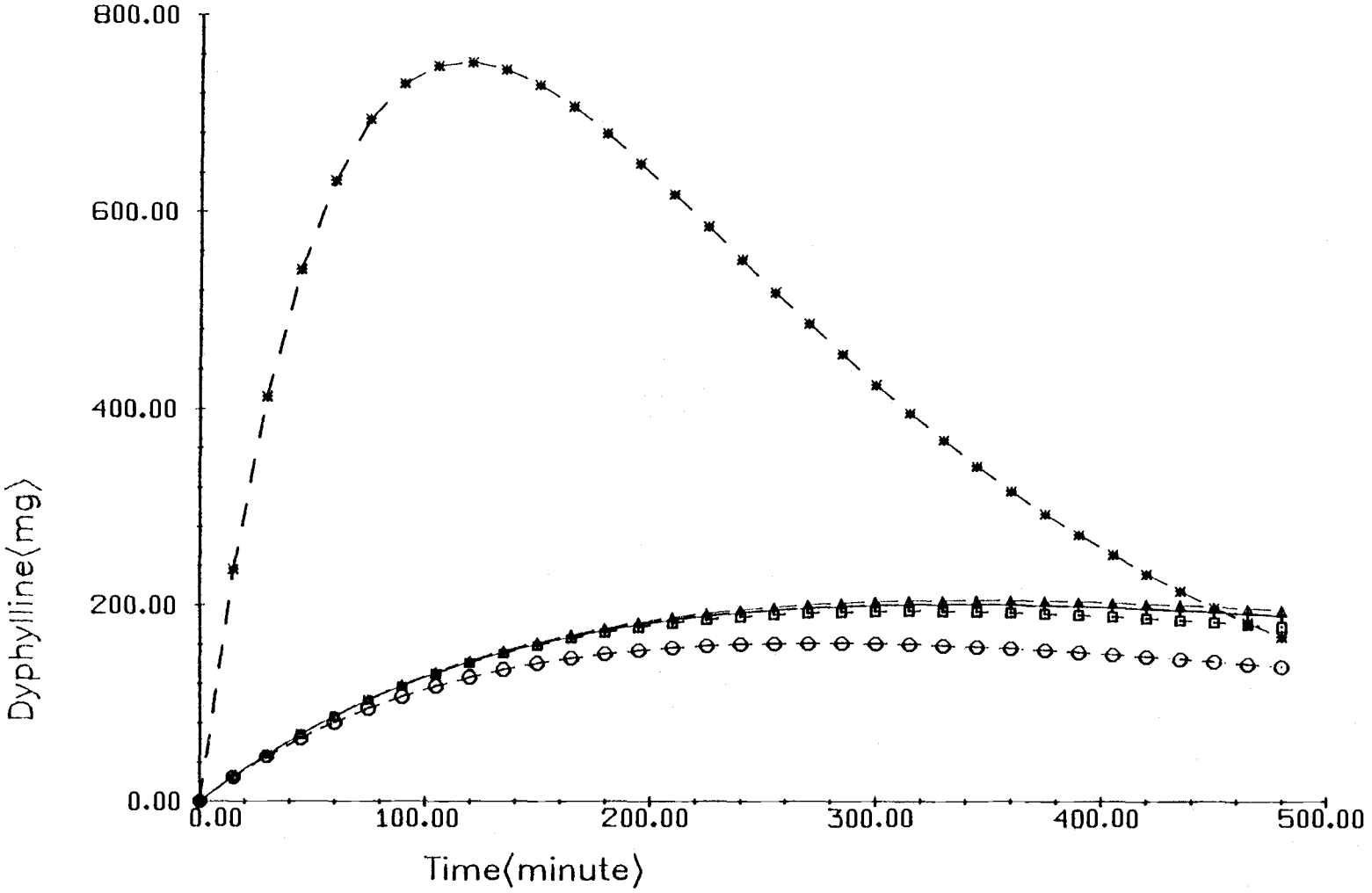
800.00
600.00
400.00
200.00
0.00
Dyphylline(mg)
0.00
100.00
200.00
300.00
400.00
500.00
Time(minute)

Figure 1

Figure 2. Dyphylline mass versus time curves generated from simulation of a three compartment open pharmacokinetic model with intravenous dosing of 1.5 g of monopropionyl dyphylline using the high-low combination number 4, 6, 7, 10, 11 and 13 in table IV:-

+ - k_{40}, k_{54} = high while k_{45}, k_{46} = k_{56} = low;

o - k_{40}, k_{45} = high while k_{54}, k_{46} = k_{56} = low;

□ - k_{40}, k_{46} = k_{56} = high while k_{45}, k_{54} = low;

△ - k_{54}, k_{45} = high while k_{40}, k_{46} = k_{56} = low;

* - k_{54}, k_{46} = k_{56} = high while k_{40}, k_{45} = low;

$\underline{\bar{x}}$ - k_{45}, k_{46} = k_{56} = high while k_{40}, k_{54} = low;

Predicted dyphylline blood concentrations could be obtained by dividing the values on the Y-axis by the volume of distribution.

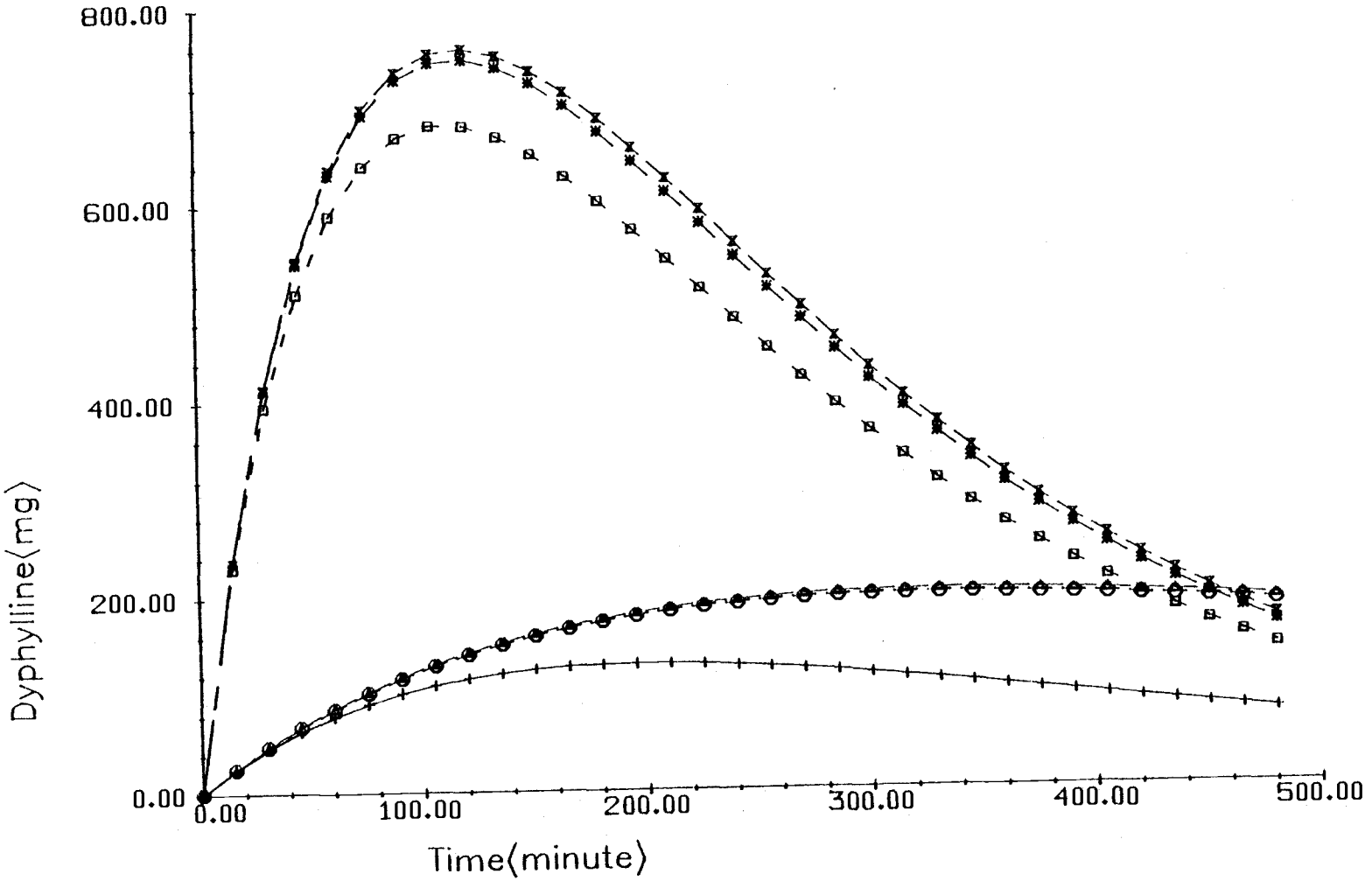
800.00
600.00
400.00
200.00
0.00
Dyphylline(mg)
0.00
100.00
200.00
300.00
400.00
500.00
Time(minute)

Figure 2

Figure 3. Dyphylline mass versus time curves generated from simulations of a three compartment open pharmacokinetic model with intravenous dosing of 1.5 g of monopropionyl dyphylline using the high-low combination number 8, 12, 14, 15 and 16 in table IV:-

+ - k_{40}, k_{54}, k_{45} = high while $k_{46} = k_{56}$ = low;

o - k_{40}, k_{54}, $k_{46} = k_{56}$ = high while k_{45} = low;

□ - k_{54}, k_{45}, $k_{46} = k_{56}$ = high while k_{40} = low;

△ - k_{40}, k_{45}, $k_{46} = k_{56}$ = high while k_{54} = low;

* - k_{40}, k_{54}, k_{45}, $k_{46} = k_{56}$ = high;

Predicted dyphylline blood concentrations could be obtained by dividing the values on the Y-axis by the volume of distribution.

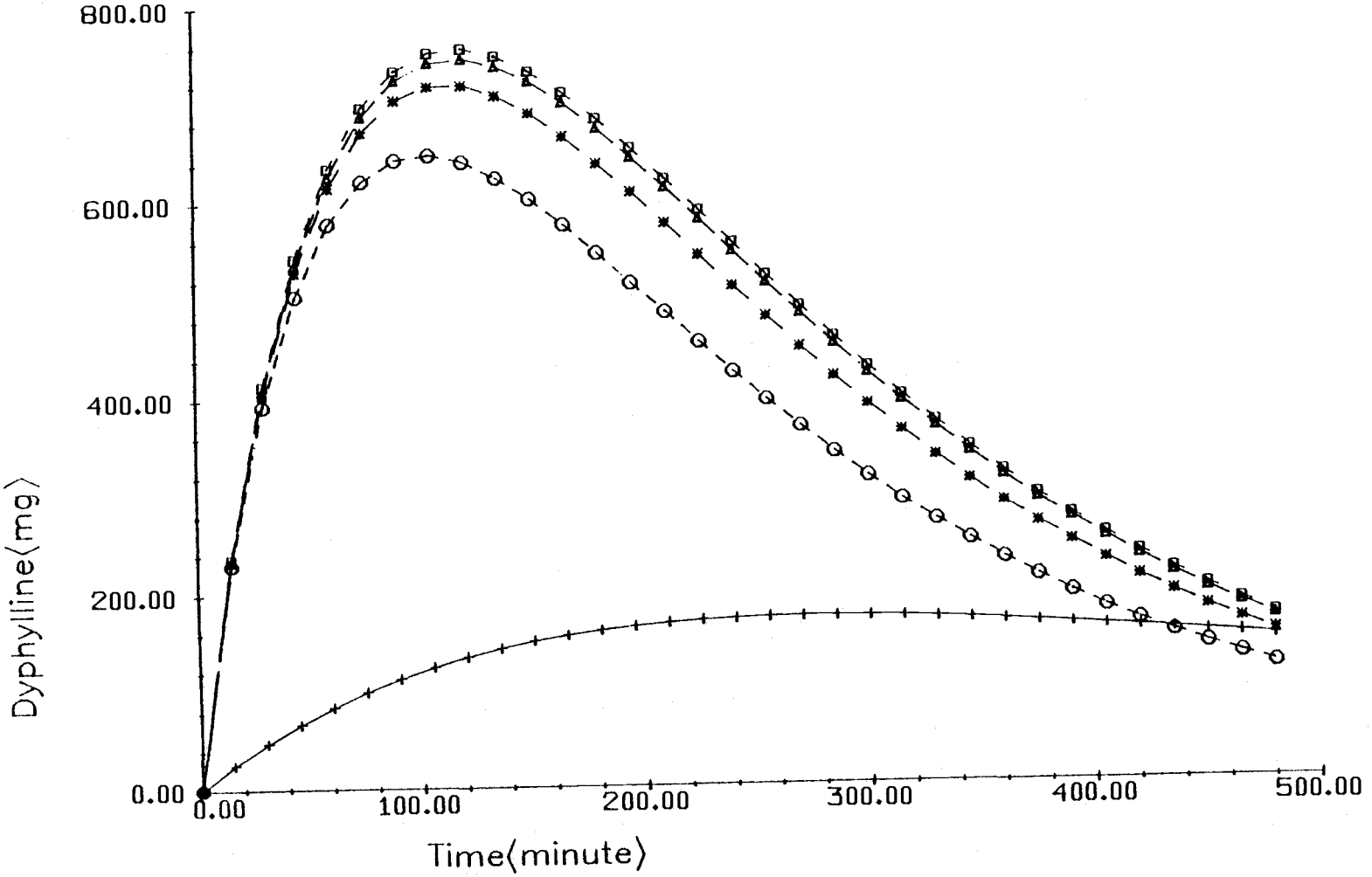
800.00
600.00
400.00
200.00
0.00
Dyphylline⟨mg⟩
0.00
100.00
200.00
300.00
400.00
500.00
Time⟨minute⟩

Figure 3

influence of the conversion rate in more detail, the second step of the simulation experiments was completed by varying the percent conversion of monoester to dyphylline while keeping constant the other rate constants. The results are shown in figure 4. The higher the conversion rate, the higher would be the dyphylline peak blood concentrations and the sooner would be the peak time. However, the higher conversion rate also resulted in production of greater fluctuation of dyphylline blood concentrations, i. e. the predicted peak went higher and the valley was lower.

The next step was to determine the predicted effect of administering the diester prodrug on dyphylline blood concentrations. The conversion rate of the diester to monoester was taken as equal to, two times higher and two times slower than the conversion rate of monoester to dyphylline. Figure 5 shows that the higher the conversion rate of the diester to monoester, the higher would be the peak dyphylline amount and the sooner would be the peak time. With rapid conversion there would also be more fluctuation in the dyphylline amount versus time curve.

Dyphylline blood concentration versus time curves for the administration of dyphylline, monoester or diester via the intravenous route are compared in figure 6. These simulation curves show that the administration of the monoester would result in a lower peak, later peak time, but more stable dyphylline blood concentrations

Figure 4. Dyphylline mass versus time curves generated from simulations of a three compartment open pharmacokinetic model with intravenous dosing of 1.5 g of monopropionyl dyphylline using mean values for k_{60}, k_{45}, k_{54} and k_{40} but varying the conversion rate of monopropionyl dyphylline to dyphylline ($k_{46}=k_{56}$):-

x - 10% hydrolysis in one hour;

o - 30% hydrolysis in one hour;

□ - 50% hydrolysis in one hour;

△ - 70% hydrolysis in one hour;

Predicted dyphylline blood concentrations could be obtained by dividing the values on the Y-axis by the volume of distribution.

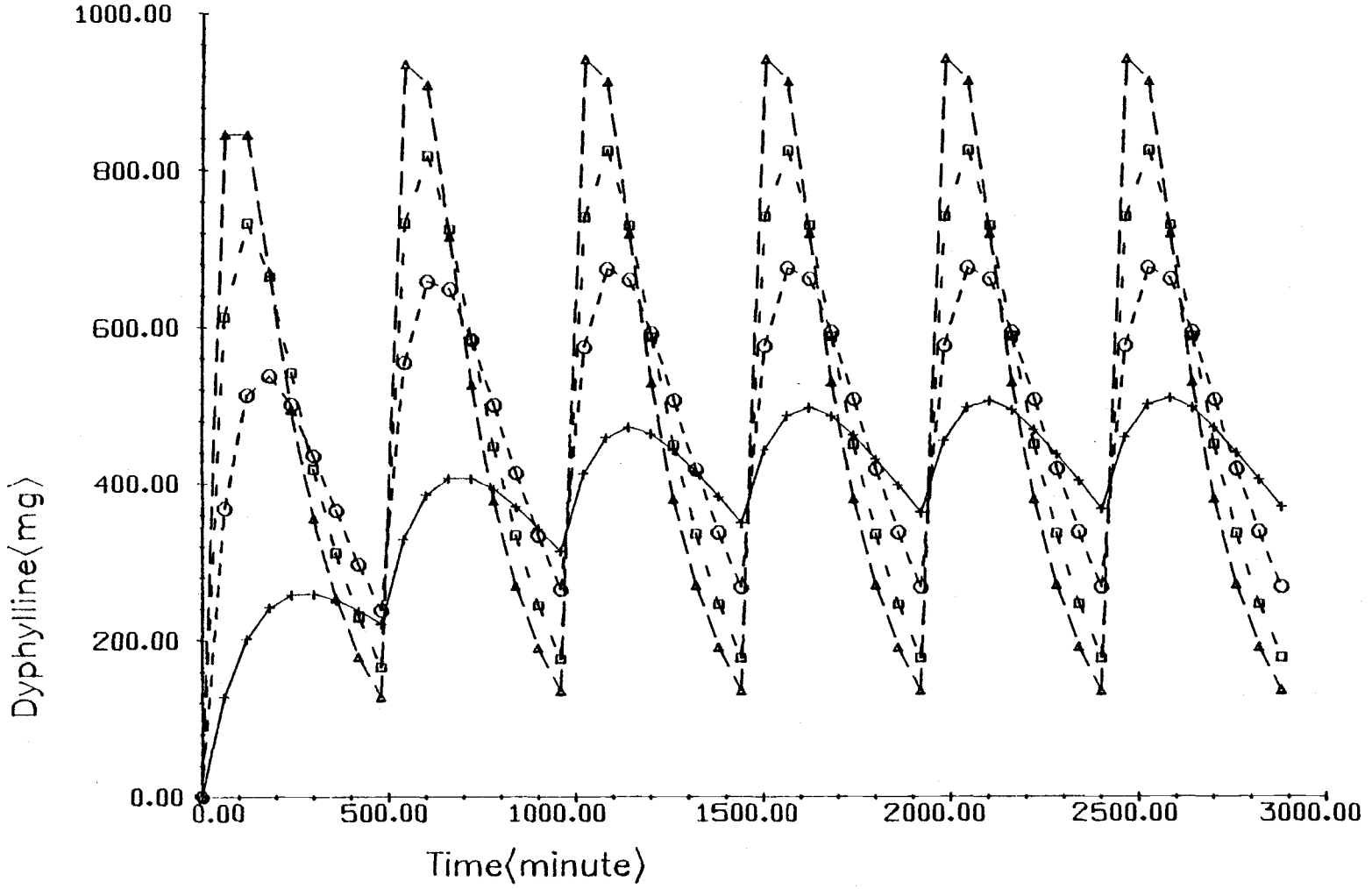
1000.00
800.00
600.00
400.00
200.00
0.00
Dyphylline(mg)
0.00
500.00
1000.00
1500.00
2000.00
2500.00
3000.00
Time(minute)

Figure 4

Figure 5. Dyphylline mass versus time curves generated from simulations of a five compartment open pharmacokinetic model with intravenous dosing of 1.5 g of dipropionyl dyphylline using mean values for k_{60}, k_{45}, k_{54}, k_{40}, k_{46} and k_{56} (table III) but varying the conversion rate of dipropionyl dyphylline to monopropionyl dyphylline ($k_{24}=k_{35}$):-

x - two times higher than the hydrolysis of monopropionyl dyphylline to dyphylline (k_{46}, k_{56});

o - two times lower than the hydrolysis of monopropionyl dyphylline to dyphylline (k_{46}, k_{56});

□ - equal to the hydrolysis rate of monopropionyl dyphylline to dyphylline (k_{46}, k_{56});

Predicted dyphylline blood concentrations could be obtained by dividing the values on the Y-axis by the volume of distribution.

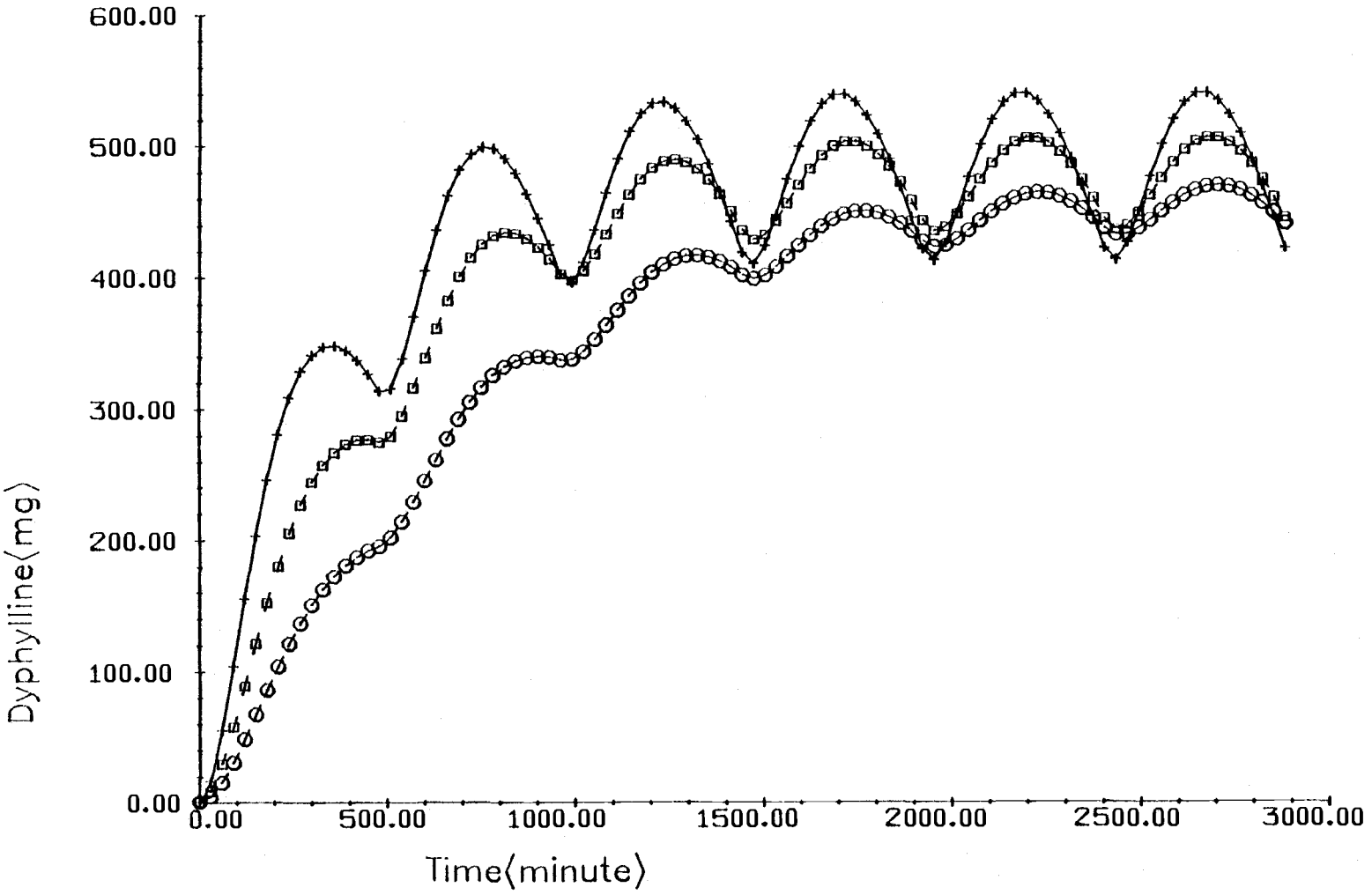
600.00
500.00
400.00
300.00
200.00
100.00
0.00
Dyphylline(mg)
0.00
500.00
1000.00
1500.00
2000.00
2500.00
3000.00
Time(minute)

Figure 5

Figure 6. Simulated dyphylline mass versus time curves generated from intravenous administration of 1.5 g of the diester, monoester or dyphylline:-

x - given dipropionyl dyphylline;

o - given monopropionyl dyphylline;

□ - given dyphylline itself;

All microconstants were equal to the mean values. Predicted dyphylline blood concentrations could be obtained by dividing the values on the Y-axis by the volume of distribution.

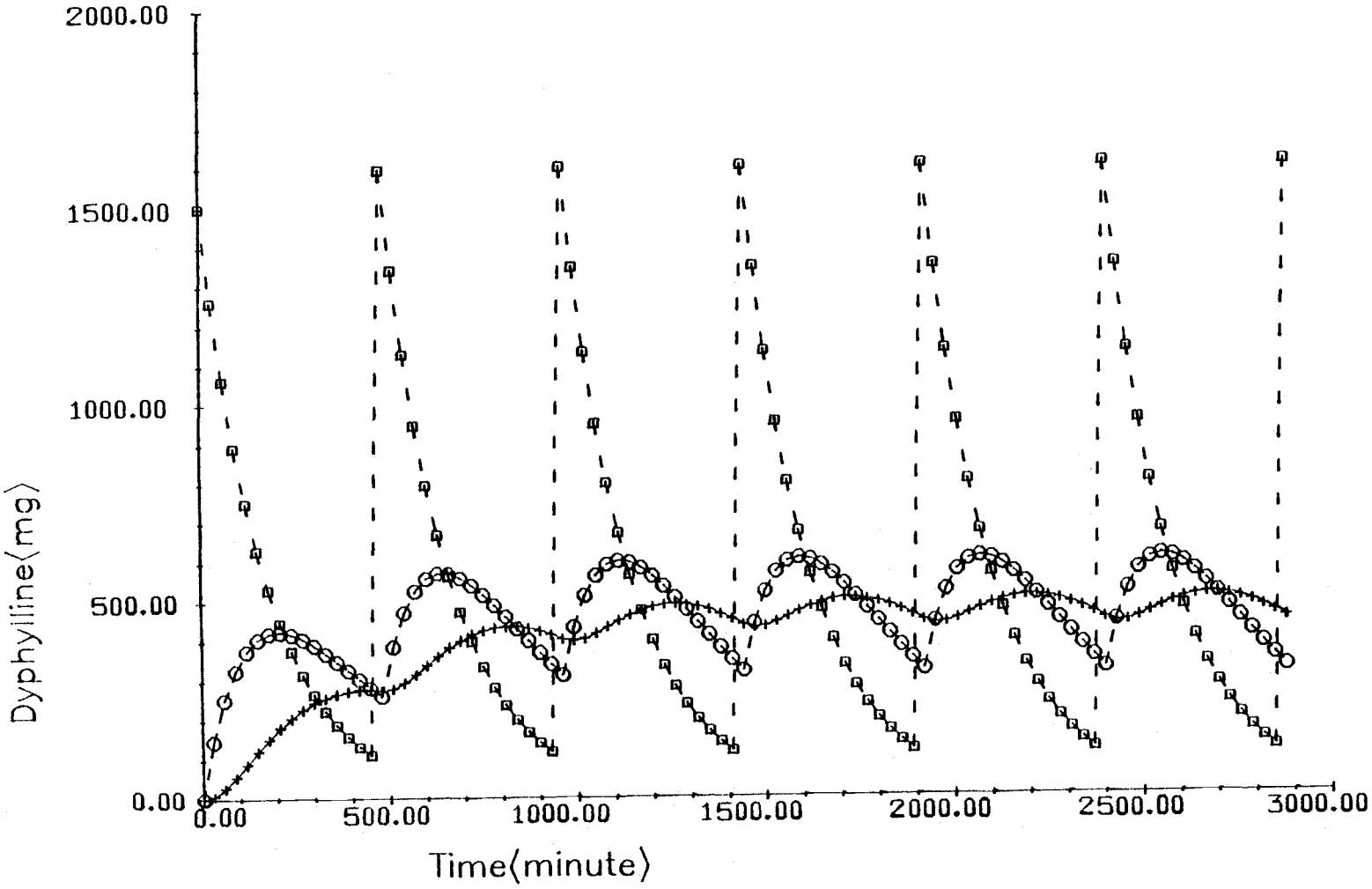
2000.00
1500.00
1000.00
500.00
0.00
Dyphylline(mg)
0.00
500.00
1000.00
1500.00
2000.00
2500.00
3000.00
Time(minute)

Figure 6

than the administration of dyphylline itself, and the administration of the diester would result in an even lower peak, later peak time, but more stable dyphylline blood concentrations than the administration of the monoester.

Figure 7 shows the influence of absorption rate on dyphylline blood concentrations when the monoester was administered and figure 8 shows the affect of the absorption rate on dyphylline blood concentrations when the diester was administered. Both figures 7 and 8 show that two of the absorption rates chosen did not have much influence on predicted dyphylline blood concentrations. Predicted dyphylline blood concentration versus time curves vary only slightly for oral administration from the dyphylline blood concentrations predicted from the intravenous route of administration. This implies that when the conversion rate was 90 percent in 10 hours ($0.0038\ min^{-1}$) as was used for most of these simulation experiments, the conversion rate was the slowest step. Since it was much slower than the absorption rates evaluated, this conversion became the rate determining step and was the main influence on predicted dyphylline blood concentrations. However, when the absorption rate was taken as one-tenth of the absorption rate of theophylline ($0.0023\ min^{-1}$), thin absorption rate became slower than the conversion step. Therefore, the absorption rate became the rate determining step and some obvious differences in dyphylline blood concentrations were predicted. The affects

Figure 7. Comparison of simulated dyphylline mass versus time curves when the route of administration of monopropionyl dyphylline was changed from intravenous (IV) to oral with varying rates of absorption:-

x - IV;

o - one-tenth of the absorption rate of theophylline;

□ - equal to the absorption rate of theophylline;

Δ - square root of the partition coeffient ratio times slower than the absorption rate of theophylline;

Dose = 1.5 g; all other microconstants were equal to the mean values. Predicted dyphylline blood concentrations could be obtained by dividing the values on the Y-axis by the volume of distribution.

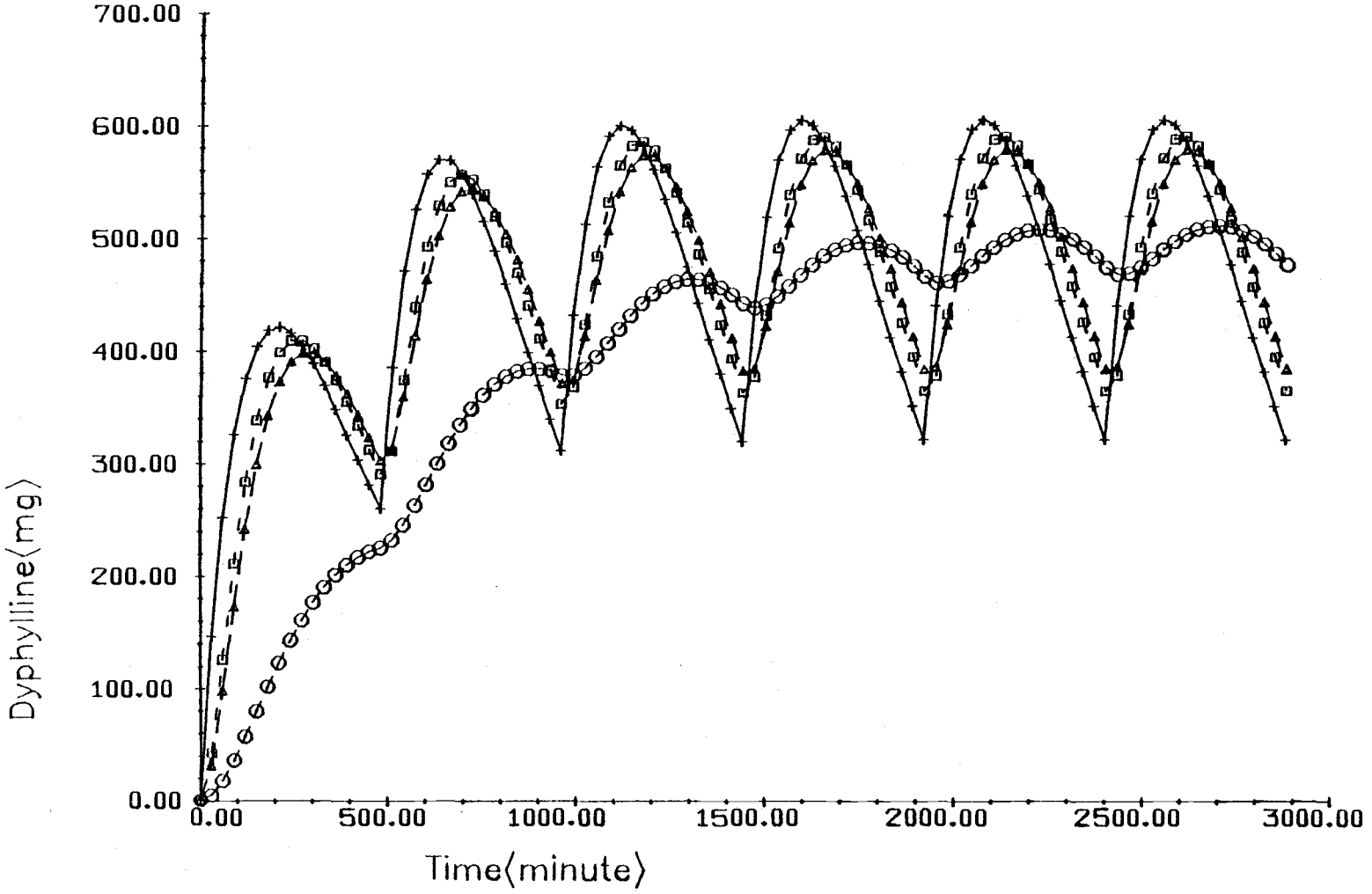
700.00
600.00
500.00
400.00
300.00
200.00
100.00
0.00
Dyphylline〈mg〉
0.00
500.00
1000.00
1500.00
2000.00
2500.00
3000.00
Time〈minute〉

Figure 7

Figure 8. Simulated dyphylline mass versus time curves when the route of administration of dipropionyl dyphylline was changed from intravenous (IV) to the oral route with varying rates of absorption:-

x - IV;

o - one-tenth of the absorption rate of theophylline;

□ - equal to the absorption rate of theophylline;

△ - square root of partition coefficient ratio times slower than the absorption rate of theophylline;

Dose = 1.5 g; all other microconstants were equal to the mean values. Predicted dyphylline blood concentrations could be obtained by dividing the values on the Y-axis by the volume of distribution.

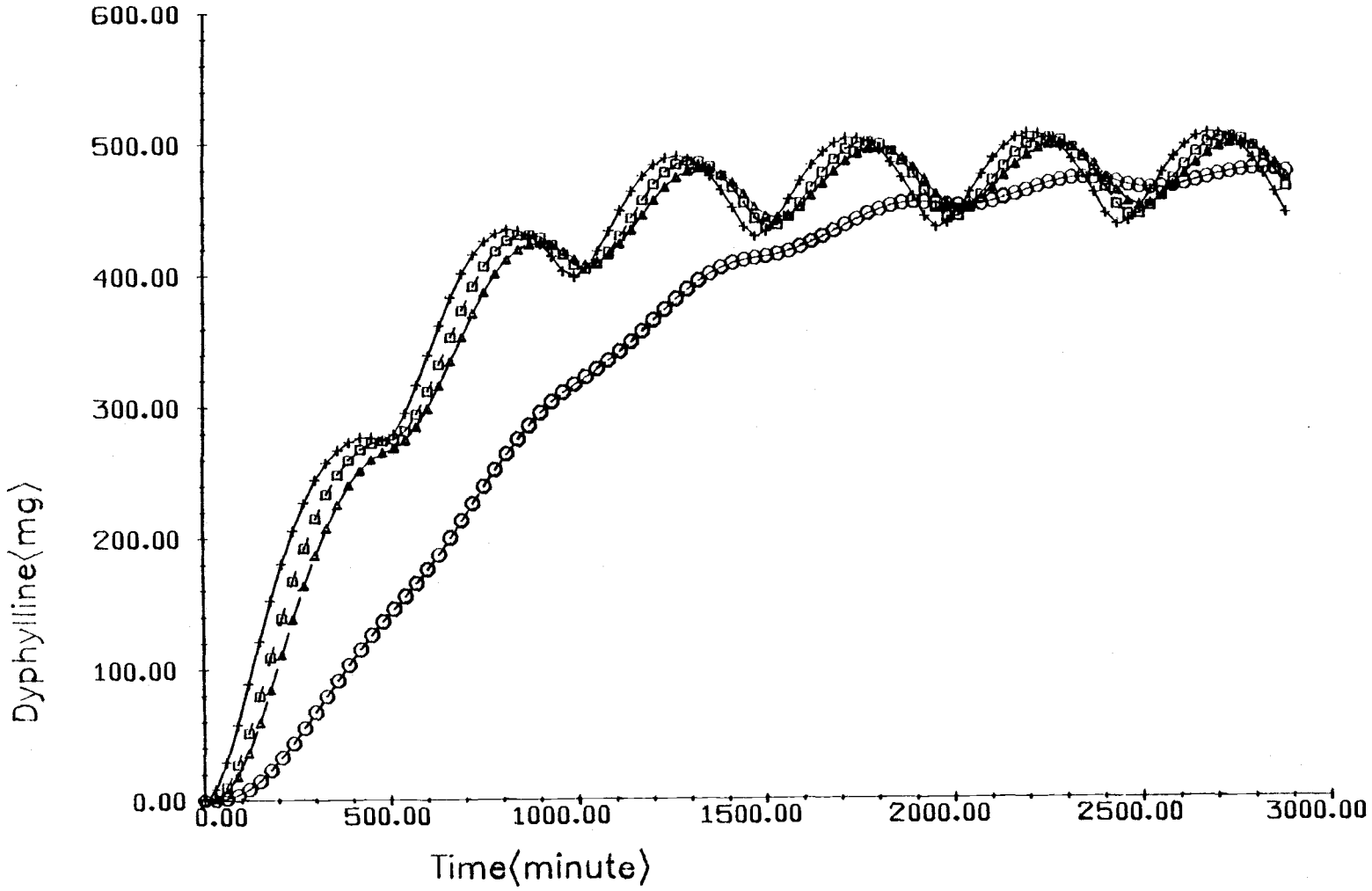
600.00
500.00
400.00
300.00
200.00
100.00
0.00
Dyphylline(mg)
0.00
500.00
1000.00
1500.00
2000.00
2500.00
3000.00
Time(minute)

Figure 8

were a lower peak, a little bit slower peak time, but more steady dyphylline blood concentrations. The dyphylline concentrations before steady state were distinctively lower with this slower absorption rate, but the time required to reach steady state was not much different. After the dyphylline concentrations obtained steady state, the curves exhibited much less fluctuation.

Figure 9 shows an example of the mass of each drug in each compartment using the mean value for each rate constant and the simulations were run according to the pharmacokinetic pattern for diesters with oral administration (Scheme I). Compartment 1, the gut, showed the most fluctuation of drug mass versus time curve as the mass went down to nearly zero at the end of each dose which indicates that absorption was nearly complete at the end of eight hours. The drug in compartment 2 (which represents the central compartment of dipropionyl dyphylline) was in the range of 40 to 270 mg. The mass in compartment 3 (which represents the peripheral compartment of dipropionyl dyphylline) was much higher than the mass in the central compartment and also fluctuated much more; the range was 227 to 1035 mg. Compartment 4, which represents the central compartment of monopropionyl dyphylline, exhibited low drug mass and little fluctuation after steady state had been reached; the range of mass levels was 123 to 172 mg. The peripheral compartment for monopropionyl dyphylline (compartment 5) at steady state showed a relatively high

Figure 9. Simulated drug mass versus time curves for six compartments generated from an open pharmacokinetic model with oral administration of the dipropionyl ester of dyphylline using the mean value for each rate constant and a dose equal to 1.5 g:-

x - dipropionyl dyphylline mass level in gut;

o - dipropionyl dyphylline mass level in central compartment;

□ - dipropionyl dyphylline mass level in peripheral compartment;

△ - monopropionyl dyphylline mass level in central compartment;

* - monopropionyl dyphylline mass level in peri-peripheral compartment;

$\underline{\bar{x}}$ - dyphylline mass level;

Predicted prodrug or drug concentrations could be obtained by dividing the values on the Y-axis by the volume of distribution of each compartment.

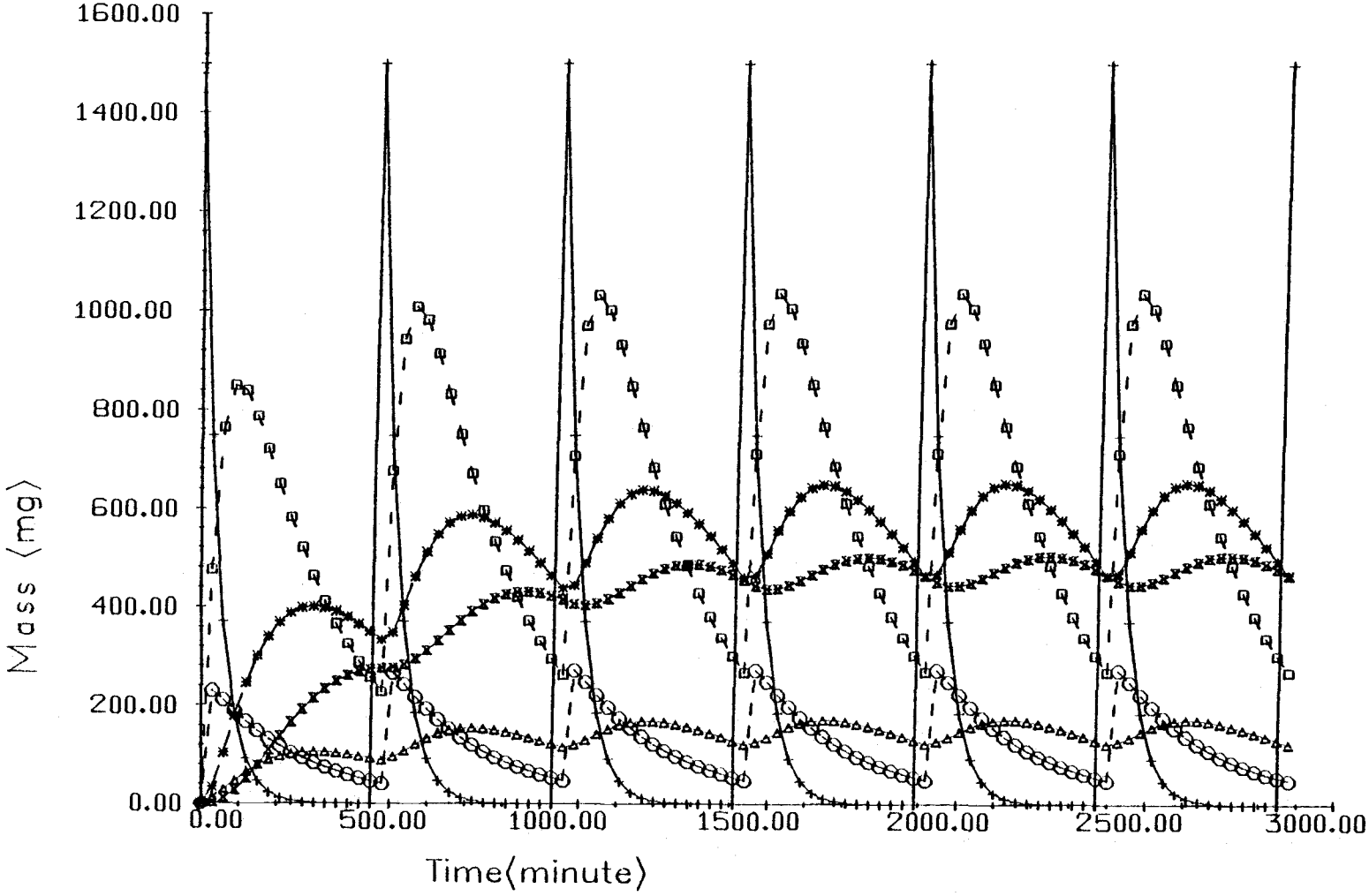
1600.00
1400.00
1200.00
1000.00
800.00
600.00
400.00
200.00
0.00
Mass (mg)
0.00
500.00
1000.00
1500.00
2000.00
2500.00
3000.00
Time(minute)

Figure 9

and steady mass versus time curves with the range of mass levels from 465 to 651 mg. Compartment 6, which represented dyphylline mass levels, exhibited very steady amounts which is highly desirable; the range was 442 to 502 mg.

The results from these simulation experiments indicated that dyphylline is a very good prospect for prolonging action through prodrugs. The results showed that predicted dyphylline blood concentrations were mainly influenced by the conversion rate of prodrug to drug, which is desirable since the conversion rate may be controlled through chain length optimization in the esters. It is also advantageous to know that the absorption rate is predicted to have little effect on dyphylline mass levels until it becomes much slower than the absorption rate of theophylline. The hydroxy ester prodrugs synthesized in chapter one are much more lipophilic than dyphylline which would result in a much lower solubility in the G-I tract and in turn a much slower absorption rate than dyphylline. If solubilized the dyphylline prodrugs should be absorbed at least as rapidly as theophylline.

The suggested minimum effective serum concentration for dyphylline is 12 μg/ml (8) and the volume of distribution in the dyphylline compartment can be calculated to be 61.5 liters,[6] if one assumes that dyphylline behavior is adequately described by a one compartment open model. Thus the minimum effective dyphylline mass should be closed to 738 mg. From the simulation experiments, dyphylline mass

Figure 10. Simulated dyphylline mass versus time curve when 3.0 g dose of dipropionyl dyphylline was administered orally every 8 hours and all the microconstants were equal to their mean values.

x - dyphylline mass;

--- - suggested minimum effective mass

Predicted dyphylline blood concentrations could be obtained by dividing the values on the Y-axis by the volume of distribution.

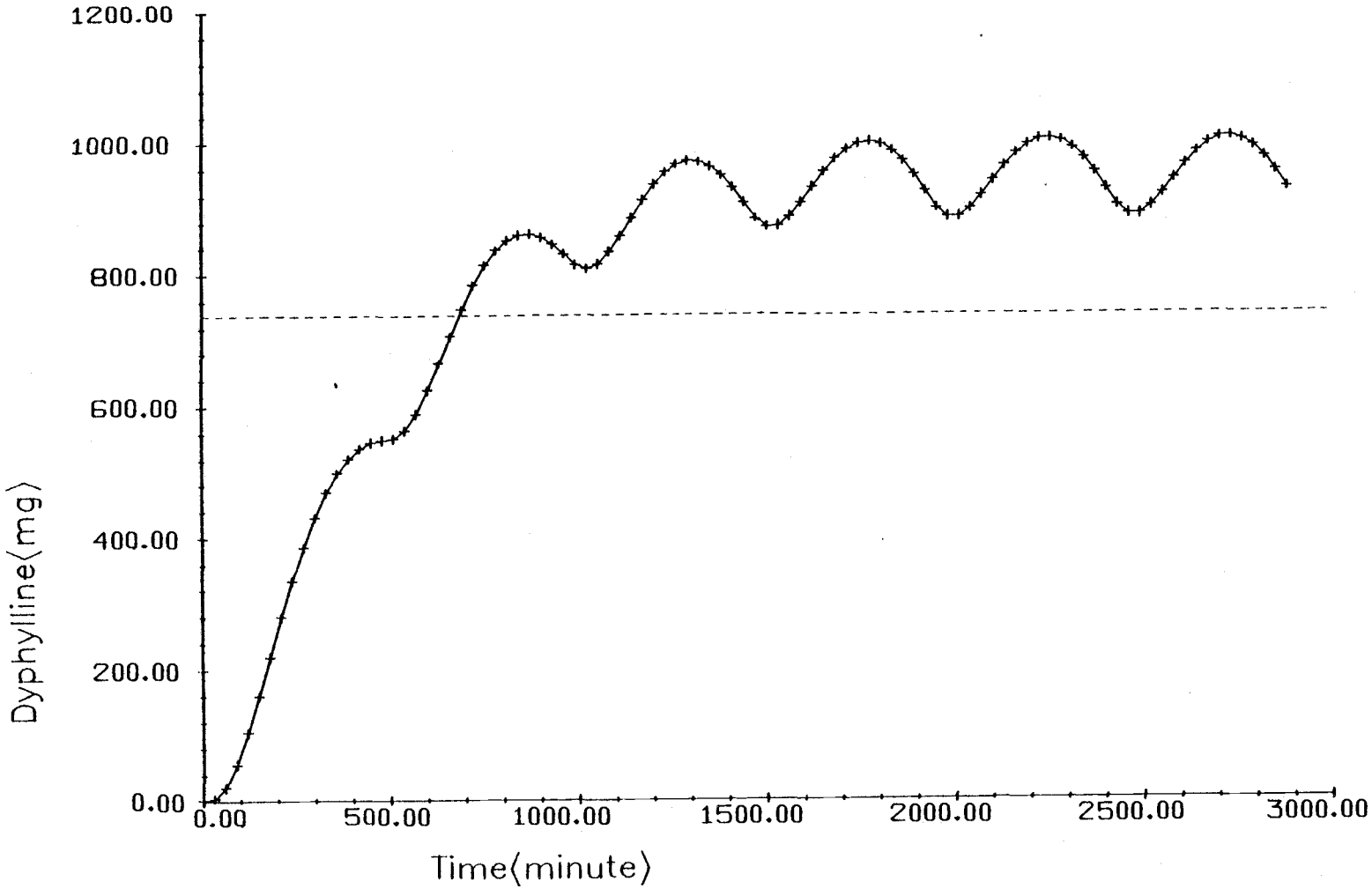
1200.00
1000.00
800.00
600.00
400.00
200.00
0.00
Dyphylline(mg)
0.00
500.00
1000.00
1500.00
2000.00
2500.00
3000.00
Time(minute)

Figure 10

amounts were much more steady when the prodrug was given than when the dyphylline itself was given. Dyphylline steady state mass amounts when given prodrugs were also higher than 400 mg when a 1.5 g dose was given every eight hours which means that by doubling the dose to 3.0 g, the dyphylline steady state mass amounts could go higher than 800 mg, i.e. higher than the suggested minimum effective amount. Figure 10 showed that dyphylline blood concentration could be maintained above the suggested minimum effective level when 3.0 g of the dipropionyl dyphylline was administered orally every 8 hours and all the microconstants were equal to their mean values.

It is true that several assumptions have been made in order to perform these simulation experiments but it is anticipated that variations from these assumptions, when the real pharmacokinetic experiments are performed in animals and/or humans, will not be so extensive that they negate the value of this simulation work.

Footnotes, Chapter III:

1. Obtain by computer fit using AUTOANII and data reported by Gisclon, Ayres and Ewing in Am. J. Hosp. Pharm., Sep. 1979
2. Program developed by Dr. T. Lindstrom, Statistics Department, Oregon State University
3. Ernest D. Menold, Lester, Pennsylvania
4. Beckman DB Spectrophotometer, Fullerton, California
5. Obtain by computer fit using AUTOANII and data reported by Gisclon, Ayres and Ewing in Am. J. Hosp. Pharm., Sep. 1979
6. Personal advice from Dr. T. Lindstrom, Statistics Department, Oregon State University
7. Program developed by D. R. Henry, a Ph. D. candidate in Medicinal Chemistry, School of Pharmacy, Oregon State University

BIBLIOGRAPHY

1. R. E. Notari, "Alteration of Pharmacokinetics through Structural Modification" in Design of Biopharmaceutical Properties through Prodrugs and Analogs, edited by R. E. Roche, American Pharmaceutical Association, Washington, D.C., 1977, Chapter 6.

2. A. Rescigno and G. Segre, "Drug and Tracer Kinetics," Blaisdell Publishing Company, Mass, 1966, p. 78-81.

3. L. Z. Benet and J. S. Turi. "Use of General Partial Fraction Theorem for Obtaining Inverse Laplace Transforms in Pharmacokinetic Analysis," J. Pharm. Sci, Vol. 60, No. 10, 1971, p. 1593-1594.

4. F. B. Hildebrand, "Introduction to Numerical Analysis," McGraw-Hill, New York, 1956, Chapter 6, p. 237.

5. Pamona College Medicinal Chemistry Project, June 1978.

6. P. A. Mitenko and R. I. Ogilvie, "Rapidly Achieved Plasma Concentration Plateaus, with Observations on Theophylline Kinetics," Clin Pharmacol Ther, Vol. 13, No. 3, 1972, p. 329.

7. M. Weinberger, L. Hendeles and L. Bighley, "The Relation of Production Formulation to Absorption of Oral Theophylline," N. Engl J Med, Vol. 299, No. 16, Oct 1978, p. 855.

8. F. R. R. Simons, C. W. Bierman and A. C. Sprenkle. "Efficacy of Dyphylline (Dihydroxypropyltheophylline in Exercise-induced Brochospasm," Peds (Suppl), Vol. 56, Nov 1975, p. 916-918.

APPENDIX

APPENDIX I

Modified Program SIMMOD

```
      PROGRAM SIMMOD(TAPE1,OUTPUT,TAPE2=OUTPUT)
      REAL K
      COMMON/DATA1/K(10,10),SUM(10)
      COMMON/DATA2/TO,TCUT,DTO,DT,PRTIN,TDOSE,DOSE(10),T,M
      COMMON/DATA4/X(10),XD(10),XNOW(10),XI1(10),
     1XDI1(10),XI2(10),XDI2(10),XI3(10),XDI3(10)
C
C     ENTER SYSTEM DIMENSION
C
 1000 READ(1,1)M
    1 FORMAT(I2)
      IF(EOF(1))50,51
   51 DO 20 I=1,M
      DO 2 J=1,M
    2 K(I,J)=0.0
   20 CONTINUE
C
C     ENTER RUN CONTROL INFORMATION
C
      READ(1,*)TO,TCUT,DTO,PRTIN,TDOSE
      READ(1,*)(DOSE(I),I=1,M)
C
C     INITIALIZE TIME AND COUNTERS
C
      T=TO
```

```
      DT=DTO
C
C  READ SYSTEM CONSTANTS
C
      DO 4 I=1,M
    4 READ(1,*)(K(I,J),J=1,M)
      DO 6 I=1,M
      SUM(I)=0.0
      DO 7 J=1,M
    7 SUM(I)=SUM(I)+K(J,I)
    6 CONTINUE
      DO 10 I=1,M
   10 K(I,I) = SUM(I)
C
      WRITE(2,25)
   25 FORMAT(2X,//)
      WRITE(2,31)
   31 FORMAT(1H ,*K(I,J) VALUES ARE:*,/)
      DO 32 I=1,M
   32 WRITE(2,28)(K(I,J),J=1,M)
   28 FORMAT (2X,10(1X,F10.6))
      WRITE(2,25)
C
C  READ INITIAL VALUES
C
```

```
      READ(1,*)(XNOW(I),I=1,M)
      DO 11 I=1,M
   11 X(I)=XNOW(I)
C
C     PRINT HEADINGS AND INITIAL LEVELS
C
      WRITE(2,12)(I,I=1,M)
   12 FORMAT(1H ,2X,4HTIME,1X,10(7X,2HX(, I1, 1H)))
      WRITE(2,13)T,(XNOW(I),I=1,M)
   13 FORMAT(1H ,G10.4,4X,10G11.4)
      TPRT=0.0
      TMUL = 0.0
C
C     SIMULATE SYSTEM OPERATION OVER TIME
C
  100 CALL INTGRL
      TPRT=TPRT+DTO
      T=T+DT
      TMUL =TMUL+DT
      IF(TMUL.LT.TDOSE) GO TO 90
      DO 9 I=1,M
    9 XNOW(I) = XNOW(I) + DOSE(I)
      TMUL = 0.0
   90 IF(TPRT.LT.PRTIN)GO TO 200
      WRITE(2,13)T,(XNOW(I),I=1,M)
```

```
      TPRT=0.0
  200 DO 14 I=1,M
   14 X(I)=XNOW(I)
      IF(T.LT.TCUT)GO TO 100
      GO TO 1000
C
C     END OF RUN
C
   50 CALL EXIT
      END
      SUBROUTINE XDOT(M,X,XD,T)
      REAL K
      COMMON/DATA1/K(10,10),SUM(10)
      DIMENSION X(10),XD(10)
C
C     COMPUTE LEVEL DERIVATIVES
C
      XD(1)=-K(1,1)*X(1)
      XD(2)=K(2,1)*X(1)-K(2,2)*X(2)+K(2,3)*X(3)
      XD(3)=K(3,2)*X(2)-K(3,3)*X(3)
      XD(4)=K(4,2)*X(2)-K(4,4)*X(4)+K(4,5)*X(5)
      XD(5)=K(5,3)*X(3)+K(5,4)*X(4)-K(5,5)*X(5)
      XD(6)=K(6,4)*X(4)+K(6,5)*X(5)-K(6,6)*X(6)

      RETURN
```

```
      END
      SUBROUTINE INTGRL
      REAL K
      COMMON/DATA1/K(10,10),SUM(10)
      COMMON/DATA2/TO,TCUT,DTO,DT,PRTIN,TDOSE,DOSE(10),T,M
      COMMON/DATA4/X(10),XD(10),XNOW(10),XI1(10),
     1XDI1(10),XI2(10),XDI2(10),XI3(10),XDI3(10)
C
C     RUNGE-KUTTA METHOD, FOURTH ORDER GLOBALLY
C
      HDT=DT/2.
      CALL XDOT(M,X,XD,T)
      DO 100 I=1,M
  100 XI1(I)=X(I)+HDT*XD(I)
      TH=T+HDT
      CALL XDOT(M,XI1,XDI1,TH)
      DO 200 I=1,M
  200 XI2(I)=X(I)+HDT*XDI1(I)
      CALL XDOT(M,XI2,XDI2,TH)
      DO 300 I=1,M
  300 XI3(I)=X(I)+DT*XDI2(I)
      TF=T+DT
      CALL XDOT(M,XI3,XDI3,TF)
      SDT=DT/6.
      DO 400 I=1,M
```

```
 400 XNOW(I)=X(I)+SDT*(XD(I)+2.*XDI1(I)+2.*XDI2(I)+XDI3(I))
     RETURN
     END
-END OF FILE-
```

APPENDIX II

Program TEKPLOT

```
      PROGRAM TEKPLOT(TAPE1,INPUT,OUTPUT,TAPE5=INPUT,TAPE6=OUTPUT,TAPE10
     1,TAPE49)
      COMMON/PLT/ICODE,WIDTH,HEIGHT,MODEL,IRATE
      DIMENSION LABX(3),LABY(3),LABL(5)
      DIMENSION ICHAR(80),ICHAR1(20),ICHAR2(20),ICHAR3(40)
      DIMENSION MARK(9),DASH(8,4),YYMIN(9),YYMAX(9),YY(240)
      DIMENSION DATA(240,20),Y(240,9),X(240)
      DIMENSION NY(9)
      NAMELIST/PLOT/NROWS,NCOLS,IX,IY,IY1,IY2,IY3,IY4,IY5,IY6,IY7,IY8,
     1 IY9,XMIN,XMAX,YMIN,YMAX,NCURVES,WIDTH,HEIGHT,MODEL,IRATE,ICODE
      DATA WIDTH,HEIGHT,MODEL,IRATE,ICODE/10.,7.,4010,300,4/
      DATA MARK/4,28,18,20,22,24,26,2,6/
      DATA IBLANK,ICOMMA/1H ,1H,/
      DATA(DASH(1,I),I=1,4)/0.1,0.1,0.1,0.1/
      DATA(DASH(2,I),I=1,4)/0.1,0.2,0.1,0.2/
      DATA(DASH(3,I),I=1,4)/0.2,0.1,0.2,0.1/
      DATA(DASH(4,I),I=1,4)/0.2,0.2,0.2,0.2/
      DATA(DASH(5,I),I=1,4)/0.1,0.1,0.2,0.2/
      DATA(DASH(6,I),I=1,4)/ 0.2,0.2,0.1,0.1/
      DATA(DASH(7,I),I=1,4)/0.15,0.05,0.05,0.05/
      DATA(DASH(8,I),I=1,4)/0.15,0.1,0.15,0.1/
    1 CONTINUE
C
C ...ZERO ALL THE ARRAYS OF IMPORTANCE
C
```

```
      DO 2001 I=1,80
2001 ICHAR(I)=IBLANK
      DO 2002 I=1,20
2002 ICHAR1(I)=ICHAR2(I)=IBLANK
      DO 2003 I=1,40
2003 ICHAR3(I)=IBLANK
      XMIN=XMAX=YMIN=YMAX=0.
      IX=1
      IY1=IY2=IY3=IY4=IY5=0
      IY6=IY7=IY8=IY9=0
      DO 2 I=1,240
      DO 3 J=1,20
    3 DATA(I,J)=0.
      DO 4 J=1,9
    4 Y(I,J)=0.
    2 CONTINUE
      DO 5 I=1,9
    5 NY(I)=0
C
C......READ THE PLOT COMMAND
C
    6 READ(5,PLOT)
      IF(EOF(5).NE.0)STOP
      IF(NROWS.GT.0.AND.NCOLS.GT.0)GO TO 7
C
```

```
C......FOR GOT TO ENTER NROWS OR NCOLS
C
      WRITE(6,8)
    8 FORMAT(* ERROR IN NROWS OR NCOLS-REENTER PLOT COMMAND*)
      GO TO 6
    7 CONTINUE
      READ(5,77)(ICHAR(I),I=1,80)
   77 FORMAT(80A1)
      IF(EOF(5).NE.0)GO TO 78
   78 CONTINUE
C
C......ASSIGN THE X AXIS TITLE
C
      NCHAR=0
      DO 73 I=1,20
      NCHAR=NCHAR+1
      IF(ICHAR(NCHAR).EQ.ICOMMA)GO TO 74
   73 ICHAR1(I)=ICHAR(NCHAR)
C
C......ASSIGN THE YAXIS TITLE
C
   74 DO 75 I=1,20
      NCHAR=NCHAR+1
      IF(ICHAR(NCHAR).EQ.ICOMMA)GO TO 76
   75 ICHAR2(I)=ICHAR(NCHAR)
```

```
C
C......ASSIGN THE PLOT TITLE
C
   76 DO 177 I=1,40
      NCHAR=NCHAR+1
      IF(NCHAR.GT.80)GO TO 79
  177 ICHAR3(I)=ICHAR(NCHAR)
C
C......WRITE THE X, Y, AND PLOT TITLES ON TAPE49, WITH THE
C......APPROPRIATE CONTROL CHARACTERS
C
   79 REWIND 49
      WRITE(49,710)(ICHAR1(I),I=1,20)
      WRITE(49,710)(ICHAR2(I),I=1,20)
  710 FORMAT(2H<!,A1,1H>,19A1,6H      )
      WRITE(49,720)(ICHAR3(I),I=1,40)
  720 FORMAT(2H<!,40A1,8H        )
      REWIND 49
      READ(49,711)(LABX(I),I=1,3)
      READ(49,711)(LABY(I),I=1,3)
  711 FORMAT(3A10)
      READ(49,712)(LABL(I),I=1,5)
  712 FORMAT(5A10)
      NY(1)=IY1
      NY(2)=IY2
```

```
      NY(3)=IY3
      NY(4)=IY4
      NY(5)=IY5
      NY(6)=IY6
      NY(7)=IY7
      NY(8)=IY8
      NY(9)=IY9
      IF(NCURVES.NE.0)GO TO 20
C
C.....NCURVES=0 MEANS ALL THE DATA IS IN ONE FILE-READ THE DATA
C.....ARRAY AND SET UP THE X AND Y ARRAYS ACCORDINGLY
C
      READ(1,*)((DATA(I,J),J=1,NCOLS),I=1,NROWS)
      IF(EOF(1).EQ.0)GO TO 11
      WRITE(6,12)
   12 FORMAT(* DATA FILE ERROR-REWIND, CHECK, AND RESTART*)
      STOP
   11 IF(NY(1).EQ.0)STOP
C
C.....FIND NCURVES
C
      NCURVES=0
      DO 15 J=1,9
      IF(NY(J).EQ.0) GO TO 15
      NCURVES=NCURVES+1
```

```
   15 CONTINUE
      DO 13 I=1,NROWS
      X(I)=DATA(I,IX)
      DO 14 J=1,NCURVES
      IF(NY(J).EQ.0)GO TO 13
   14 Y(I,J)=DATA(I,NY(J))
   13 CONTINUE
      GO TO 30
C
C......IF NCURVES NE 0 MUST REPEAT READ OF DATAFILE FOR SUCCESSIVE
C......Y VALUES-X IS TAKEN FROM THE IXTH COLUMN OF THE FIRST FILE
C
   20 READ(1,*)((DATA(I,J),J=1,NCOLS),I=1,NROWS)
      IF(EOF(1).EQ.0)GO TO 1020
      WRITE(6,12)
      STOP
 1020 DO 1021 I=1,NROWS
 1021 X(I)=DATA(I,IX)
C
C......CHECK IF IY IS SPECIFIED-IF SO, SET NY TO IY - OTHERWISE USE NY
C
      IF(IY.EQ.0)GO TO 25
      DO 2021 J=1,NCURVES
 2021 NY(J)=IY
   25 DO 21 I=1,NROWS
```

```
   21 Y(I,1)=DATA(I,NY(1))
C
C......REREAD THE DATA FILE AND FILL THE REMAINING Y COLUMNS, UP TO
C......NCURVES
C
      IF(NCURVES.LT.2)GO TO 30
      DO 22 M=2,NCURVES
      READ(1,*)((DATA(I,J),J=1,NCOLS),I=1,NROWS)
      IF(EOF(1).EQ.0)GO TO 23
      WRITE(6,12)
      STOP
   23 DO 24 I=1,NROWS
   24 Y(I,M)=DATA(I,NY(M))
   22 CONTINUE
C
C......CHECK MIN AND MAX VALUES
C
   30 IF(XMIN.NE.XMAX)GO TO 50
      CALL CHECK(X,NROWS,XMIN,XMAX)
   50 IF(YMIN.NE.YMAX)GO TO 60
      DO 51J=1,NCURVES
      DO 52 I=1,NROWS
   52 YY(I)=Y(I,J)
   51 CALL CHECK(YY,NROWS,YYMIN(J),YYMAX(J))
      YMIN=YYMIN(1)
```

```
      YMAX=YYMAX(1)
      IF(NCURVES.LT.2) GO TO 60
      DO 53 J=2,NCURVES
      YMIN=AMIN1(YMIN,YYMIN(J))
   53 YMAX=AMAX1(YMAX,YYMAX(J))
C
C.....NOW HAVE X,Y,XMIN,XMAX,YMIN,AND YMAX
C.....MUST FIND SUITABLE RANGES FOR THE AXES
C
   60 CALL RANGE(XMIN,XMAX, 5,XMIN1,XMAX1,XTIC )
      CALL RANGE(YMIN,YMAX,5,YMIN1,YMAX1,YTIC)
C
C.....SET UP THE PLOT PARAMETERS
C
      CALL SETUP(XMIN1,XMAX1,YMIN1,YMAX1)
      XORG=XMIN1
      YORG=YMIN1
      XMAX=XMAX1
      YMAX=YMAX1
C
C.....DRAW AND LABEL THE AXES
C
      CALL ERASE
       CALL AXISL(XMIN1,XMAX1,XORG,YMIN1,YMAX1,YORG,XTIC,YTIC,4,4,2,1,
     1 1.0,1.0,0.15,0)
```

```
C
C......DRAW THE FIRST LINE SOLID
C
      DO 70 I=1,NROWS
   70 YY(I)=Y(I,1)
      CALL VECTORS
      CALL LINE(X,YY,MARK(1),NROWS)
C
C......DRAW SUCCESSIVE LINES WITH VARIOUS DASHED LINE
C......COMBINATIONS AND DATA MARKS
C
      IF(NCURVES.LT.2)GO TO 201
      DO 100 J=2,NCURVES
      CALL DASHES
      JJ=J-1
      CALL DASHSZ(DASH(JJ,1),DASH(JJ,2),DASH(JJ,3),DASH(JJ,4))
      DO 99 I=1,NROWS
   99 YY(I)=Y(I,J)
  100 CALL LINE(X,YY,MARK(J),NROWS)
C
C......DRAW THE X AND Y AXES AND THE PLOT TITLE
C
  201 XRANGE=XMAX-XORG
      YRANGE=YMAX-YORG
      XFACT=WIDTH/XRANGE
```

```
      YFACT=HEIGHT/YRANGE
C
C.....LABEL THE XAXIS
C
      XPOS=XORG+0.2*XRANGE
      YPOS=YORG-0.1*YRANGE
      CALL SYMBEL(XPOS,YPOS,0.,0.2,30,LABX)
C
C.....LABEL THE Y-AXIS, AT A 90 DEGREE ANGLE
C
      XPOS=XORG-0.15*XRANGE
      YPOS=YORG+0.1*YRANGE
      CALL SYMBEL(XPOS,YPOS,90.,0.2,30,LABY)
C
C.....TITLE THE PLOT AT THE TOP
C
      XPOS=XORG+0.1*XRANGE
      YPOS=YMAX
      CALL SYMBEL(XPOS,YPOS,0.,0.3,50,LABL)
  200 CALL PLOTEND
      STOP
      END
      SUBROUTINE SETUP (XMIN,XMAX,YMIN,YMAX)
      COMMON/PLT/ICODE,WIDTH,HEIGHT,MODEL,IRATE
      CALL PLOTYPE(ICODE)
```

```
      CALL TKTYPE(MODEL)
      CALL BAUD(IRATE)
      CALL SIZE(WIDTH+0.5*WIDTH,HEIGHT+0.5*HEIGHT)
       XFACT=WIDTH/(XMAX-XMIN)
      YFACT=HEIGHT/(YMAX-YMIN)
      CALL SCALE(XFACT,YFACT,2.,2.,XMIN,YMIN)
      RETURN
      END
-END OF FILE-
```